

THE KÜHNEL TRIANGULATION OF THE COMPLEX  
PROJECTIVE PLANE FROM THE VIEW POINT OF  
COMPLEX CRYSTALLOGRAPHY

by

Bernard MORIN and Masaaki YOSHIDA  
with appendices by Alexis MARIN

B. MORIN  
Univ. Louis Pasteur  
7, rue René Descartes  
67084 Strasbourg

FRANCE

M. YOSHIDA  
Max-Planck-Institut  
für Mathematik  
Gottfried-Claren-Str. 26  
5300 Bonn 3

BRD

A. MARIN  
Univ. Paris XI Orsay  
91405 Orsay

FRANCE

MPI 86-13

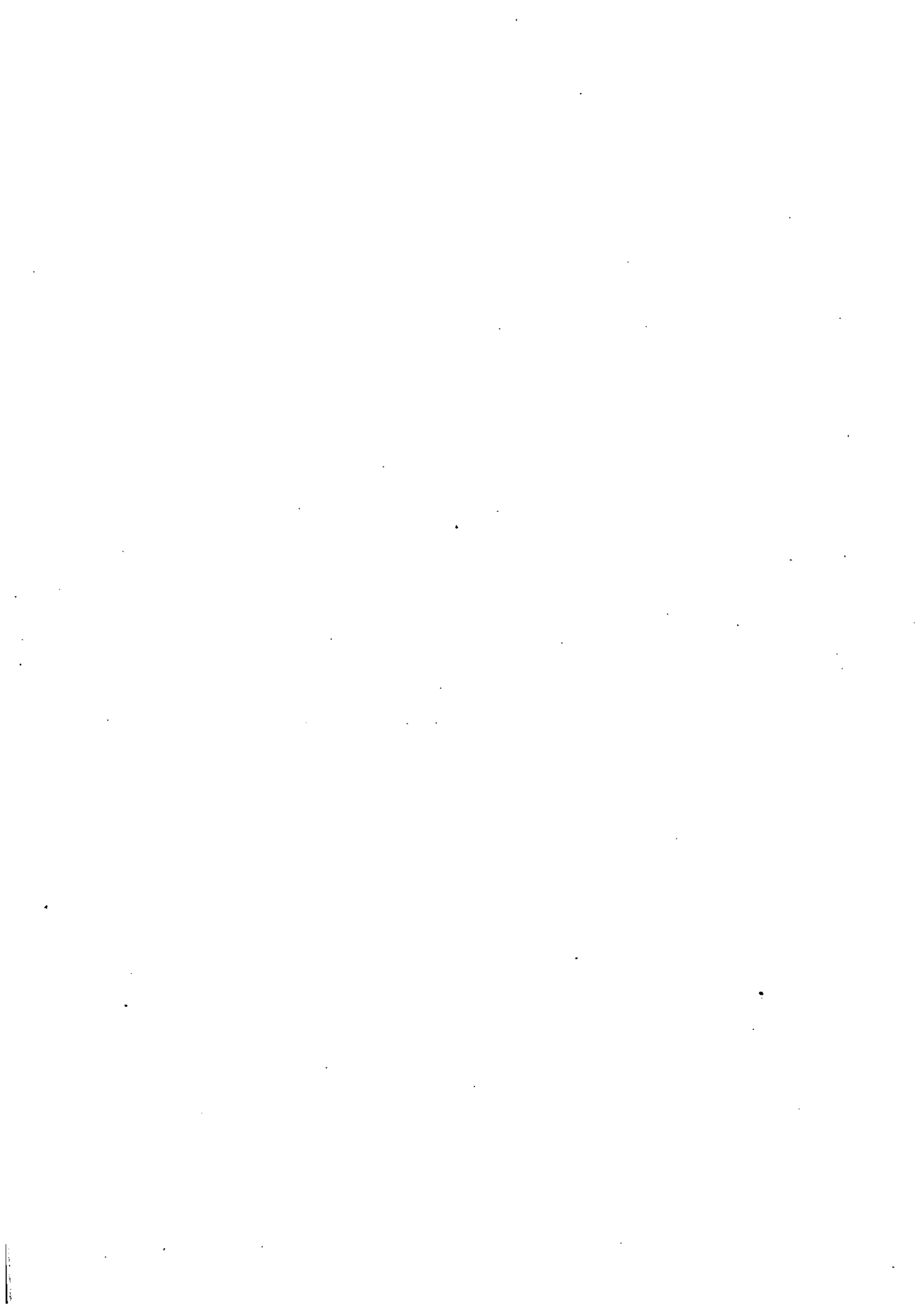


## TABLE OF CONTENTS

### Introduction

- Chapter I      The Kühnel complex viewed as a PL-manifold
- § 1      Kühnel's simplicial complex  $K$
  - § 2      The Grünbaum-Brückner link  $M$
  - § 3      A topological insight into  $|K|$
  - § 4      The direct proof that  $|K| \cong \mathbb{C}P^2$
- Chapter II     The Kühnel complex viewed as an orbifold
- § 5      The  $G$ -invariant torus  $T$  in  $K$
  - § 6      The six fold cover  $\tilde{M}$  of  $M$
  - § 7      Some lattices and crystallographic groups of  $\mathbb{C}^2$
  - § 8      The rectilinear triangulation  $\tilde{K}$  of  $\mathbb{C}^2$
  - § 9      An explicit triangulation of  $\mathbb{C}P^2$  by  $K$   
(the crystallographic proof)
- Chapter III    Additional material
- § 10     Two interesting fundamental domains for  $\Gamma$  in  $\tilde{K}$
  - § 11     How does  $\mathbb{R}P^2$  fit into the picture
  - § 12     The ontological proof forcing  $\mathbb{C}P^2$  to admit the  
triangulation  $K$  (A. Marin)
  - § 13     The lattice  $L[f]$  decorated with 81 colors (A. Marin)
  - § 14     How to make paper models (A. Marin)

### References



## Introduction

In this paper we give three new proofs of the fact that the geometric realization  $|K|$  of the Kühnel triangulation  $K$  defined in § 1 is homeomorphic to the complex projective plane  $\mathbb{C}P^2$ .

The original proof is due to W. Kühnel and T. F. Banchoff and can be found in [K-B]. It compares an explicit map from  $|K| - |\overset{\circ}{\Delta}|$  to the sphere  $S^2$  with the Hopf map  $\mathbb{C}P^2 - B \rightarrow \mathbb{C}P^1 \cong S^2$ . (Here  $\Delta$  is any 4-simplex in  $K$  and  $B$  is the complement of a closed tubular neighborhood of a complex line in  $\mathbb{C}P^2$ .) In fact, using the same idea, there exists also an unpublished but completely straightforward combinatorial argument (see end of § 2, where we reproduce A. Marin's version of it). Moreover Freedman's classification of simply connected closed 4-manifolds tells us that there are only two topological manifolds having the homotopy type of  $\mathbb{C}P^2$ , one of which admits no PL-structure. Therefore it suffices to show that  $K$  has the homotopy type of  $\mathbb{C}P^2$  and has a PL-structure (see § 2 Power hammer proof).

The first of our three proofs (referred to in § 4 as the direct proof) was presented in Oberwolfach in 1981 and notes of this talk have been circulated by K. Jänich, whom we thank for having drawn the wonderful pictures they contain. This proof uses the fact that  $\mathbb{C}P^2$  maps naturally onto the 2-simplex  $\Delta_2$ ; this map is compared with a simplicial mapping

from a subdivision  $\bar{K}$  of  $K$  to a subdivision  $\bar{\Delta}_2$  of  $\Delta_2$  constructed in § 3. The second proof (referred to in § 9 as the crystallographic proof) is by showing that the Kühnel triangulation  $K$  is in fact the quotient of a rectilinear triangulation  $\tilde{K}$  of  $\mathbb{C}^2$  by the action of complex crystallographic group  $\Gamma$  (defined in § 7) preserving  $\tilde{K}$ . An explicit mapping  $\gamma: \mathbb{C}^2 \rightarrow \mathbb{C}P^2$  is then defined (see § 9) which factorizes through  $|K| = \mathbb{C}^2/\Gamma$ . The last proof (referred to in § 12 as the ontological proof) is a very efficient attack on the problem that was developed by Alexis Marin after reading drafts of the present work. We include it here as an appendix under his signature, to which we will occasionally refer in the course of the paper. Other contributions by Marin will be mentioned as we encounter them, so that this paper should be considered as a dialogue between the authors and him.

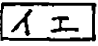
A question naturally arises: "Why three new proofs when at least two satisfactory ones already exist?" Answer: Many mathematicians asked for a spatial representation of the phenomenon discovered by Kühnel. In order to respond to this demand, we thought that as many view points as possible should be given. Each proof (including the one in [K-B]) does indeed throw a different light from a different angle of vision, on a simple but tricky four dimensional fact. The trickiness comes from the constraint that human vision has been divised to grasp only three dimensional happening. We have tried our best to make the

four dimensional world - at least one corner of it -  
as palatable as possible to the reader.

In § 1 we recall that what is the Kühnel triangulation  $K$  (a simplicial complex of dimension 4 with 9 vertices, the star of all vertices being isomorphic to each other). In § 2 we recall that the link  $M$  at a given vertex is homeomorphic to the 3-sphere which implies that  $|K|$  is a topological 4-manifold. We show that  $K$  is PL, which allows Freedman's Power hammer proof to work, and we cite Marin's version of the straightforward combinatorial proof. § 3 defines a piecewise linear projection  $p:|K| \rightarrow \Delta_2$  and studies their topological properties. § 4 introduces a map  $\pi:\mathbb{C}P^2 \rightarrow \Delta_2$  and compares it with  $p$  thus showing  $|K| \approx \mathbb{C}P^2$  and making the triangulation explicit. § 5 shows that  $K$  contains a combinatorial torus  $T$  with remarkable properties. This fact enables one to connect Kühnel's result with complex crystallography. § 6 constructs a 6 fold branched cover  $\tilde{M}$  of  $M$  which will turn out to be isomorphic to the link of any vertex of  $\tilde{K}$ . In order to explain the crystallographic proof, § 7 introduces lattices and various crystallographic ingredients needed later, in particular, the vertices of  $\tilde{K}$  and the groups  $\Gamma$  and  $\Gamma''$ . The construction of  $\tilde{K}$  is completed in § 8. In § 9, a  $\Gamma$ -invariant holomorphic mapping  $Y:\mathbb{C}^2 \rightarrow \mathbb{C}P^2$  is constructed by using Weierstrass functions, producing a second explicit homeomorphism  $|K| \xrightarrow{\sim} \mathbb{C}P^2$ . As a dessert § 10

constructs a highly symmetric Dirichlet domain for the action of  $\Gamma$  in  $\mathbb{C}^2$  and uses it to exhibit a fundamental domain for  $\tilde{K}$ . It also prepares the construction of § 12 by embedding in  $\tilde{K}$  the fundamental domain discovered by A. Marin. In § 11 one sees how the real projective plane  $\mathbb{R}P^2 \subset \mathbb{C}P^2$  fits inside our picture.

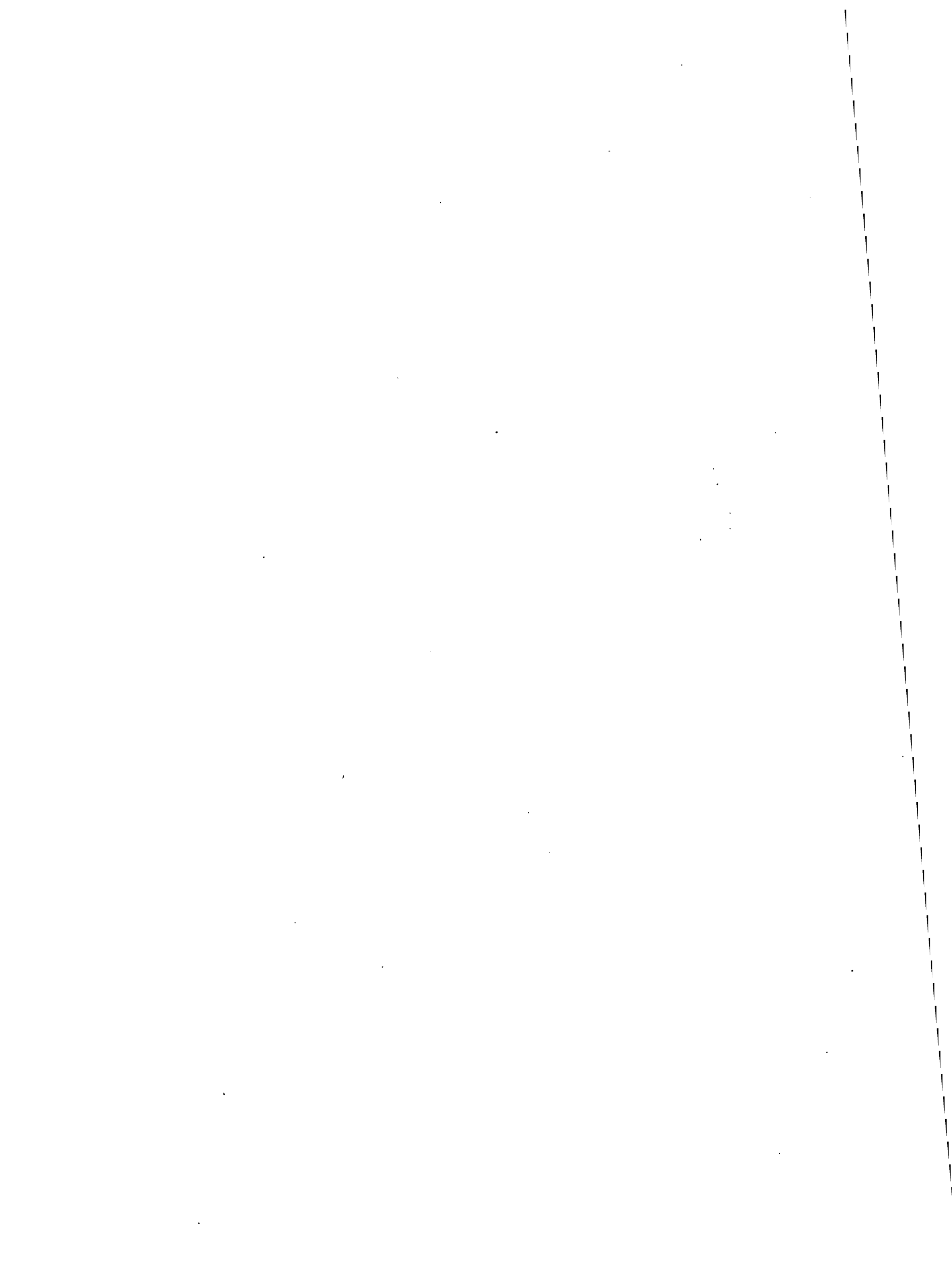
In § 12 (the appendix), it is shown how, by considering a fundamental domain of  $|\tilde{K}|$  which is isomorphic to the product of  $\Delta_2$  with a hexagon, and by using a priori requirements, A. Marin forces the Kühnel triangulation to exist. This provides a way for the hurried mathematician, not interested in visualizing things, to avoid most of the effort imposed on him in the present article. § 13 will study the quotient of the lattice  $L[f]$  of vertices of  $\tilde{K}$  by a sublattice of index 81 which should provide the reader with a global understanding of the whole scenery. § 14 will explain how to obtain 3-dimensional paper models of various constructions used in the course of the article.

The pictures of K. Jänich, already cited, were of invaluable help in communicating our ideas, and are reproduced here with the logo  (the Katakana sign pronounced as the English word "Yea"). We also include four drawings made for us by George K. Francis which we attribute to him as they occur.

We would like to acknowledge the importance to us of the contribution of Jänich, numerous discussions with



Kühnel (who gave us much useful information and made many helpful suggestions) and the deep interest shown by A. Marin, in particular his stern checking, his rigorous criticisms and the solidity of his contribution. We are grateful to Alex Flegmann who tried his best to make our Franco-Japanese English book less clumsy. Without the facilities offered both by the IRMA (ULP Strasbourg, France) and by the MPI für Mathematik (Bonn, West Germany), the authors could not thank each other for their mutual collaboration. A special mention should be made of Marie-Claire Grima, who showed great patience in tabulating a huge quantity of tedious diagrams. Some of these appear below while the remainder will, we hope, serve as the basis for a computerised audiovisual animation of the pictures we have in mind.



## Chapter I The Kühnel complex viewed as a PL-manifold

§ 1 Kühnel's simplicial complex  $K$ 

Let the vertices  $1, 2, \dots, 9$  of the 8-simplex  $\Delta_8$  be arranged in an array as follows:

$$\begin{pmatrix} 1 & 4 & 7 \\ 2 & 5 & 8 \\ 3 & 6 & 9 \end{pmatrix}$$

In the course of this paper we like to keep in mind the idea that the three columns of this matrix are respectively blue, white and red, so that for instance 1 belongs to the blue family 5 to the white family and 9 to the red family.

Let  $G$  be the subgroup of the symmetric group  $\mathfrak{S}_9$  (acting on  $\Delta_8$ ) be generated by  $\alpha, \beta$  and  $\gamma$ , where  $\alpha$  and  $\beta$  cyclicly permute respectively the columns and the rows of the above matrix, while  $\gamma$  is  $\beta$  on the first column,  $\beta^{-1}$  on the second and the identity on the third:

$$\alpha \begin{pmatrix} 1 & 4 & 7 \\ 2 & 5 & 8 \\ 3 & 6 & 9 \end{pmatrix} = \begin{pmatrix} 4 & 7 & 1 \\ 5 & 8 & 2 \\ 6 & 9 & 3 \end{pmatrix}, \quad \beta \begin{pmatrix} 1 & 4 & 7 \\ 2 & 5 & 8 \\ 3 & 6 & 9 \end{pmatrix} = \begin{pmatrix} 2 & 5 & 8 \\ 3 & 6 & 9 \\ 1 & 4 & 7 \end{pmatrix}$$

$$\gamma \begin{pmatrix} 1 & 4 & 7 \\ 2 & 5 & 8 \\ 3 & 6 & 9 \end{pmatrix} = \begin{pmatrix} 2 & 6 & 7 \\ 3 & 4 & 8 \\ 7 & 5 & 9 \end{pmatrix}.$$

Thus we have

$$\alpha\beta = \beta\alpha, \quad \beta\gamma = \gamma\beta, \quad \alpha^{-1}\gamma\alpha\gamma = \beta,$$

showing that the order of  $G$  is 27. Moreover  $G$  acts transitively on the vertices of  $\Delta_8$ . For later use, let us also define  $\delta$  and  $\epsilon$ :

$$\delta \begin{pmatrix} 1 & 4 & 7 \\ 2 & 5 & 8 \\ 3 & 6 & 9 \end{pmatrix} = \begin{pmatrix} 2 & 5 & 8 \\ 1 & 4 & 7 \\ 3 & 6 & 9 \end{pmatrix} \quad \epsilon \begin{pmatrix} 1 & 4 & 7 \\ 2 & 5 & 8 \\ 3 & 6 & 9 \end{pmatrix} = \begin{pmatrix} 4 & 1 & 7 \\ 5 & 2 & 8 \\ 6 & 3 & 9 \end{pmatrix}.$$

As an alternative possibility, let us write a sub-simplex of  $\Delta_8$  just by making the places of its vertices in the  $3 \times 3$ -matrix (Braille notation), for instance,

$$(1 \ 2 \ 4 \ 5 \ 9) = \begin{array}{|c|c|} \hline \bullet & \bullet \\ \hline \bullet & \bullet \\ \hline & \\ \hline \end{array}, \quad (1 \ 2 \ 4 \ 5 \ 6) = \begin{array}{|c|c|} \hline \bullet & \bullet \\ \hline \bullet & \bullet \\ \hline & \bullet \\ \hline \end{array}.$$

The type of a sub-simplex of  $\Delta_8$  is the collection of non-zero occupation numbers of its vertices in the columns, for instance,  $(1 \ 2 \ 4 \ 5 \ 9)$  is of type  $2-2-1$  and  $(1 \ 2 \ 4 \ 5 \ 6)$  is of type  $3-2$ . The marked vertex of a  $2-2-1$  simplex is the vertex which lives alone in its column. For example 9 is the marked vertex in the example above. The color of a  $2-2-1$  simplex is the color of its marked vertex; thus  $(1 \ 2 \ 4 \ 5 \ 9)$  is red. The color of a  $3-2$  simplex is the color of the missing column; thus  $(1 \ 2 \ 4 \ 5 \ 6)$  is red. Obviously the type is invariant under the five actions defined above, while  $\alpha$  and  $\epsilon$  permute

the colors which are  $\beta, \gamma$  and  $\delta$  - invariant.

Let  $K'$  and  $K''$  be the sub-complexes of  $\Delta_8$  respectively generated by the  $G$ -orbits of  $(1\ 2\ 4\ 5\ 9)$  and  $(1\ 2\ 4\ 5\ 6)$  and let  $K$  be the  $G$ -invariant complex  $K' \cup K''$ . Notice that  $K$  contains the 2-skelton of  $\Delta_8$  and that it has 36 4-simplices. Figure 1-1 shows the  $G$ -orbit of  $(1\ 2\ 4\ 5\ 9)$ , which consists of 27 4-simplices of type 2-2-1. The segments indicate that the joined simplices share a common hyperface. Note that the figure actually contains 30 simplices, but of course the opposite corners of the hexagon must be identified in order to produce a toridal arrangement. Note also that  $\alpha$  acts on the diagram as an anticlockwise rotation of  $2\pi/3$  about the center of the figure and that  $\beta$  and  $\gamma$  are respectively the four step eastward and the two step southeastward translations on the torus. The intersection of  $K'$  with the star of  $K$  at vertex 9 is represented on the diagram by the central northwest-southeast ship of width three. Figure 1-2 shows the  $G$ -orbit of  $(1\ 2\ 4\ 5\ 6)$ , which consists of 9 4-simplices of type 3-2.

The Kühnel complex

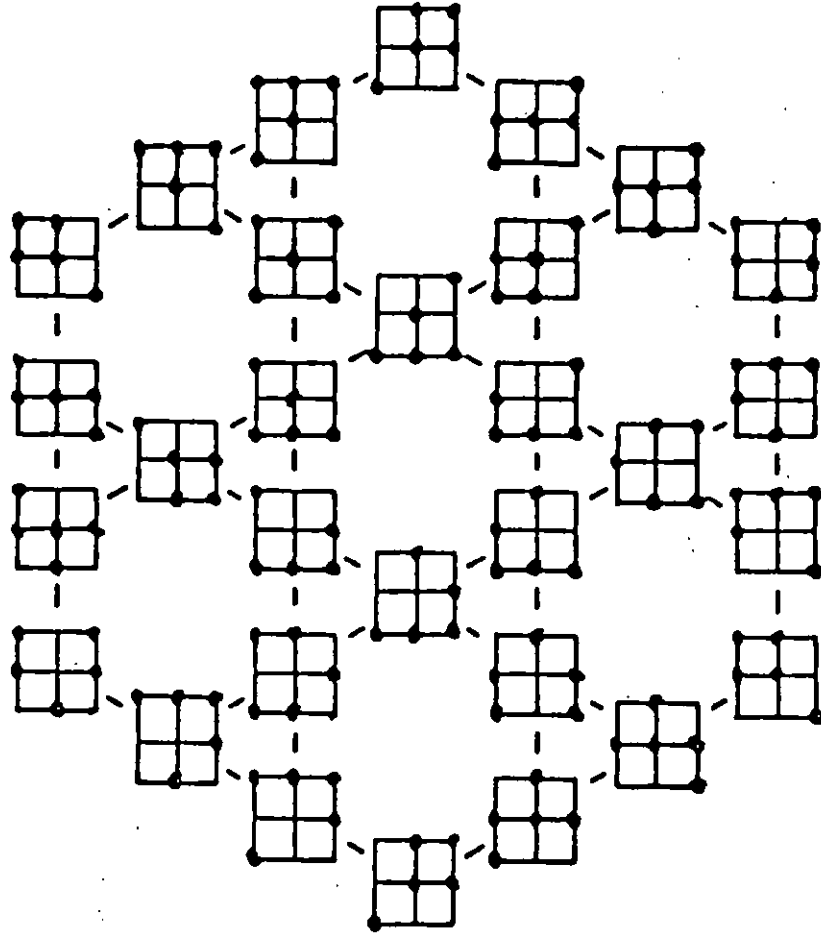


Figure 1-1

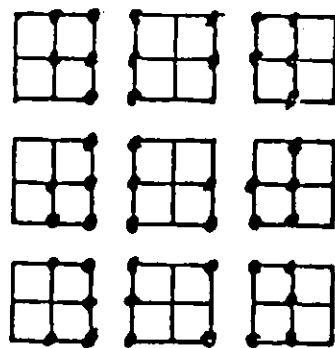


Figure 1-2

IE

§ 2 shows that the topological realization  $|K|$  of  $K$  is a PL-manifold and recalls two proofs of the fact that  $|K| \cong \mathbb{C}P$ . § 3 studies the topology of  $|K'|$  and  $|K''|$ , and § 4 presents the first of our new demonstrations showing that  $|K| \cong \mathbb{C}P^2$ .

Note The present definitions of  $\beta$  and  $\gamma$  have been interchanged compared with those in [K-B]. It is essentially due to the fact that, as we will see in § 12, our  $\gamma$  (that is to say Kühnel and Banchoff's  $\beta$ ) is some how less important than our  $\beta$ , although  $\alpha$  and  $\gamma$  generate  $G$ .





§ 2 The Grünbaum-Brückner link  $M$ 

In this section we show that  $|K|$  is a topological and also a PL-manifold. We study the stars of vertices of  $K$  (cf. [G]). Since  $G$  is transitive on these vertices, all stars are combinatorially isomorphic. The link in  $K$  of vertex 9 (i.e. the boundary of the star at this vertex) is the complex generated by the following twenty 3-simplices:

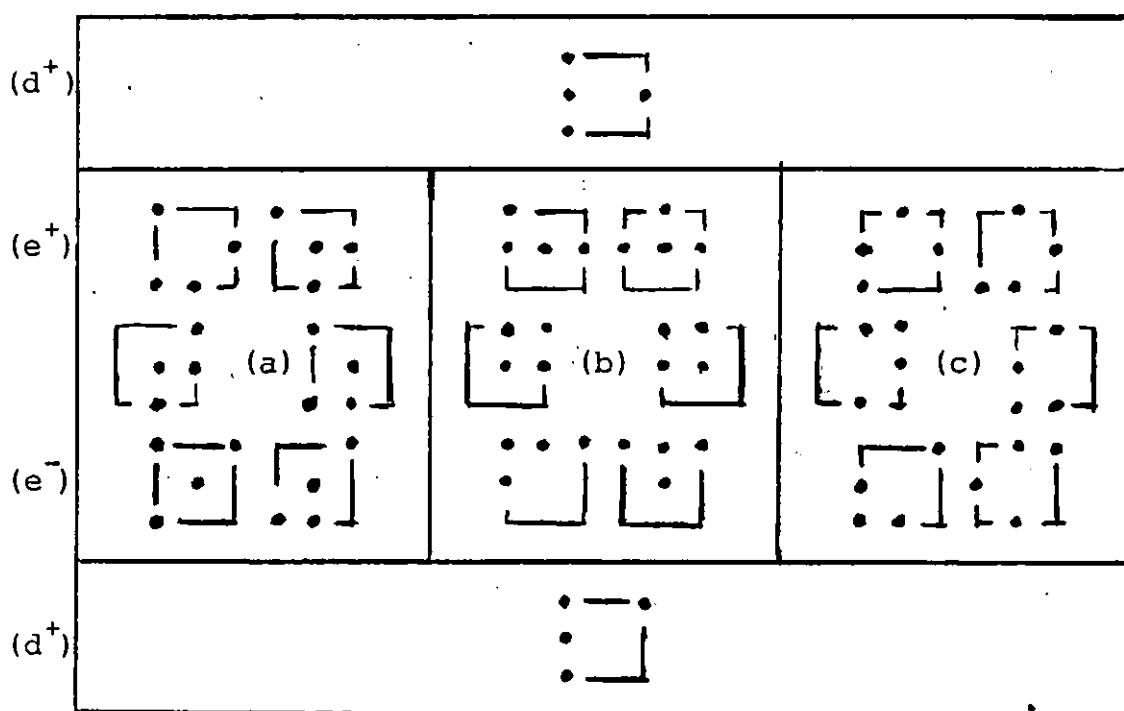


Figure 2-1

(We remark that (b) and (c) are obtained by respectively applying  $\gamma$  and  $\gamma^2$  to (a), while the two simplices in boxes  $(d^+)$  and  $(d^-)$  are  $\gamma$ -invariant.)

The union of the topological realizations of the six simplices displayed in each of the boxes (a), (b) and (c) is a 3-ball. Now  $(a) \cup (b) \cup (c)$  and  $(d^+) \cup (d^-)$  are two 3-balls glued along their common boundary, showing that the link of vertex 9 in  $K$  is a 3-sphere (and hence that  $|K|$  is a topological manifold).

The complex displayed in Figure 2-1 (denoted  $M$  in  $[G]$ ) is one of the four ways described by M. Brückner (1909) and B. Grünbaum (1967) to triangulate the 3-sphere  $S^3$  with 8 vertices, 28 edges, 40 triangles and 20 tetrahedrons.

Description of  $M$  In order to have a good grasp on  $M$  one can describe it as follows.

(1) Notice first that the union of the three simplices appearing on the right of boxes (a), (b) and (c) can be non-rectilinearly arranged into a quilted annulus as shown on Figure 2-2.

The quilted annulus formed by three 3-simplices (1635), (2514)  
and (3426)

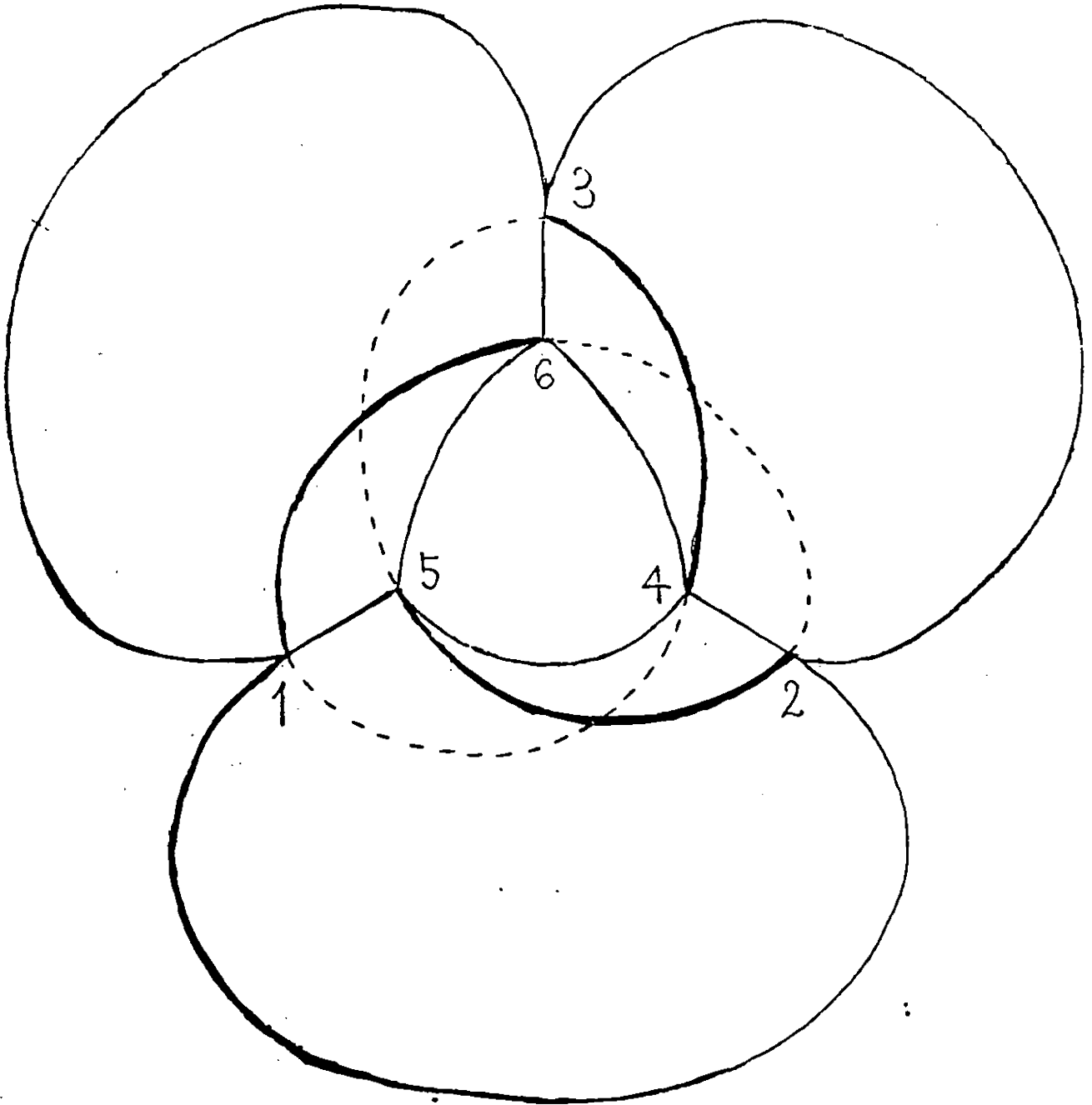
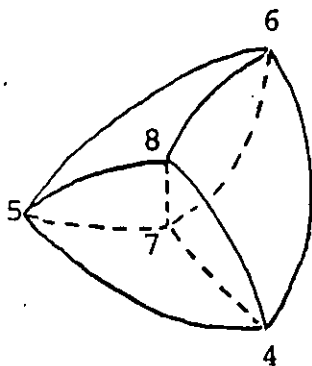


Figure 2-2

(2) On the axis of symmetry of Figure 2-2 let us place vertex 7 and vertex 8 respectively below and above the plane of the picture. The simplices appearing on the left of boxes (a), (b) and (c) are obtained by joining 7 to 8 and then (78) respectively to (56), (45) and (64).



(3) Notice now that the collection of simplices respectively listed on lines  $(e^+)$  and  $(e^-)$  can be interpreted as representing the visual cone when one looks to the quilted annulus respectively from 8 and 7. From 8 you see the top part of the annulus namely the six triangles:

• (316), (615), (125), (524), (234), (436).

From 7 you see the bottom part of the annulus namely the six triangles:

(135), (536), (214), (415), (326), (624).

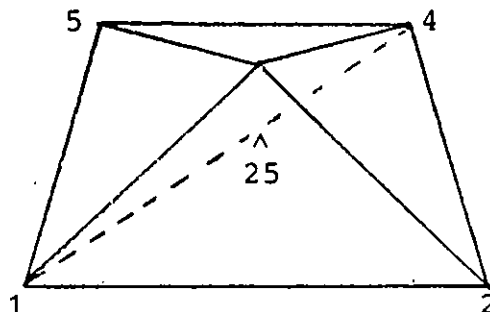
See Figure 2-2.

(4) The union of the 18 tetrahedra already constructed is a ball whose complement in  $S^3$  can be decomposed into the two tetrahedra in  $(d^+)$  and  $(d^-)$  which share the face (123) (a triangle having the point at infinity as its center).

The combinatorial manifold K. There are several reasons why the topological manifold K is in fact PL. Firstly because  $S^3$  has a unique PL-structure (see [Moi]); secondly because the way we described the triangulation is obviously  $C^1$  in the sense of J.H.C. Whitehead (see [Wh 2]); and lastly because, by adding the three midpoints  $\hat{16}$ ,  $\hat{25}$  and  $\hat{34}$  of respective edges (16), (25) and (34) as new vertices, one easily gets a subdivision of M with eleven vertices and twenty nine 3-simplices.

For instance, the ball considered above consisting of six non-rectilinear tetrahedra now decomposes into the nine following rectilinear simplices:

$$\begin{array}{lll}
 (1 \ 2 \ 8 \ \hat{25}) & (2 \ 4 \ 8 \ \hat{25}) & (4 \ 5 \ 8 \ \hat{25}) \\
 (5 \ 1 \ 8 \ \hat{25}) & (1 \ 4 \ 5 \ \hat{25}) & (1 \ 2 \ 4 \ \hat{25}) \\
 (1 \ 2 \ 4 \ 7) & (1 \ 4 \ 5 \ 7) & (4 \ 5 \ 7 \ 8)
 \end{array}$$



Claim 0:  $|K| \cong \mathbb{C}P^2$

Power hammer proof (mentioned by W. Kühnel). Since  $K$  contains the 2-skeleton of  $\Delta_8$ ,  $|K|$  is simply connected; its Euler characteristic is 3: Hence  $|K|$  has the homotopy type of  $\mathbb{C}P^2$  (c.f. [E-K]). Using the Freedman classification of simply connected 4-manifolds (c.f. [S]), one sees that the combinatorial manifold  $K$  is homeomorphic to  $\mathbb{C}P^2$ .

Nevertheless in § 3 - § 12 we intend to present three new proofs of this fact. Before doing this, we conclude the present section by giving the straight-forward combinatorial argument following the idea of Kühnel and Banchoff mentioned in the introduction and as explained by A. Marin.

The straightforward combinatorial proof of claim 0 (A. Marin)

Let  $\Delta$  be any one of the 4-simplicies of  $K$ . The subcomplex  $\Sigma$  generated by the vertices outside  $\Delta$  is a 2-sphere.

Let  $r:K \rightarrow [0,1]$  be the simplicial mapping which sends  $\Delta$  to 1 and  $\Sigma$  to 0.

Consider the decomposition:

$$|K| = r^{-1}([0,1/2]) \cup \underset{r^{-1}(1/2)}{r^{-1}([1/2,1])} = T \cup B.$$

The second term  $B$  of this decomposition is a regular neighbourhood of  $\Delta$  in the 4-manifold  $|K|$  (cf. [Wh 1] or [R-S, chap 3]) and hence it is a 4-ball. The first term  $T$  is a regular neighbourhood of the sphere  $\Sigma$  in  $|K|$ . Therefore by claims 1 and 2 below,  $T$  is PL-isomorphic to a disc bundle over  $\Sigma$ . Since the boundary of this bundle is the 3-sphere  $\partial B$ , the Euler class of the bundle is  $\pm 1$ . With a suitable orientation,  $T$  is PL-isomorphic to a tube around a complex line in  $\mathbb{C}P^2$ , i.e. the complement of a 4 ball in  $\mathbb{C}P^2$ . By the Alexander trick there is essentially one way to glue  $\partial T$  to  $\partial B$ , so  $|K| = T \cup_{\partial} B$  is PL-isomorphic to  $\mathbb{C}P^2$ .

Claim 1 The sphere  $\Sigma$  is locally flat in the manifold  $|K|$ .

Proof Notice that  $\Sigma$  is combinatorially the boundary of a 3-simplex not contained in  $K$ . In order to prove Claim 1, it suffices to check that the boundary of each 2-simplex in  $\Sigma$  is unknotted in the link in  $K$  of the remaining vertex of  $\Sigma$ . Now it suffices to look at Figure 2-2 to observe that any closed curve formed by three edges is unknotted in  $M$ .

Claim 2 A regular neighbourhood of a locally flat 2-sphere  $S$  in a PL-4-manifold  $V$  is PL-isomorphic to a 2-disc bundle over  $S$ .

Proof A regular neighbourhood in the manifold pair  $(V, S)$  (cf. [R-S] chap 4) of a point interior to a triangle of  $S$  is an unknotted ball pair  $(B_1, D_1)$ .

The closed disc  $D_2 = S - \overset{\circ}{D}_1$  is locally flat in the manifold  $V - \overset{\circ}{B}_1$ . Hence a regular neighbourhood of this disc in  $(V - \overset{\circ}{B}_1, D_2)$  is also an unknotted ball pair  $(B_2, D_2)$ .

The pair  $(B_1 \cup B_2, D_1 \cup D_2)$  is then a regular neighbourhood of  $S$  in  $V$ . It is the union of two unknotted ball pairs which are glued along regular neighbourhoods of the circles bounding the 2-balls in the 3-spheres bounding the 4-balls (therefore along unknotted solid tori), the pair  $(B_1 \cup B_2, D_1 \cup D_2)$  is a disc bundle.

■



§ 3 A topological insight into  $|K|$ 

This section introduces a piecewise linear mapping  $|K| \rightarrow \Delta_2$  in order to give in § 4 an intuitive approach to Claim 0 of § 2 which is completely different to the attack adopted in [K-B].

As suggested by Figure 1-2 the complex  $K''$  decomposes into three complexes called  $K_a, K_b$  and  $K_c$  :

$$K_a = \partial(456) * (789),$$

$$K_b = \partial(789) * (123),$$

$$K_c = \partial(123) * (456),$$

where  $\partial$  denotes the boundary of a simplex and  $*$  the join operator between complexes. Thus  $|K''|$  appears as a union of three 4-balls touching each other along a great circle of their boundaries; the boundary of each ball being thought of as the join of the two circles of contact which it contains. If we let  $10, 11$  and  $12$  denote the barycenter of the simplices  $(789), (123)$  and  $(456)$  then we can interpret  $K_a, K_b$  and  $K_c$  as cones with vertices  $10, 11$  and  $12$  and bases

$$\partial K_a = \partial(456) * \partial(789)$$

$$\partial K_b = \partial(789) * \partial(123)$$

and  $\partial K_c = \partial(123) * \partial(456)$  .

Let us denote by  $K_{10}, K_{11}$  and  $K_{12}$  the subdivision of  $K_a, K_b$  and  $K_c$  so defined and by  $\bar{K}$  the complex  $K' \cup K_{10} \cup K_{11} \cup K_{12}$  which is a subdivision of  $K$ . Continuing the suggestion in § 1, we like to think of 10, 11 and 12 as respectively belong to the blue, the white and the red family. Accordingly  $K_a, K_b$  and  $K_c$  as well as their subdivisions  $K_{10}, K_{11}$  and  $K_{12}$  will be respectively thought of as a combinatorial decomposition of a blue, a white and a red 4-ball.

Define:

$$\alpha : 10 \mapsto 11, 11 \mapsto 12, 12 \mapsto 10$$

$$\beta, \gamma, \delta : 10 \mapsto 10, 11 \mapsto 11, 12 \mapsto 12$$

$$\epsilon : 10 \mapsto 10, 11 \mapsto 12, 12 \mapsto 11$$

so that now  $\alpha, \beta, \gamma, \delta, \epsilon$  and in particular the group  $G$  acts on  $\bar{K}$ .

In order to understand the topology of the entire space  $|K|$ , we construct a combinatorial map

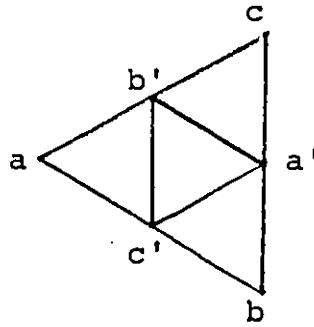
$$p: \bar{K} \longrightarrow \bar{\Delta}_2$$

where  $\bar{\Delta}_2$  is the subdivision of the 2-simplex  $abc$  using middles  $a', b'$  and  $c'$  of the sides and the central triangle

$$\Delta'_2 = a'b'c'$$

as shown on the following figure.

$$\Delta'_2 \subset \overline{\Delta}_2$$



Keep in mind that the vertices  $a$  and  $a'$ , sides  $bc$  and  $b'c'$  as well as the corner triangle  $(ac'b')$  must be thought of as being blue. Accordingly vertices  $b$  and  $c$ , vertices  $b'$  and  $c'$  as well as their opposite sides and the corresponding corner triangles must be respectively considered as being white and red. Check that the map between vertices shown in the following table does indeed extend to a  $G$ -invariant combinatorial map  $p: \overline{K} \rightarrow \overline{\Delta}_2$ , where  $G$  acts in an obvious manner on  $\overline{\Delta}_2$ .

	1	4	7	10	11	12
	2	5	8			
P:	3	6	9			
	↓	↓	↓	↓	↓	↓
	a'	b'	c'	a	b	c

Then

$$p^{-1}(ac'b') = K_{10},$$

$$p^{-1}(ba'c') = K_{11},$$

$$p^{-1}(cb'a') = K_{12},$$

$$p^{-1}(\Delta'_2) = K'.$$

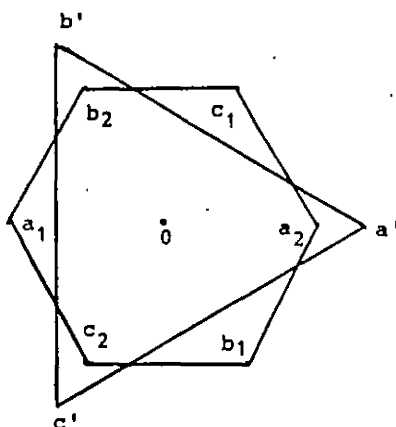
Let us think of  $\Delta'_2$  as an equilateral triangle in the euclidian plane  $\mathbb{E}^2$  with its barycenter at the origin. Furthermore let  $H$  be the regular hexagon with vertices  $a_1, c_2, b_1, a_2, c_1$  and  $b_2$  where

$$a_2 = -a_1 = 3a'/4 ,$$

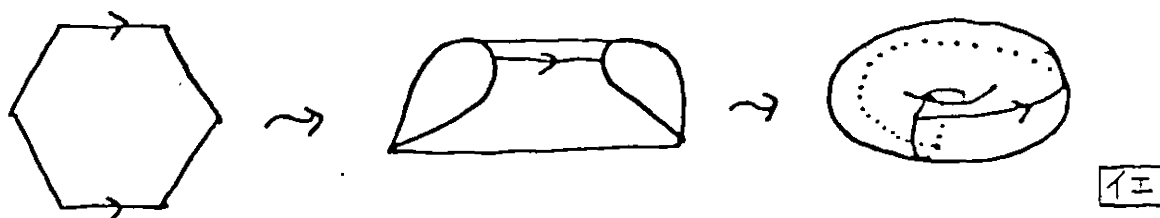
$$b_2 = -b_1 = 3b'/4 ,$$

$$c_2 = -c_1 = 3c'/4 ,$$

as shown in the picture.



Let  $\bar{H}$  be the torus obtained by identifying opposite sides of  $H$ .



It is the quotient of  $\mathbb{E}^2$  by the lattice  $L$  generated by  $a_1 + b_2$  and  $b_1 + c_2$ . Call  $\pi_f$  the canonical projection of  $\bar{H} = \mathbb{E}^2/L$  on  $\mathbb{E}^2/f(f\mathbb{R})^\perp + L \cong S^1$  where  $f = a', b', c'$  and  $\perp$  stands for the orthogonal complement.

Let  $U$  be the topological space obtained by factoring  $\Delta'_2 \times \bar{H}$  by the following equivalence relation:

$(d,e) \sim (d',e')$  whenever  $(d',e') = (d,e)$  or  $d = d' = f$  and  $\pi_f(e) = \pi_f(e')$  where  $f = a', b'$  or  $c'$ .

Claim: The geometric realization  $|K'|$  is homeomorphic to  $U$ .

Proof Let  $S$  be a  $2-2-1$  simplex in  $K$  and  $v$  its marked vertex (see § 1). We will say  $S$  is of class  $f$  if  $p(v) = f$ . The column decomposition of  $S$  shows the marked vertex  $v$  and two  $1$ -simplices of type  $2-0-0$  called  $S_1$  and  $S_2$ . Now  $S$  can be thought of as the triple join  $S_1 * S_2 * \{v\}$  and  $p:S \rightarrow \Delta'_2$  as the canonical projection of the triple join onto its base.

Let us define the standard realization of a  $2-2-1$  simplex of class  $f$  to be the following simplex  $S_f$  (where  $f = a', b', c'$ ) in  $\Delta'_2 \times \mathbb{R}^2$ , which canonically projects on  $\Delta'_2$  using the first projection:

$$S_{a'} = ((b', b_1), (b', b_2)) * ((c', c_1), (c', c_2)) * \{(a', 0)\},$$

$$S_{b'} = ((c', c_1), (c', c_2)) * ((a', a_1), (a', a_2)) * \{(b', 0)\},$$

$$S_{c'} = ((a', a_1), (a', a_2)) * ((b', b_1), (b', b_2)) * \{(c', 0)\}.$$

Notice that all  $2-1-1$  hyperfaces of the three standard realizations are linearly isometric by type preserving

isomorphisms.

For any simplex  $S$  of class  $f$ , there are four type-preserving identifications  $S \rightarrow S_f$  which also preserve projections to  $\overline{\Delta_2}$ . They can be deduced from each other by a linear isometry of  $S_f$ :

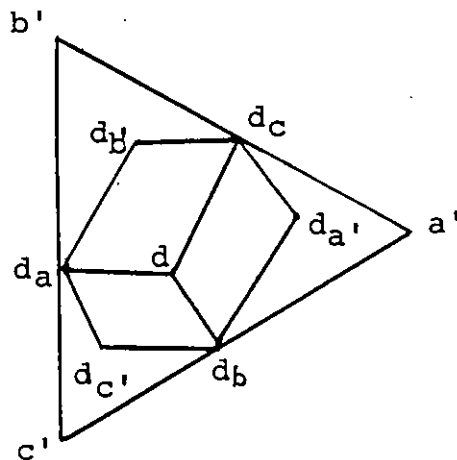
For all  $d \in \Delta_2'$ , let  $d_a, d_b$  and  $d_c$  be the projections of  $d$  onto the sides of  $\Delta_2'$ . Let

$$P_{a'} = d \ d_b \ d_a \ d_c,$$

$$P_{b'} = d \ d_c \ d_b \ d_a,$$

$$P_{c'} = d \ d_a \ d_c \ d_b.$$

be the three parallelograms shown on the following figure



Notice that  $P_f$  degenerates into a segment when  $d$  is on a side of  $\Delta_2'$  containing  $f$ , and into a point when  $d = f$ . Notice also that the inverse image of  $d$  in  $S_f$  ( $\subset \{d\} \times \mathbb{R}^2$ ) projects to the second factor  $\mathbb{R}^2$  as the parallelogram obtained by translating  $P_f$  so that it becomes centered at the origin.

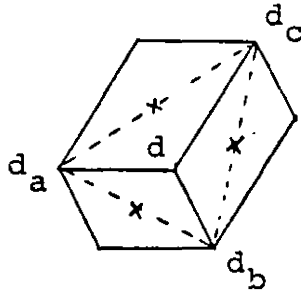
Now one can readily realize  $K'$  by identifying to  $S_f$  its simplices of class  $f$  (using any type-preserving identification) and by gluing along  $2-1-1$  hypersurfaces the copies of the  $S_f$ 's thus obtained by linear isometries (commuting with projections to  $\overline{\Delta_2}$  according to the pattern shown in Figure 1-1.

Now for all  $d \in \Delta'_2$ ,  $p^{-1}(d)$  appears to be a patchwork made of the 27 parallelograms (some of which may be degenerate) corresponding to the intersections of  $p^{-1}(d)$  with the 27  $2-2-1$  simplices of  $K$ . For instance the inverse image of the origin is the torus obtained by identifying the opposite sides of the hexagon shown in Figure 3-1 where the parallelograms are now rombi. Notice that this hexagon is homothetic to  $H$  and can therefore be canonically identified with it. When  $d$  moves away from the center, the hexagonal pattern gets continuously distorted assuming for instance the following dispositions. But after the suitable identifications are done, the patchwork remains topologically a torus. The universal cover of the patchedwork torus  $p^{-1}(d)$  is obtained by letting the lattice

$$\mathbb{Z}(d_c - d_a) + \mathbb{Z}(d_b - d_a)$$

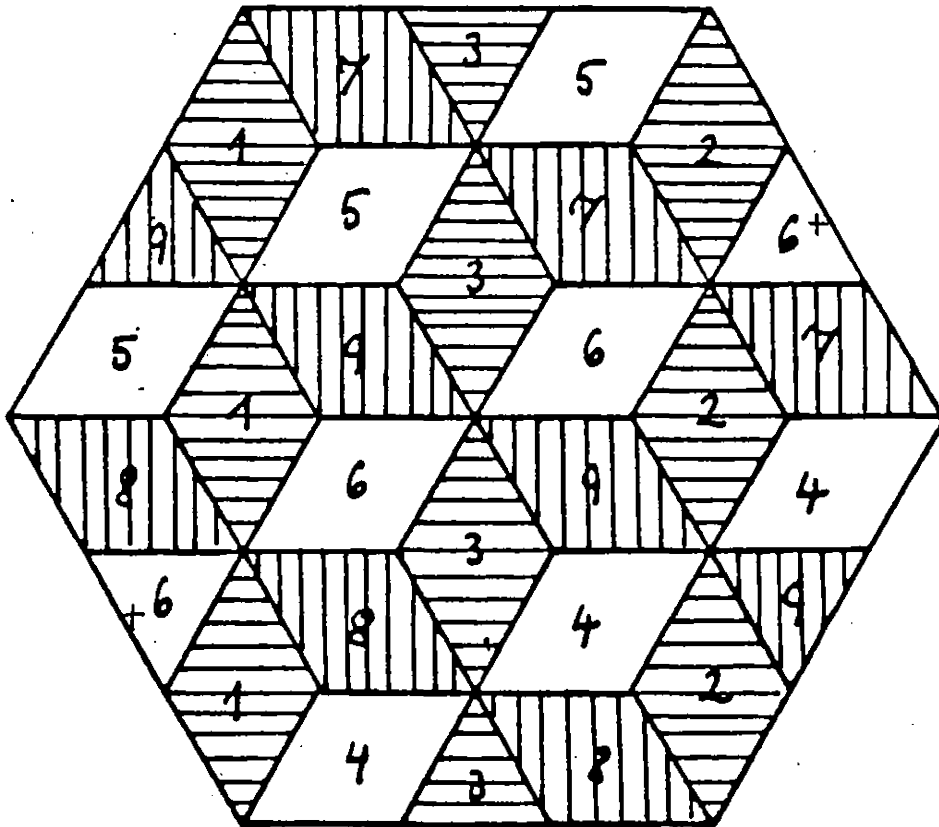
act on the union of the three parallelograms  $P_a$ ,  $P_b$ , and  $P_c$ . One can also use the triangular fundamental domain obtained by considering the union of the three half parallelograms cut along the long diagonals as shown below and tessellating under the action of the group

generated by rotations of  $\pi$  centered at the midpoints of the sides of the triangle.



When  $d$  arrives to the interior of one of the sides of  $\Delta'_2$  18 out of the 27 parallelograms degenerates into segments but  $p^{-1}(d)$  still remains a topological torus (Figure 3-2). When  $d$  finally reaches a vertex  $f$  then 9 of the parallelograms become points while the 18 others are segments. So that the torus degenerates to a circle according to projection  $\pi_f$  (Figure 3-3). This completes the proof of the claim.



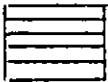




Strasbourg 14-07-81

Figure 3-1

イエ

In this picture each rhombus shows the marked vertex of the 2-2-1 simplex it represents. In order to list all the vertices of the represented simplex, consider its marked vertex as well as those of the four adjacent rhombi. For example, the union of the two halves of the hexagon marked with a cross is the intersection with the torus of the simplex (1 2 6 7 8). The picture also shows the blue white red coloring of each of the 2-2-1 represented simplexes using the Heraldic convention

for colors, namely  for blue,  for white and  for red.

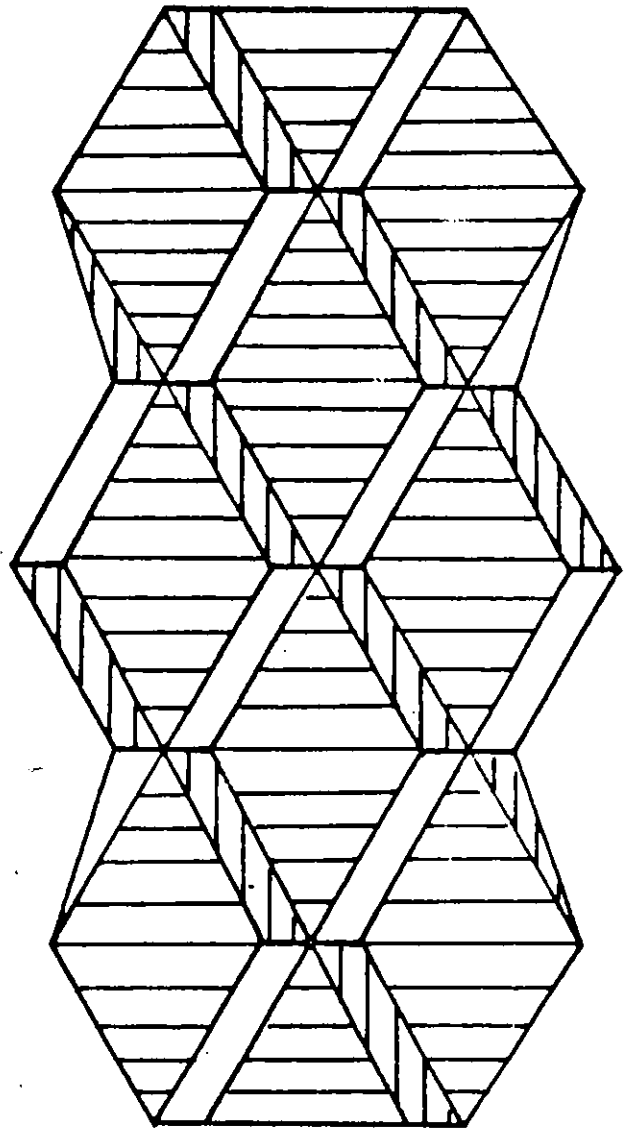
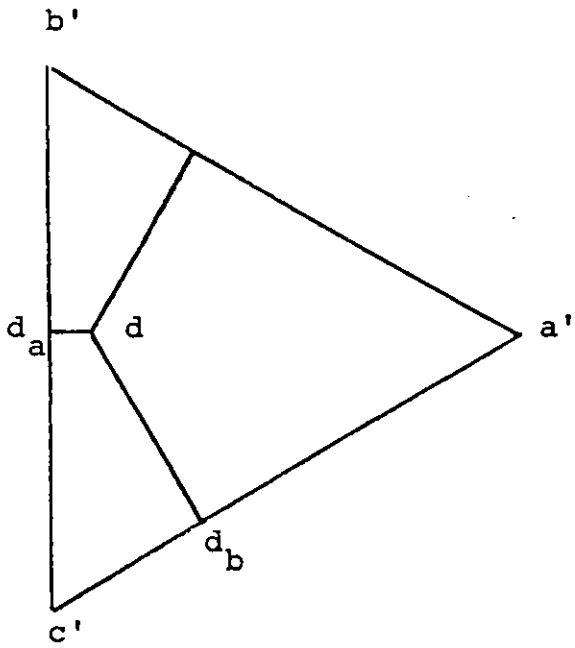


Figure 3-2

12

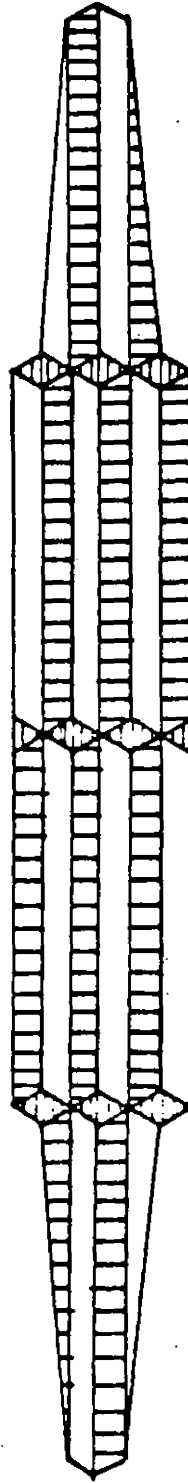
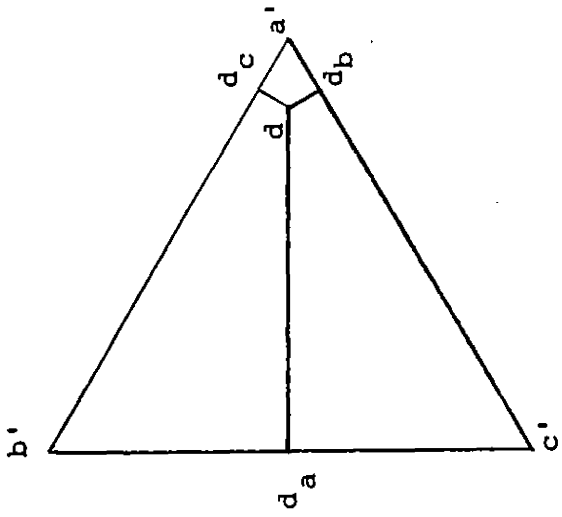


Figure 3-3

イ

§ 4 The direct proof that  $|K| \cong \mathbb{C}P^2$  [Jä]

In this section, we introduce a map  $\pi: \mathbb{C}P^2 \rightarrow \Delta_2$  and show that the decomposition of  $\mathbb{C}P^2$  induced by the inverse image under  $\pi$  of the subdivision  $\overline{\Delta_2}$  is isomorphic to the decomposition

$$|K| = |K_a| \cup |K_b| \cup |K_c| \cup |K'|.$$

This shows that  $|K| \cong \mathbb{C}P^2$ .

Let us now think of  $\Delta_2$  as being the standard 2-simplex in  $\mathbb{R}^3$  with coordinates  $t_0, t_1, t_2$ , so that the points previously introduced now become

$$\begin{aligned} a &= e_0 = (1, 0, 0), & b &= e_1 = (0, 1, 0), & c &= e_2 = (0, 0, 1) \\ a' &= (0, 1/2, 1/2), & b' &= (1/2, 0, 1/2), & c' &= (1/2, 1/2, 0). \end{aligned}$$

Let us identify the standard 5-sphere  $S^5$  in  $\mathbb{C}^3$  (with coordinates  $y_0, y_1, y_2$ ) to the join  $S^1 * S^1 * S^1$  which embeds into  $\mathbb{C}^3$  as the set of points of the form

$$y = (\sqrt{t_0} \exp 2\pi i s_0/t_0, \sqrt{t_1} \exp 2\pi i s_1/t_1, \sqrt{t_2} \exp 2\pi i s_2/t_2)$$

where  $t = (t_0, t_1, t_2) \in \Delta_2$  and  $s = (s_0, s_1, s_2) \in \mathbb{R}^3$ . Notice that the formula makes sense even if some  $t_j$ 's equal zero. The canonical mapping  $S^1 * S^1 * S^1 \rightarrow \Delta_2$  induces on  $S^5$  the map

$$(y_0, y_1, y_2) \mapsto (|y_0|^2, |y_1|^2, |y_2|^2).$$

On  $S^1 * S^1 * S^1$  the Hopf action of  $S^1$  onto  $S^5$  induces the diagonal action of the join defined by  $(\theta, y)$  goes to  $(\sqrt{t_0} \exp i(\theta + 2\pi s_0/t_0), \sqrt{t_1} \exp i(\theta + 2\pi s_1/t_1), \sqrt{t_2} \exp i(\theta + 2\pi s_2/t_2))$ , where  $\theta \in \mathbb{R}$  and  $y$  is as above. Now the quotient  $\mathbb{C}P^2$  of  $S^5$  under the Hopf action identifies to the quotient of  $S^1 * S^1 * S^1$  under the diagonal action. Let  $\pi: \mathbb{C}P^2 \rightarrow \Delta_2$  be the quotient under diagonal action of the canonical mapping of the join so that we now have the commutative diagram:

$$\begin{array}{ccc}
 S^5 = S^1 * S^1 * S^1 & \xrightarrow{\quad} & \mathbb{C}P^2 \\
 & \searrow & \swarrow \pi \\
 & \Delta_2 &
 \end{array}$$

Notice that  $S^1 * S^1 * S^1$  is the quotient of  $\Delta_2 \times \mathbb{R}^3$  under the equivalence relation defined by  $(t, s) \sim (t', s')$  if

$$t = t' \quad \text{and} \quad s - s' \in L_t := t_0\mathbb{Z} \times t_1\mathbb{Z} \times t_2\mathbb{Z}$$

where it is assumed that  $0\mathbb{Z} = \mathbb{R}$ . Therefore  $\mathbb{C}P^2$  appears to be the quotient of  $\Delta_2 \times \mathbb{R}^3$  under the equivalence relation defined by  $(t, s) \sim (t', s')$  if

$$t = t' \quad \text{and} \quad s - s' \in L_t + D_t$$

where  $D_t$  is the line in  $\mathbb{R}^3$  generated by  $t = (t_0, t_1, t_2) \in \Delta_2$ .

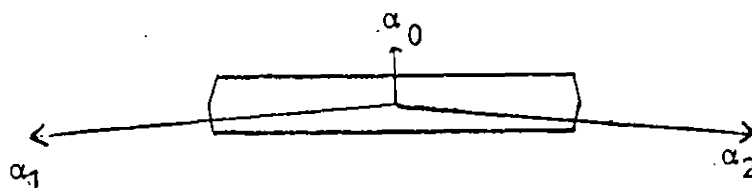
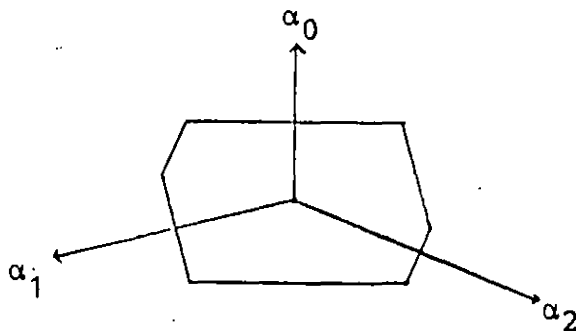
In order to study  $\pi^{-1}(t)$  for  $t \in \Delta_2$ , it suffices to look at the image of  $L_t$  in the quotient of the euclidean

space  $\mathbb{R}^3$  by the greatest vector space  $V_t$  contained in the subgroup  $L_t + D_t$ .

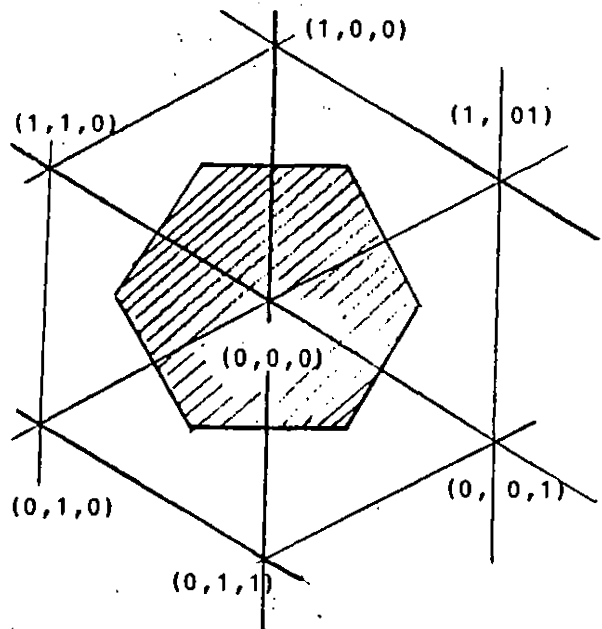
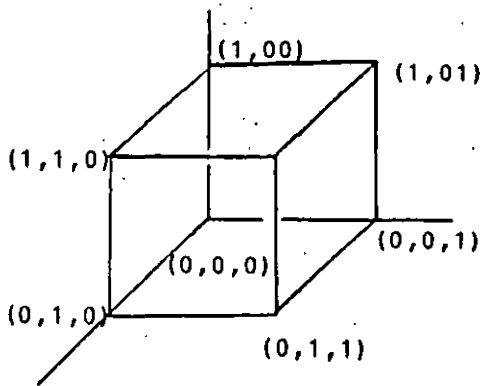
Notice that

$$V_t = \begin{cases} D_t & t \in \text{the interior of } \Delta_2, \\ D_t + \mathbb{R}e_i & t \in \text{the interior of the side} \\ & \text{opposite to } e_i, \\ \mathbb{R}^3 & t \in \text{the vertices of } \Delta_2. \end{cases}$$

For each  $t$  in the interior of  $\Delta_2$ , the Dirichlet domain of the image of  $L_t$  is given by the following figure, where  $\alpha_0, \alpha_1$  and  $\alpha_3$  are the images of  $(t_0, 0, 0), (0, t_1, 0), (0, 0, t_2)$ .  $\alpha_0, \alpha_1$  and  $\alpha_2$  generate the image lattice, one has  $\alpha_0 + \alpha_1 + \alpha_2 = 0$  and all angles  $\alpha_j \cap \alpha_k$  ( $j \neq k$ ) are in the interval  $] \pi/2, \pi[$ . When  $t$  approaches some interior point of the side opposite to the vertex  $e_i$ , the angle  $\alpha_j \cap \alpha_k$  ( $i \neq j \neq k \neq i$ ) tends to  $\pi$  and  $\alpha_i$  tends to 0.



In the limit,  $\alpha_j$  and  $\alpha_k$  are on the same line but the dimension of  $V_t$  has increased and one has to project everything orthogonally onto the line  $\alpha_j\alpha_k$ . Now  $\mathbb{R}^3/V_t$  is isomorphic to  $\mathbb{R}$  in which the image of  $L_t$  has to be a discrete additive subgroup tending to  $\mathbb{R}$  itself when  $t$  remains on the side and tends to a vertex. Notice that when  $t$  is at the center of  $\Delta_2$ , the Dirichlet fundamental domain of  $\pi^{-1}(t)$  is regular hexagon, that  $L_t$  is the cubical lattice and that  $D_t$  is the diagonal of  $\mathbb{R}^3$ .



The previous remarks can be summarized as follows:  
 $\pi^{-1}(t)$  is a torus which degenerates into a circle when  $t$  tends to a side and to a point when  $t$  tends to a vertex.



There are three ways (analogous to those studied in § 3) in which the torus can degenerate to the circle, according to which side  $t$  approaches. It therefore should now be obvious that

$$\pi^{-1}((ab'c') \cup (ca'b') \cup (bc'a'))$$

is the union of three smooth 4-balls touching each other in  $\mathbb{C}P^2$  along linked circles as explained in § 3 while  $\pi^{-1}(a'b'c')$  appears to be homeomorphic to  $U$  (c.f. Claim in § 3). By the Alexander trick,  $\mathbb{C}P^2$  is therefore homeomorphic to  $|K|$ .

In order to make this clearer, we specify an explicit triangulation of  $\mathbb{C}P^2$ , isomorphic to  $\bar{K}$ . The idea stems from the suggestion by A. Marin simplified and modified in order to resemble the construction in § 3, which in some sense it dualises.

The explicit triangulation of  $\mathbb{C}P^2$  by  $\bar{K}$ . Let

$$\begin{array}{lll} v_1 = [0, 1, \omega] & v_4 = [\omega, 0, 1] & v_7 = [1, \omega, 0] \\ v_2 = [0, 1, \omega^2] & v_5 = [\omega^2, 0, 1] & v_8 = [1, \omega^2, 0] \\ v_3 = [0, 1, 1] & v_6 = [1, 0, 1] & v_9 = [1, 1, 0] \\ v_{10} = [1, 0, 0] & v_{11} = [0, 1, 0] & v_{12} = [0, 0, 1] \end{array}$$

be the images in  $\mathbb{C}P^2$  of the vertices  $1, \dots, 12$  in  $\bar{K}$ , where  $\omega = \exp 2\pi i/3$ . Let  $\tilde{\chi}: \Delta_2 \times Q \rightarrow \mathbb{C}P^2$  be defined by setting

$$\tilde{\chi}(t, \psi) = [\sqrt{t_0} e^{2\pi i \psi_0}, \sqrt{t_1} e^{2\pi i \psi_1}, \sqrt{t_2} e^{2\pi i \psi_2}]$$

where  $t = (t_0, t_1, t_2) \in \Delta_2$ ,  $\psi = (\psi_0, \psi_1, \psi_2) \in Q$  and

$$Q = \{(\psi_0, \psi_1, \psi_2) \in \mathbb{R}^3 \mid \psi_0 + \psi_1 + \psi_2 = 0\}.$$

The map  $\tilde{\chi}$  is onto and factors through  $\Delta_2 \times Q/L_0$  where  $L_0$  is the orthogonal projection of  $\mathbb{R}^3$  to  $Q$ . Call  $\chi$  the quotient map

$$\Delta_2 \times Q/L_0 \longrightarrow \mathbb{C}P^2.$$

Restricted to  $\overset{\circ}{\Delta}_2 \times Q/L_0$ ,  $\chi$  is a homeomorphism onto the complement of the three complex lines

$$y_0 = 0, y_1 = 0, y_2 = 0$$

where  $[y_0, y_1, y_2]$  denotes the system of homogeneous coordinates in  $\mathbb{C}P^2$ .

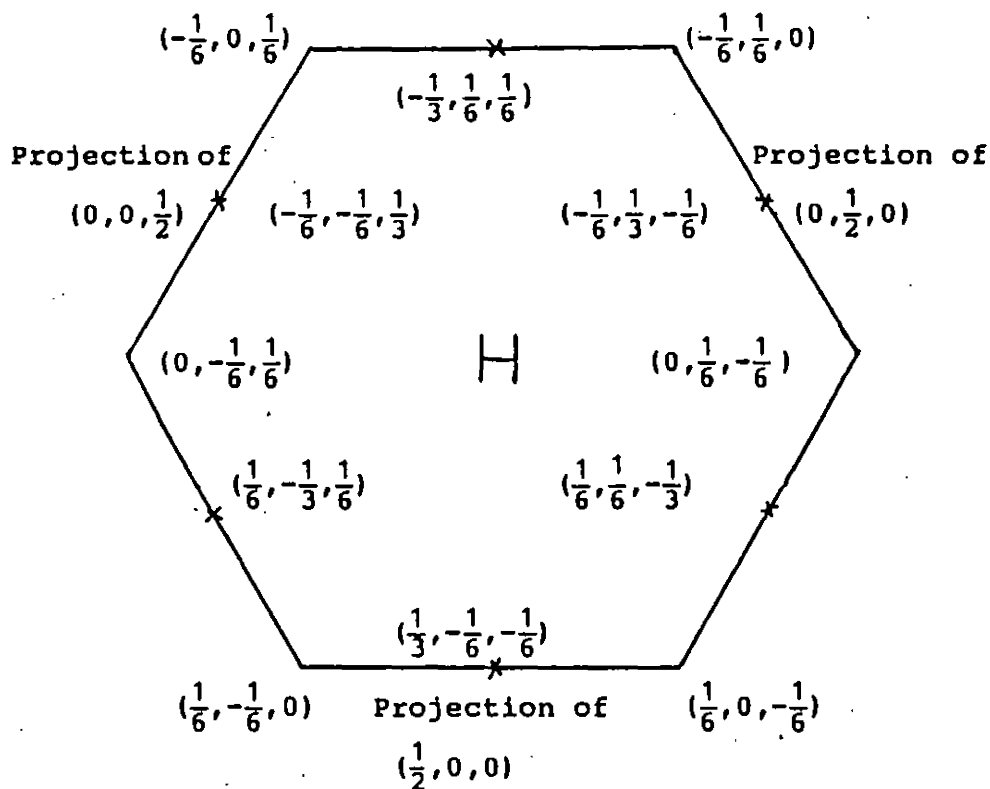
In order to describe the triangulation of  $\mathbb{C}P^2$  in terms of  $(t, \psi)$ -coordinates, we need to compute the projections  $\text{Pr}_2$  onto the second factor of

$$\chi^{-1}(v_i) \subset \Delta_2 \times Q/L_0 \quad (i = 1, \dots, 9).$$

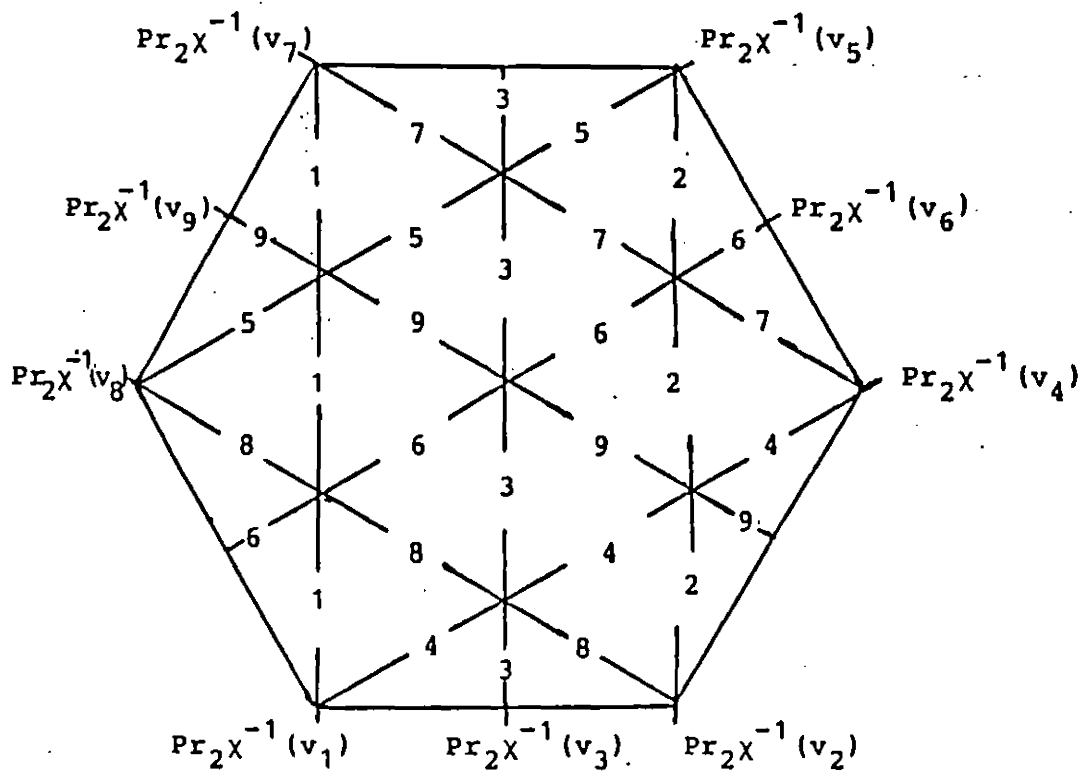
These are circles on the torus  $Q/L_0$ .

Let us now think of the hexagon  $H$  as being the Dirichlet domain of  $Q$  at the origin under the action of  $L_0$ .

Using the translations  $e_0, e_1$  and  $e_2$ , one can color all the medians and small diagonals in such a way as to obtain the following diagrams.



The following figure represents the circles  $\text{Pr}_2\chi^{-1}(v_i)$  ( $i = 1, \dots, 9$ ) viewed in  $H$ .



This picture illustrates the fact that these 9 circles decompose  $Q/L_0$  into 18 triangles. Let us denote by  $\Delta(ijk)$  the triangle with sides labelled  $i, j$  and  $k$  ( $1 \leq i, j, k \leq 9$ ), and assume that vertices opposite to sides have been given the order  $ijk$ . Let  $C: \Delta_2 \rightarrow \Delta_2$  be the Cremona transformation of the standard 2-simplex in  $\mathbb{R}^3$  defined by

$$C(t_0, t_1, t_2) = (t_1 t_2, t_2 t_0, t_0 t_1) / t_1 t_2 + t_2 t_0 + t_0 t_1 .$$

This is a one-to-one involution on  $\overset{\circ}{\Delta}_2$ , which shrinks each side to the opposite vertex and blows up each vertex to the opposite side. An ordering of the vertices of two triangles  $T_1$  and  $T_2$  defines, in an obvious and unique manner, reciprocal Cremona transformations  $T_1 \rightarrow T_2$  and  $T_2 \rightarrow T_1$ . Let  $C_{692}$  be the Cremona transformation

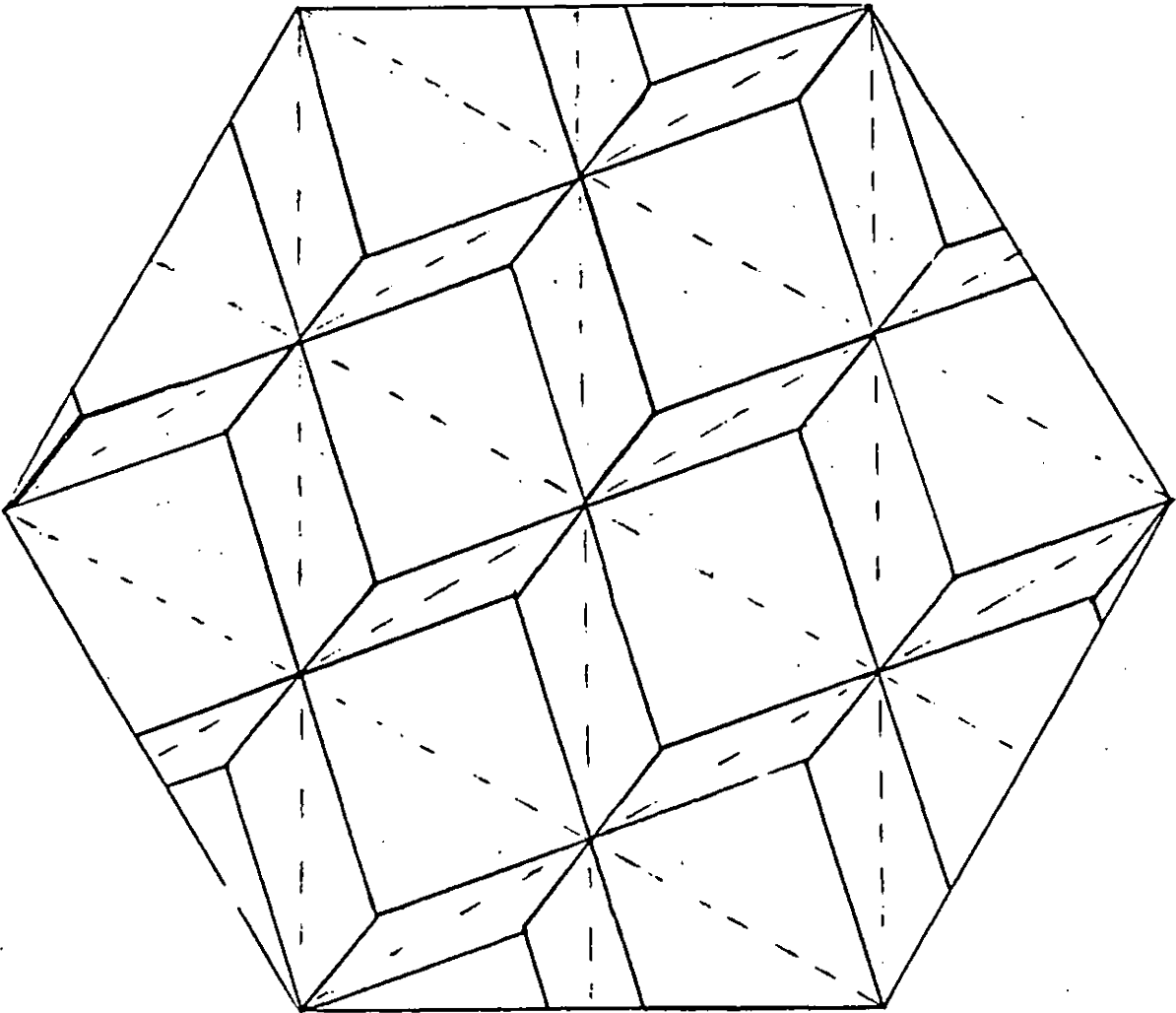
$$(a'b'c') \rightarrow \Delta(692)$$

and define the 17 other  $C_{ikj}$ 's by composing  $C_{692}$  with rotations of angle  $\pi$  centered at the middle of the sides with  $\Delta(692)$ , thus defining

$$C_{673}, C_{934}, C_{247}$$

and so on using the newly introduced sides. For all  $t \in (a'b'c')$  consider the decomposition of  $Q/L_0$  into

27 parallelograms obtained by joining each  $C_{ijk}(t) = P_{ijk}$  to the vertices of  $\Delta(ijk)$  and then erasing the sides of  $\Delta(ijk)$ .



As in § 3 we thus obtain a decomposition of the torus depending on  $t$  but this time the shape of the torus is fixed, while the angles of the parallelograms vary. Notice that some of the parallelograms degenerate when the  $p_{ijk}$ 's are on the boundaries of  $\Delta(ijk)$ 's, namely when  $t$  is on the boundary of  $(a'b'c')$ . Notice also that when  $t$  is at a vertex, the  $p_{ijk}$ 's live on the corresponding sides with no definite location but remember that when such is the case,  $\chi$  precisely quotients  $Q/L_0$  along circles parallel to these sides. From this fact one immediately sees that the previous construction defines an explicit homeomorphism from  $|K'|$  (realized as in § 3) to  $\pi^{-1}(a'b'c')$  sending the parallelograms of § 3 to the present one. In order to define the homeomorphism over all of  $|\bar{K}|$ , notice that each of the three 3-spheres bounding  $\pi^{-1}(a'b'c')$  is decomposed into 9 3-simplices; extend radially the three considered decompositions in  $\mathbb{CP}^2$  using  $v_{10}, v_{11}$  and  $v_{12}$  as origins. This operation is completely well defined since for instance  $\pi^{-1}(ab'c')$  is the standard unit 4-ball in the 2-dimensional complex plane  $\mathbb{CP}^2 - \pi^{-1}(bc)$  with coordinates  $(z_1/z_0, z_1/z_0)$ .

No doubt the severe reader will decide that the triangulation presented in this section is self-sufficient and that the construction of § 3 is needless. This is indeed true, but we like § 3 since we got it long ago, while § 4 became clear to us very recently. On the other hand as we

pointed out in the introduction, it is useful to show many approaches to the same phenomenon in order to get a good intuitive grasp of it. That is why we hoped most readers would also enjoy reading § 3.



## Chapter II The Kühnel complex viewed as an orbifold

§ 5 The  $G$ -invariant torus  $T$  in  $K$ 

The existence of the combinatorial torus  $T \subset K$  presented in this section is the basic fact that enables one to connect Kühnel's triangulation with crystallography.

Figure 5-1 represents the union  $T$  of the  $G$ -orbits of (269) (positive orbit) and (169) (negative orbit) where opposite sides should be identified and the erased.

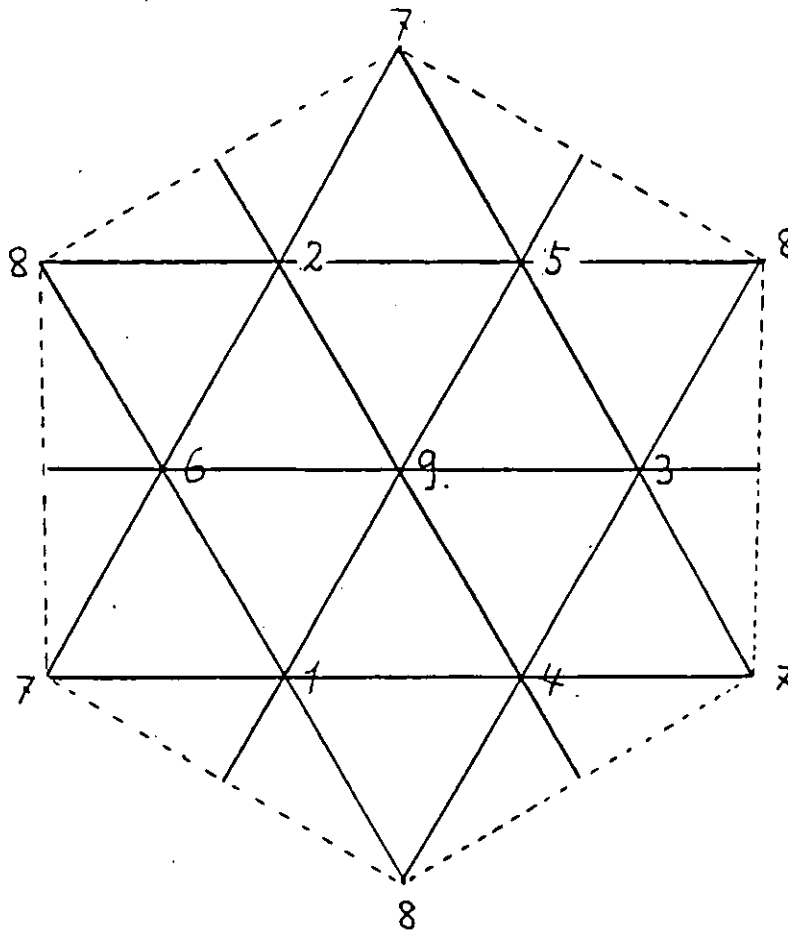


Figure 5-1

The topological space  $|T|$  is homeomorphic to a torus. Considered as a sub-torus of  $\mathbb{C}P^2$ , it is the set of  $\chi(t, C_{ijk}(t))$  of § 4 for all possible  $ijk$ 's as  $t$  varies in  $(a'b'c')$ . The complex  $T$  contains all those simplices of type  $1-1-1$  whose link is a triangle.

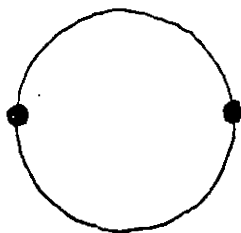
Notice that the links of the remaining simplices of type  $1-1-1$  (all belonging to the  $G$ -orbit of (147)) are hexagons, and that those simplices are in one-to-one correspondence with the hexagons in Figure 1-1. Notice also that the intersection of  $T$  with the link  $M$  of vertex 9 is the combinatorial trefoil knot:

$$14 U 43 U 35 U 52 U 26 U 61$$

shown in Figure 2-1. Therefore  $T$  has 9 combinatorial cusps.

In § 9, it will be shown that  $T$  is the combinatorial model for the embedding in  $\mathbb{C}P^2$  of a complex curve of genus 1 with 9 cusps (the dual of a non-singular cubic). In § 8 Remark 2, we will show the existence of a 6 fold cover of  $|K|$  branched over  $T$ , which is isomorphic to the 4-torus, and on which  $K$  induces an improper triangulation:

This means a decomposition into simplices which is not a triangulation because each simplex is not uniquely determined by its vertices, such as the case of the decomposition of the circle  $S^1$  by two intervals.



Suitably identified with  $\mathbb{C}^2$  the universal cover of this improperly triangulated 4-torus will appear to be the rectilinear triangulation  $\tilde{K}$  of  $\mathbb{C}^2$  defined in § 8, which is invariant under the action of the complex crystallographic group  $\Gamma''$  defined in § 7. In  $\tilde{K}$  the inverse image of  $T$  will turn out to be the union  $A$  of a family of complex lines each of which maps onto  $|T|$  as its universal cover (see § 8 Remark 1). Links of all simplices of type 1-1-1 in  $\tilde{K}$  will be hexagons. Associated with a crystallographic subgroup  $\Gamma$  of  $\Gamma''$ , there exists a map  $\gamma: \mathbb{C}^2 \rightarrow \mathbb{C}P^2$  branched along  $A$ , which will produce a new explicit homeomorphism between  $|K| = |\tilde{K}/\Gamma|$  and  $\mathbb{C}P^2$  (cf. § 9). In order to visualize the triangulation  $\tilde{K}$ , we construct in the next section a combinatorial 6 fold cover  $\tilde{M}$  of  $M$  branched along the trefoil knot  $T \cap M$ . The complex  $\tilde{M}$  will then be realized as the boundary of a 4 dimensional polytope  $N$  in  $\mathbb{C}^2$  namely as the link of the origin in the triangulation  $\tilde{K}$ . Since  $\Gamma''$  is transitive on vertices of  $\tilde{K}$ , all links of vertices in  $\tilde{K}$  are isomorphic to  $\tilde{M}$ . The realization  $\partial N$

is not strict in the sense that the star  $N$  (at the origin in  $\tilde{K}$ ) is not convex and some of its faces are unions of more than one 3-simplex of  $\tilde{M}$  (i.e. it has inward and also flat dihedral angles). The detailed study of the convex hull of  $\tilde{M}$  (i.e. of  $N$ ) is the bulk of the proof of the claim 1 of § 8.

Observe that it would not be difficult to deform the polytope  $N$  so that its boundary becomes a strict realization of  $\tilde{M}$ , in other words, so that it becomes a convex polytope whose hypersurfaces are 3-simplices decomposing its boundary accordingly to the pattern  $\tilde{M}$ . Recall that contrary to  $\tilde{M}$ , the Grünbaum-Brückner triangulation  $M$  is the only triangulation of  $S^3$  with 8 vertices which refuses to be strictly realized in  $\mathbb{R}^4$  (in the previous sense), essentially because it contains the combinatorial trefoil knot  $T \cap M$ , which is the union of 6 edges. Indeed we have

Proposition In the boundary of a 4 dimensional polytope, any PL closed curve with not more than 6 edges either is unknotted or is a trefoil knot with 6 edges contained in one hyperface of the polytope.

§ 6 The six fold cover  $\tilde{M}$  of  $M$ 

A 6 fold cover  $\tilde{M}$  (with 120 3-simplices and 30 vertices) of  $M$  branched along the trefoil knot  $M \cap T$  can be described as the union of 6 copies of a triangulation (with 20 simplices and 11 vertices) of the prism  $\Delta_2 \times \Delta_1$ . Three of these copies are glued to each other along their triangular faces in order to produce a solid torus with 9 square faces. The complement in  $S^3$  of such a solid torus is again a solid torus with 9 square faces. It is in turn obtained by gluing similarly the 3 remaining copies. Figure 6-1 shows a prism of one of the tori surrounded by the 3 prisms of the other torus.

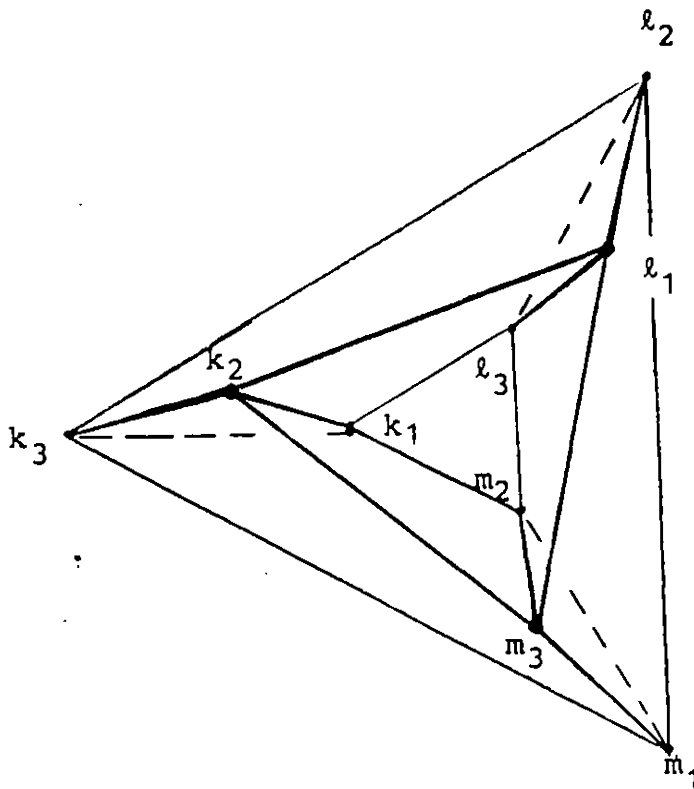


Figure 6-1

The inverse image of  $M \cap T$  in  $\tilde{M}$  is the union of three linked circles contained in the common boundary of the two solid tori. Each of these circles is the union of diagonals of three of the nine square faces and maps bijectively onto  $M \cap T$ . We first construct the triangulation  $\tilde{M}$ , that we realize in  $\mathbb{C}^2$ , and next show that the obvious projection  $\tilde{M} \rightarrow M$  is indeed the required branched covering.

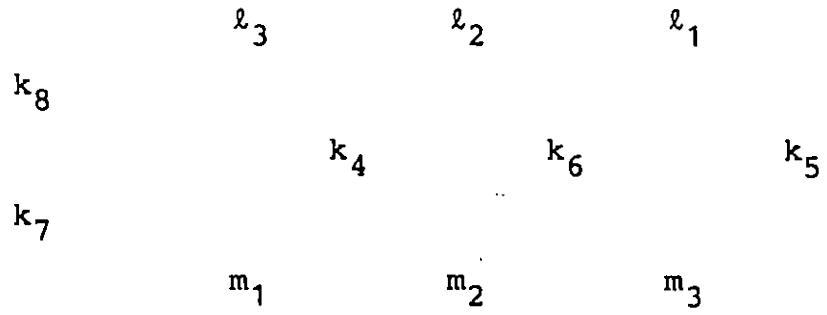
Construction of  $\tilde{M}$  We now proceed to describe the triangulation of the first prism  $M' \cong \Delta_2 \times [0,1]$  where we call  $m_1, m_2$  and  $m_3$  the vertices of the triangle  $\Delta_2 \times \{0\}$ ;  $l_2, l_3$  and  $l_1$  the vertices of the triangle  $\Delta_2 \times \{1\}$ ; where  $k_6, k_5$  and  $k_4$  are the centers of the rectangular faces

$$(m_2, m_3, l_1, l_3), (m_3, m_1, l_2, l_1), (m_1, m_2, l_3, l_2)$$

and where

$$k_7 = (b, \frac{1}{4}), \quad k_8 = (b, \frac{3}{4})$$

(in which  $b$  stands for the barycenter of  $\Delta_2$ ) so that  $k_7$  and  $k_8$  lie on the axis of symmetry of the prism. Now  $M'$  is the complex with vertices



generated by the following twenty 3-simplices.

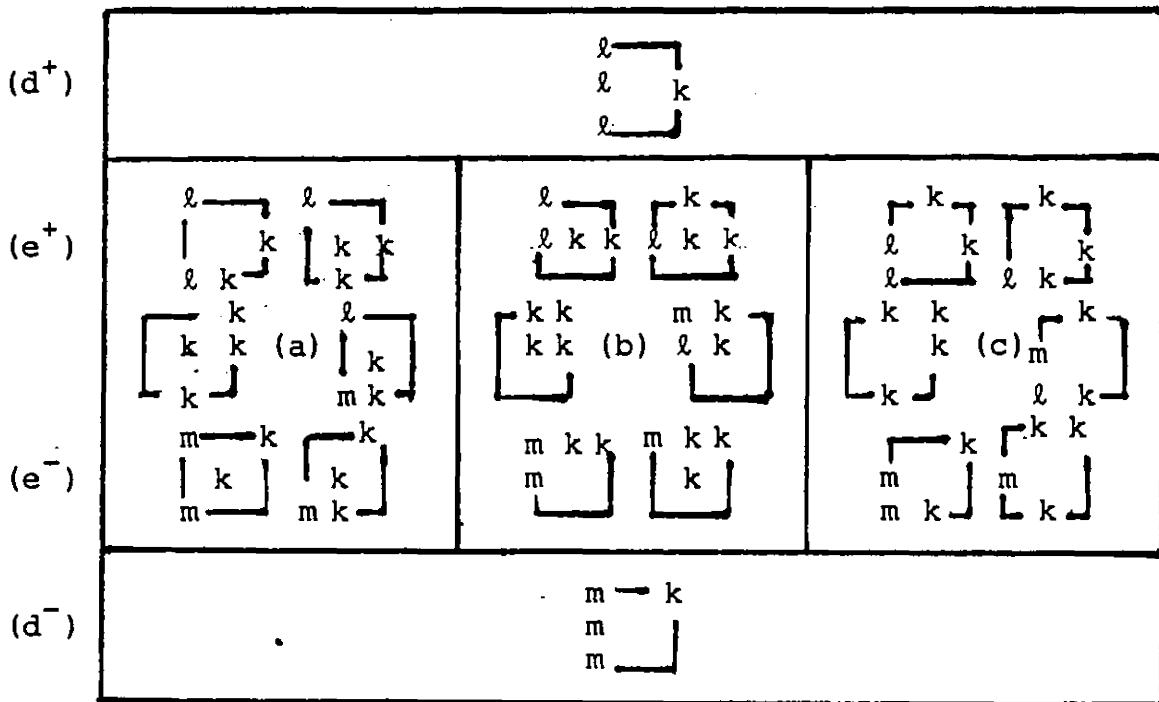


Figure 6-2

In this figure we introduce for the first time the colored Baille notation which should be understood as follows; every letter appearing in a given Braille cell is assumed to carry the color of the place it occupies in the cell. For instance,

$$\begin{array}{|c|} \hline \ell \\ \hline | \quad k \\ \hline m \quad k \\ \hline \end{array}$$

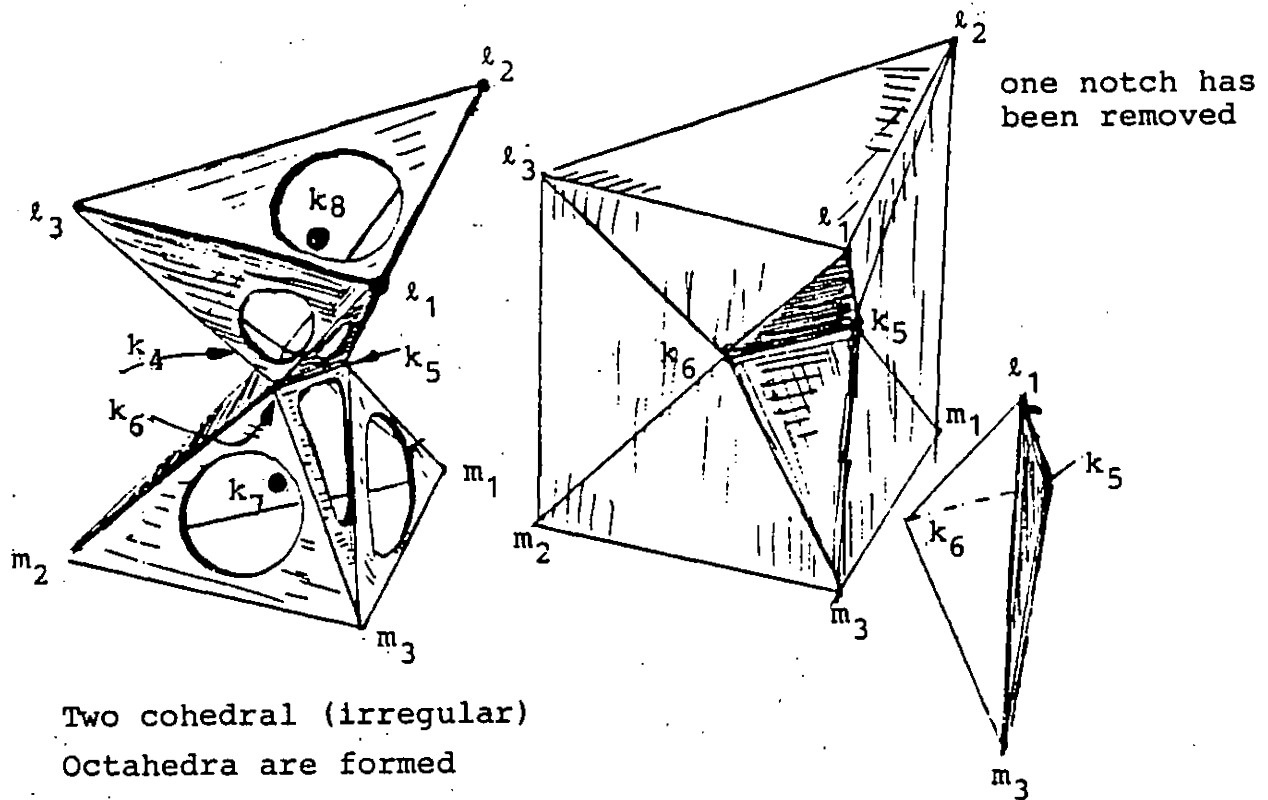
means  $(\ell_1, m_3, k_5, k_6)$ .

The three simplices appearing on the right of boxes (a), (b) and (c) are called notches, while the union of the three simplices appearing on the left of the same boxes is called the central core of  $M'$ . This central core can also be traingulated as the union of two 3-simplices

$$\begin{array}{|c|} \hline k \quad k \\ \hline k \\ \hline k \\ \hline \end{array} \quad \text{and} \quad \begin{array}{|c|} \hline k \\ \hline k \quad k \\ \hline k \\ \hline \end{array} .$$



G. Francis



Two cohedral (irregular) Octahedra are formed by removing 3 notches from a triangular prism. [in the model, windows reveal an illuminated interior with a ball vertex at the center of each octahedron. ]

Figure 6-3

Now  $M'$  minus the union of its three notches, with the central core re-triangulated as explained, can be considered as the union of the two octahedra

$$\begin{array}{l} m \ k \\ m \ k \\ m \ k \end{array} \left. \vphantom{\begin{array}{l} m \ k \\ m \ k \\ m \ k \end{array}} \right] \quad \text{and} \quad \begin{array}{l} l \ k \\ l \ k \\ l \ k \end{array} \left. \vphantom{\begin{array}{l} l \ k \\ l \ k \\ l \ k \end{array}} \right]$$

triangulated as cones on their boundaries with barycenters  $k_7$  and  $k_8$  respectively. Thus if one now restores the original triangulation of the central core one gets a very good understanding of the way  $M'$ -{notches} is constructed.

In order to build the 5 other prisms, it suffices to list their vertices according to a chosen order for those of  $M'$ . The following table does this for you.

$m_1, m_2, m_3$	;	$k_7$	;	$k_6, k_5, k_4$	;	$k_8$	;	$l_2, l_3, l_1$
$l_1, l_2, l_3$	;	$m_7$	;	$m_6, m_5, m_4$	;	$m_8$	;	$k_2, k_3, k_1$
$k_1, k_2, k_3$	;	$l_7$	;	$l_6, l_5, l_4$	;	$l_8$	;	$m_2, m_3, m_1$
$k_1, m_2, l_3$	;	$k_{-7}$	;	$k_6, m_5, l_4$	;	$k_{-8}$	;	$k_2, m_3, l_1$
$l_1, k_2, m_3$	;	$m_{-7}$	;	$l_6, k_5, m_4$	;	$m_{-8}$	;	$l_2, k_3, m_1$
$m_1, l_2, k_3$	;	$l_{-7}$	;	$m_6, l_5, k_4$	;	$l_{-8}$	;	$m_2, l_3, k_1$

Figure 6-4

The logic of the previous table is represented by the following pattern showing the vertices on the common boundary of the two solid tori as well as the vertices of the core of each torus, and thus displaying all vertices of  $\tilde{M}$ . Please identify opposite sides of the square to obtain a torus.

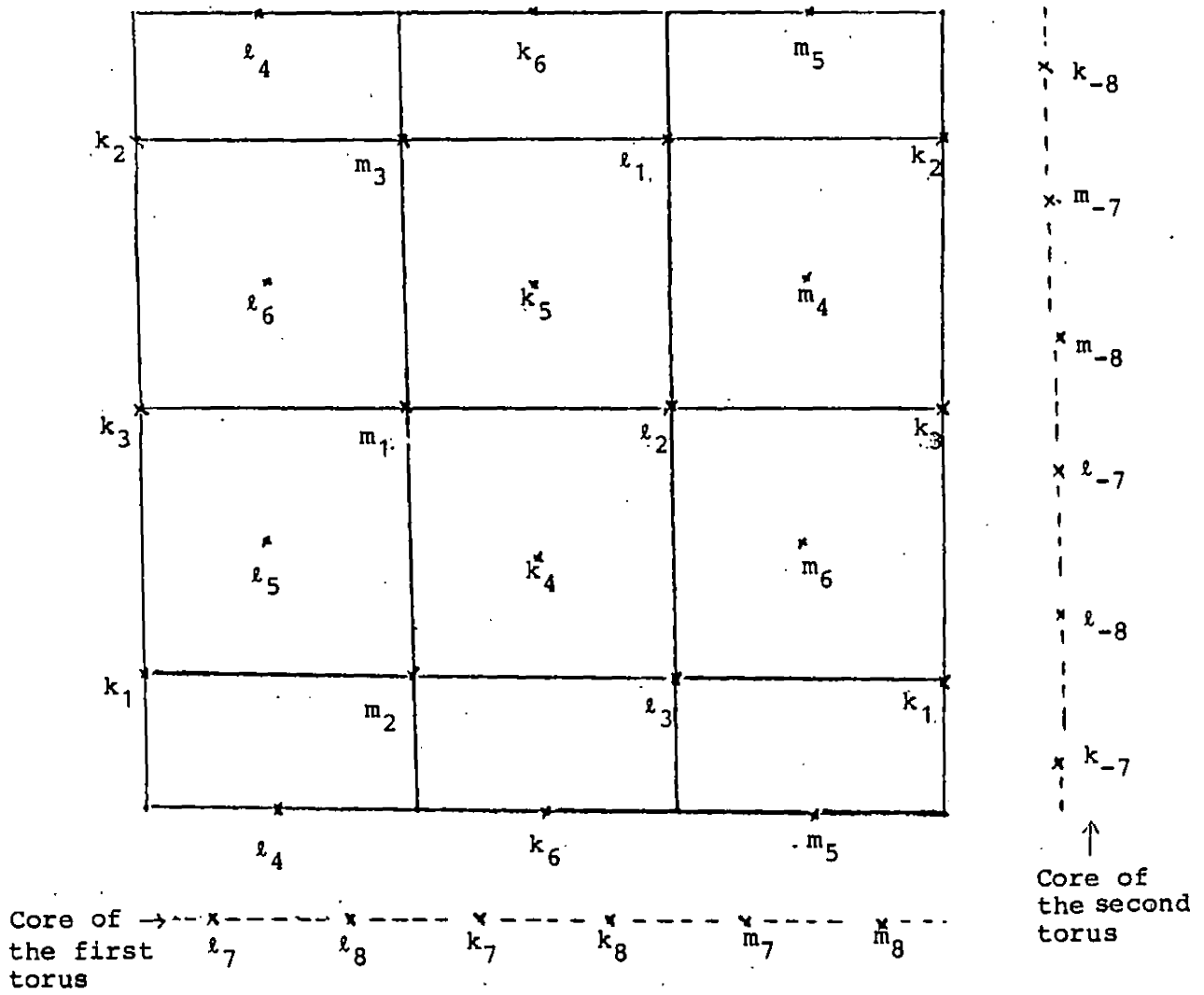


Figure 6-5

Claim 1    The natural projection  $\tilde{M} \longrightarrow M$  is a  
6 fold cover of  $M$  branched along  $T \cap M$ , in such a way  
that the inverse image of each simplex of  $M$  is the union  
of 6 simplices of the same dimension except for the edges  
and vertices of  $T \cap M$  which are covered only thrice.

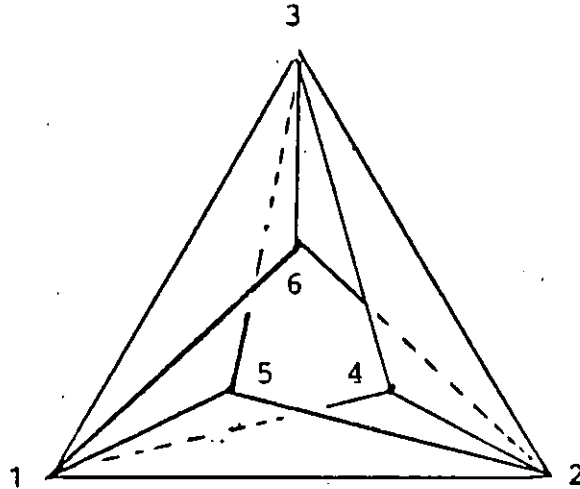
Proof. By assigning to each of the 30 vertices of  $\tilde{M}$  its color (namely the index attached to it), one readily sees that each of the 120 3-simplices of  $\tilde{M}$  is mapped to a 3-simplex of  $M$ . This defines a natural projection of  $\tilde{M}$  to  $M$ . Notice that the restriction of this projection to each of the six prisms,  $\tilde{M}$  has been decomposed into, is a surjective map from the considered prism to  $M$ . For instance observe that  $M$  is combinatorially equivalent to the quotient of  $M'$  obtained by identifying together the  $k_i$ 's  $l_i$ 's and  $m_i$ 's ( $i = 1, 2, 3$ ) of same index. These identifications force each lateral face to be folded along one of its diagonals and in addition the following pairs of triangles are glued together

$$\begin{aligned} l_3 k_6 l_1 &\longleftrightarrow m_3 k_6 l_1 \\ l_3 m_2 k_6 &\longleftrightarrow m_3 m_2 k_6 \end{aligned}$$

Similarly for the two other faces. This operation induces an anti-clockwise twist of the top and the bottom triangular faces with respect to each other. In the quotient, the image of  $\partial\Delta_2 \times \Delta_1$  in  $M$  is the Möbius strip  $S$  formed by the

union of the six triangles:

(124), (125), (236), (234), (315), (316)



bounded by  $M \cap T$ . In order to complete the quotienting procedure do not forget to identify together the simplices  $\ell_1 \ell_2 \ell_3$  and  $m_1 m_2 m_3$  (otherwise the object would not be a simplicial complex i.e. it would not be properly triangulated in the sense of § 5). The last identification gives you the Grünbaum-Brückner triangle (123) centered at infinity. The way the mapping  $\tilde{M} \rightarrow M$  has been described makes Claim 1 obvious.

Claim 2 The mapping  $\tilde{M} \rightarrow M$  is a normal covering with Galois group the symmetric group  $\mathfrak{S}_3$ . Moreover the alternating group  $A_3$  acts freely on  $\tilde{M} \cong S^3$  so that  $\tilde{M}/A_3$  is the lens space  $L(3,1)$  and that the projection  $\tilde{M}/A_3 \rightarrow \tilde{M}/\mathfrak{S}_3 \cong M \cong S^3$

is the 2 fold cover of  $M$  branched along the right hand trefoil knot  $M \cap T$ .

Proof Notice that  $A_3$  acts on each of the two solid tori, into which  $\tilde{M}$  has been splitted (see Figure 6-1). The quotient of the first torus under this action can be described as being the prism  $M'$  with the two triangular faces  $(m_1, m_2, m_3)$  and  $(l_1, l_2, l_3)$  identified together. One is now left with an improperly triangulated solid torus  $\bar{M}_1$  whose boundary  $\partial\bar{M}_1 = \tilde{\mathcal{S}}$  is obtained by doubling the Möbius strip  $S$ . The Deck involution  $\iota: \tilde{\mathcal{S}} \rightarrow \tilde{\mathcal{S}}$ , with respect to the projection  $\tilde{\mathcal{S}} \rightarrow \mathcal{S}$  fixes the curve  $\iota^{-1}(T \cap M) \sim 2\mu + 3\lambda$  :

$$1 \text{ --- } \cdot \text{ --- } 4 \text{ --- } \cdot \text{ --- } 3 \text{ --- } \cdot \text{ --- } 5 \text{ --- } \cdot \text{ --- } 2 \text{ --- } \cdot \text{ --- } 6 \text{ --- } \cdot \text{ --- } 1$$

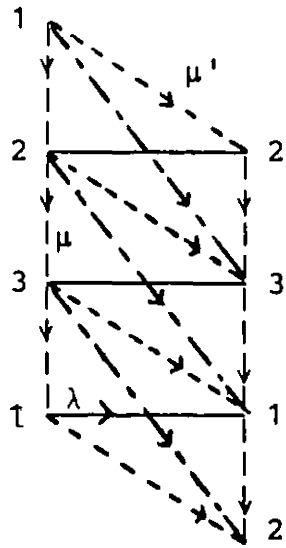
and sends the meridian  $\mu$  :

$$1 \text{ --- } 2 \text{ --- } 3 \text{ --- } 1$$

to the curve  $\mu' \sim \mu + 3\lambda$  :

$$1 \cdots 2 \cdots 3 \cdots 1$$

where  $\lambda$  is the chosen longitude indicated in the picture below.



Next consider a second copy  $\bar{M}_2$  of  $\bar{M}_1$  representing the quotient under the  $A_3$ -action of the second torus of Figure 6-1. Now  $\tilde{M}/A_3$  splits into  $\bar{M}_1$  and  $\bar{M}_2$  glued along their common boundary using the involution  $\iota$ . Observe that the meridian of  $\bar{M}_2$  is mapped to the curve  $\mu'$  on  $\bar{M}_1$ . According to [Sie],

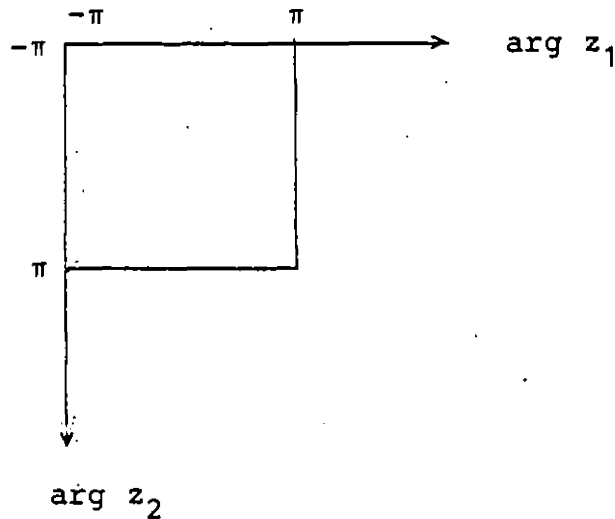
$$\bar{M}_1 \cup_{\iota} \bar{M}_2$$

appears to be the improperly triangulated lens space  $L(3,1)$  whose universal cover has three sheets and identifies with  $S^3$ , properly triangulated by  $\tilde{M}$ . This ends the proof of Claim 2.

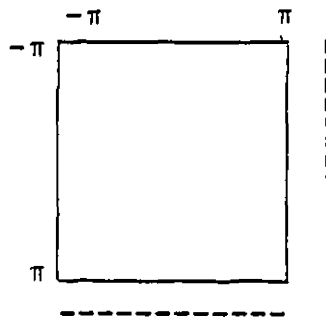
### The realization of $\tilde{M}$ in $\mathbb{C}^2$

The promised representation of  $\tilde{M}$  as the boundary of a star-polytope  $N$  will be completely determined by giving

coordinates for its 30 vertices in  $\mathbb{C}^2$ . In order to obtain these coordinates we first represent the torus of all vectors  $(z_1, z_2) \in \mathbb{C}^2$  satisfying  $z_1 \bar{z}_1 = z_2 \bar{z}_2 = 1$  as a square horizontally parameterized by the argument of  $z_1$  and vertically by the argument of  $z_2$  as indicated:



Place the 18 vertices of Figure 6-5 of colors  $1, \dots, 6$  in this square as they appear on the previous diagram. Now the cores of the tori should be treated as circles of radius  $\sqrt{3}$  in each coordinate axis represented in Figure 6-5 as dashed segments parameterized by the arguments running from  $-\pi$  to  $\pi$  from left to right for the first cone and from top to bottom for the second one.





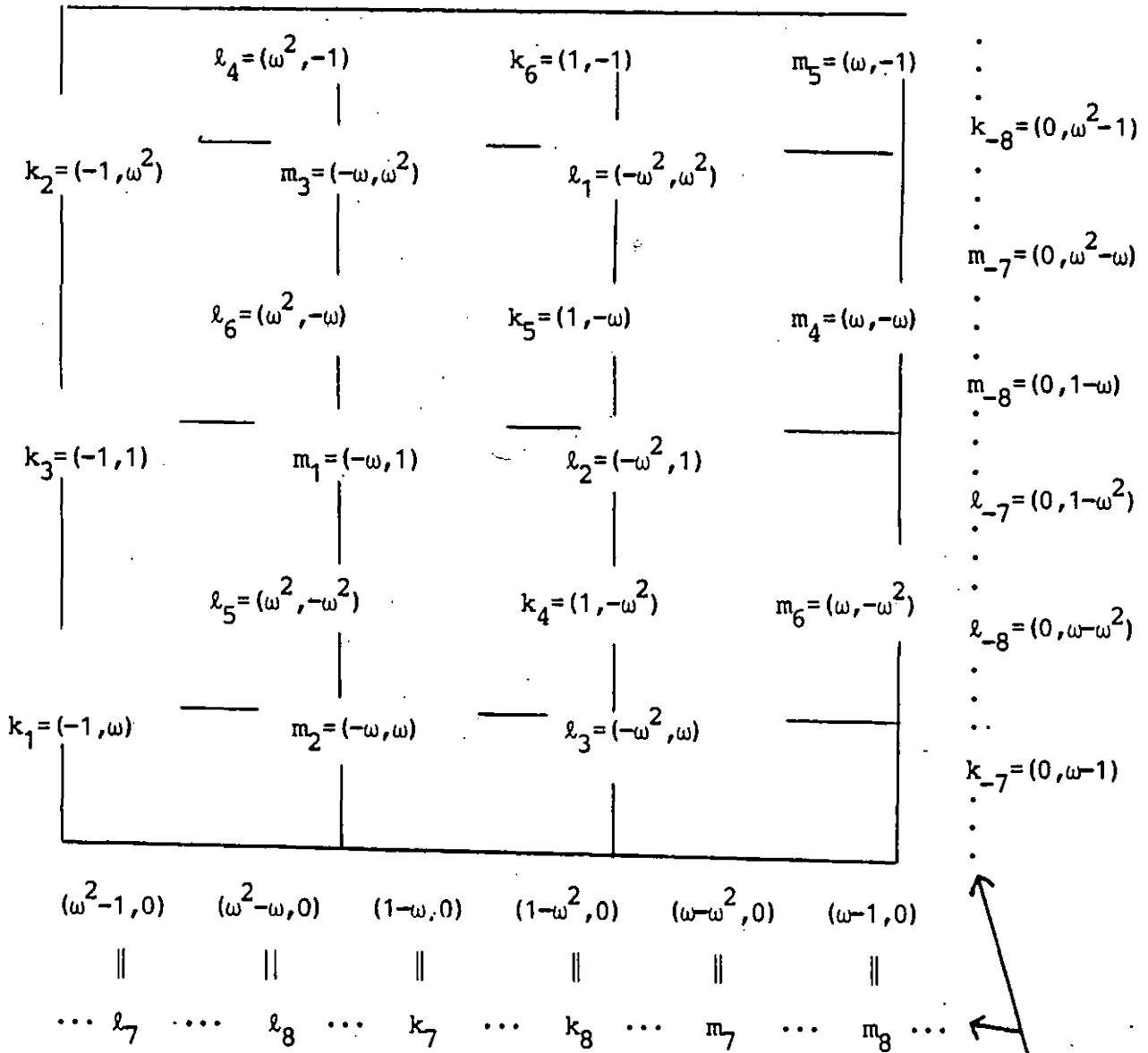
On these circles, place the 12 remaining vertices of Figure 6-5 in such a way that each of these 12 points can be obtained as the sum of two of the 18 points described above: e.g.

$$k_7 = m_1 + k_6$$

Therefore these 12 points belong to the lattice  $L[f]$  (defined in § 7) generated by the 18 points of Figure 6-5.

In order not to get mixed up while performing this very tedious exercise, the aid of Figure 7-0 might be helpful. If you are patient enough to complete this homework, you will get the following table.

Vertices at distance  $\sqrt{2}$  from 0

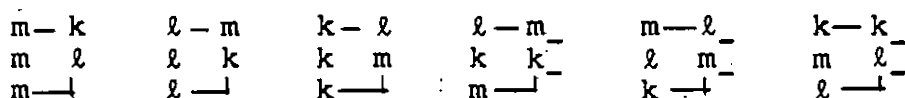


vertices at distance  $\sqrt{3}$  from 0

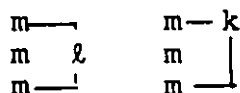
In § 7 and § 8 we will see that this set of 30 points is the intersection of the lattice  $L[f]$  (constructed in § 7) with the ball of radius  $\sqrt{3}$  centered at the origin of  $\mathbb{T}^2$  minus zero.

Now that we know the vertices of  $N$ , it is easy to

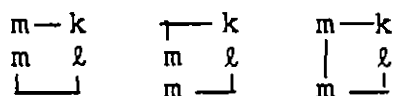
construct its boundary  $\partial N$  by taking the convex hulls in  $\mathbb{R}^2$  of all the vertices of each of the 120 3-simplices triangulating  $\tilde{M}$ . Then  $N$  is just the cone on  $\partial N$  with vertex the origin. In order to obtain the convex hull  $\bar{N}$  of  $N$  it suffices to fill 6 notches carved in  $N$  by adding 6 new 4-simplices to the 120 4-simplices into which  $N$  splits when considering the triangulation of its boundary. Here are the notch 4-simplices to be added:



To derive the triangulation of  $\partial \bar{N}$  from the triangulation  $\tilde{M}$ , it will be sufficient to replace the pair of simplices

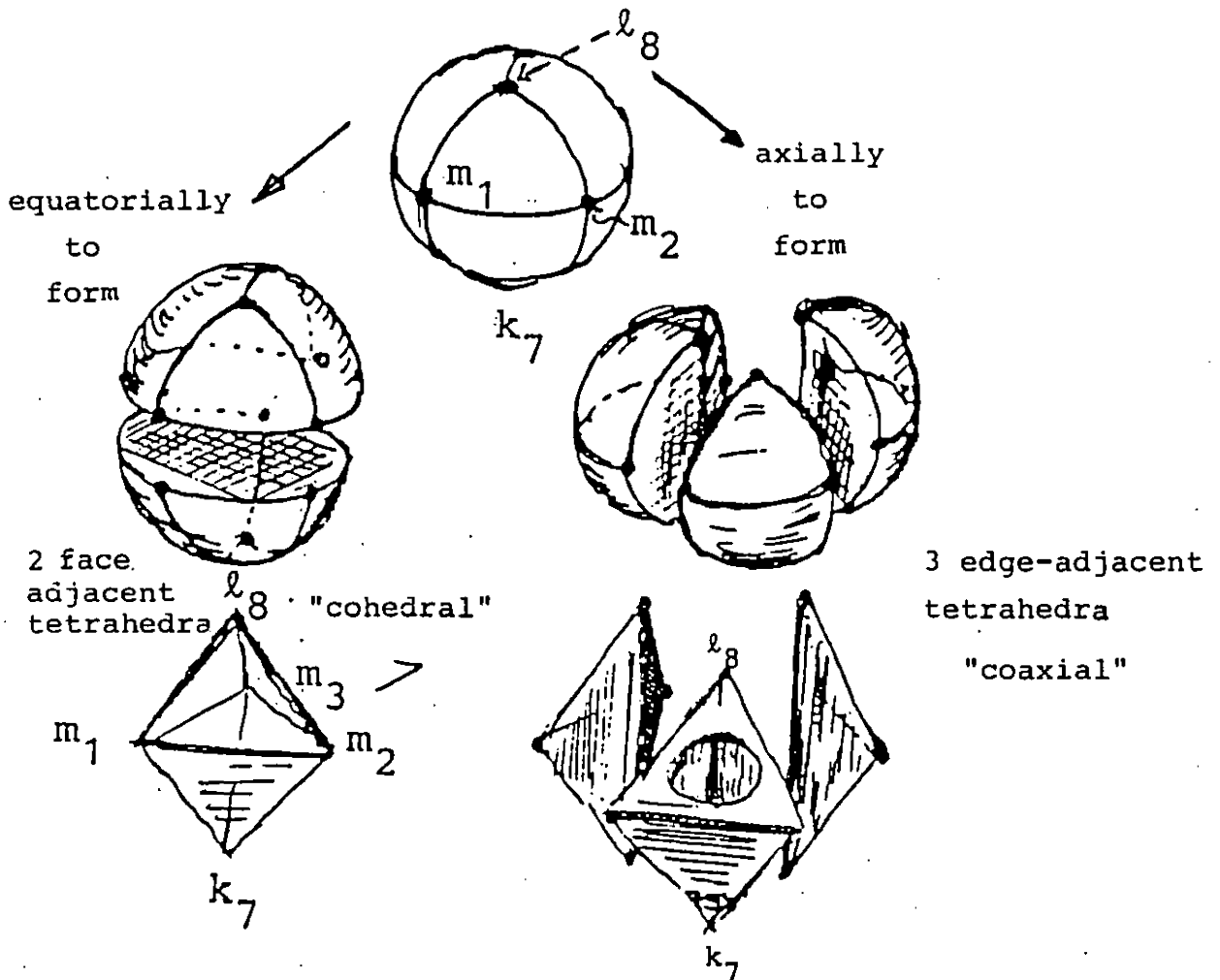


contained in the boundary of  $\begin{matrix} m-k \\ m \ \ell \\ m \ \lrcorner \end{matrix}$  by the three simplices

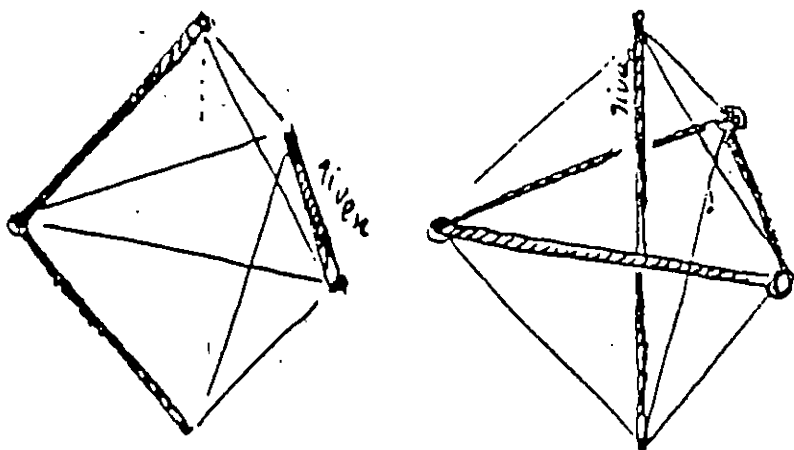


and similarly for the five pairs of simplices associated to the other notches.

There are 2 ways of triangulating the solid hexahedron



A tetrahedron is the join of two skew segments



join a diangle of segments to a given skew segment to obtain the co-hedral triangulation of the hexahedron -  
 join a triangle of segments to a given skew segment for the coaxial triangulation

Although the boundary  $\partial\bar{N}$  is naturally triangulated with 126 3-simplices, we will see in § 8 that  $\bar{N}$  is a polytope with only 18 hyperfaces (called pegs). Each of these is the union of seven 3-simplices of the triangulation. It will then be clear that both  $\bar{N}$  and  $N$  have flat dihedral angles when considered as polytopes with 126 and 120 simplicial hyperfaces respectively.



§ 7 Some lattices and crystallographic groups on  $\mathbb{C}^2$ 

In order to understand how the image of  $\tilde{M}$  in  $\mathbb{C}^2$  was obtained, we need the definitions of this section, the construction of § 8 and the map  $Y$  in § 9.

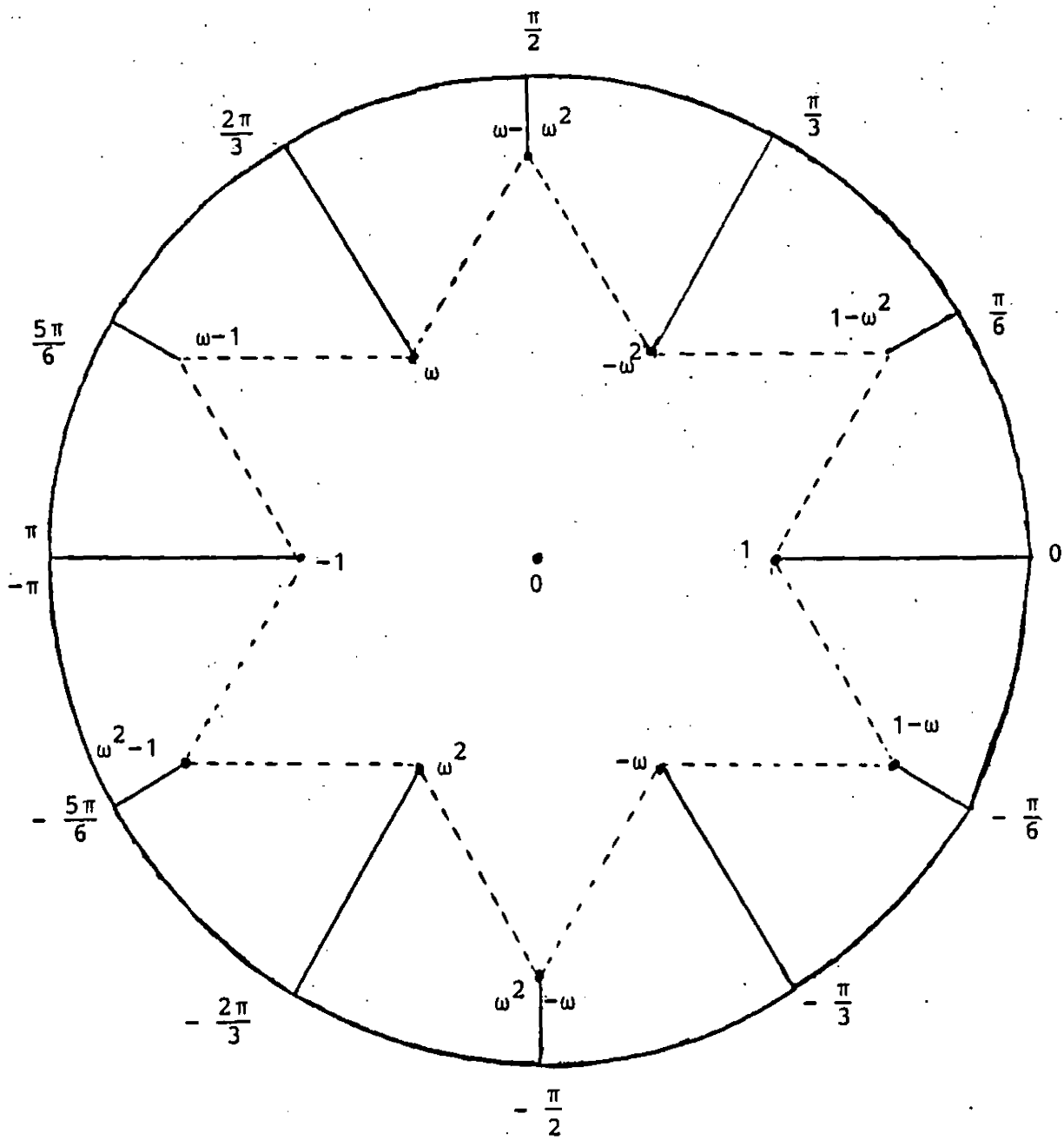
Let

$$L(\omega) = \mathbb{Z} + \mathbb{Z}\omega$$

be the hexagonal lattice in  $\mathbb{C}$ . \*)

---

\*) In § 12 the lattice considered will be  $\mathbb{Z} + \mathbb{Z}\tau$  where  $\tau$  is any complex number such that  $\text{Im } \tau > 0$ , not necessarily equal to  $\exp 2\pi i/6$ , thus losing the symmetry  $\gamma$  but still obtaining a triangulation combinatorially equal to  $\tilde{K}$ .



arguments

Figure 7-0



In  $\mathbb{C}^2$  with standard coordinates  $(z_1, z_2)$ , we define the following vectors

$$\begin{aligned} e_1 &= (1, 0), & e_2 &= (0, 1), \\ f_0 &= (-1, 1), & f_1 &= (-\omega, \omega^2), & f_2 &= (-\omega^2, \omega) \\ h_0 &= f_1 - f_2, & h_1 &= f_2 - f_0, & h_2 &= f_0 - f_1 \\ &= (\omega^2 - \omega)(1, 1) & &= (\omega^2 - \omega)(\omega, \omega^2) & &= (\omega^2 - \omega)(\omega^2, \omega). \end{aligned}$$

Note that

$$f_0 + f_1 + f_2 = h_0 + h_1 + h_2 = 0.$$

Let  $F \subset \mathbb{C}^2$  be the real plane given by

$$F = \sum_{j=0}^2 \mathbb{R} f_j \quad (= \sum_{j=0}^2 \mathbb{R} h_j).$$

We can define the following lattices in  $\mathbb{C}^2$  :

$$L[e] = L(\omega) e_1 + L(\omega) e_2$$

$$L[f] = \sum_{j=0}^2 L(\omega) f_j, \quad L[h] = \sum_{j=0}^2 L(\omega) h_j,$$

which have inclusion relations given by the marks attached below the inclusion notations:

$$L[h] \subset_9 L[f] \subset_3 L[e]$$

Let us consider the following elements and finite subgroups of the  $2 \times 2$  unitary group  $U(2)$ . The matrices act, as usual, on points of  $\mathbb{C}^2$  considered as columns:

$$\sigma = \begin{pmatrix} \omega & \\ & \omega^2 \end{pmatrix}, \quad \tau = \begin{pmatrix} & -1 \\ -1 & \end{pmatrix}, \quad \tilde{\gamma} = \begin{pmatrix} \omega^2 & \\ & \omega^2 \end{pmatrix}$$

$$G_6 = \langle \sigma, \tau \rangle$$

$$= \left\{ \begin{pmatrix} \omega & \\ & \omega^2 \end{pmatrix}, \begin{pmatrix} \omega^2 & \\ & \omega \end{pmatrix}, \begin{pmatrix} \omega^2 & \omega \\ & \omega^2 \end{pmatrix}, \begin{pmatrix} \omega & \omega^2 \\ & \omega^2 \end{pmatrix}, \begin{pmatrix} & -1 \\ -1 & \end{pmatrix}, 1 \right\}$$

$$G_{18} = \langle G_6, \tilde{\gamma} \rangle$$

Here  $\langle a, b, \dots \rangle$  stands for the group generated by  $a, b, \dots$ . Notice that  $G_6$  acts on the set  $\{f_0, f_1, f_2\}$  as the symmetric group and  $G_6 \triangleleft_3 G_{18}$ , that is to say,  $G_6$  is a normal subgroup of  $G_{18}$  of index 3.

We are now in a position to define the following two dimensional complex crystallographic groups (that is to say, cocompact discrete subgroups of  $\mathbb{C}^2 \rtimes U(2)$ ), presented as semi-direct products of their point groups with their lattices:

$$\Gamma = L[h] \rtimes G_6,$$

$$\Gamma'' = L[f] \rtimes G_{18}.$$

It is known ([Y2]) and easy to show that  $\Gamma$  is generated by a finite number of complex reflections of order 2, and that the set of points in  $\mathbb{C}^2$  fixed by some non-trivial

element of  $\Gamma$  is the union  $A$  of the following lines

$$L[f] + \mathbb{C} f_j \quad j = 0, 1, 2,$$

which intersect in threes at each element of  $L[f]$  and intersect nowhere else.

Identifying vectors with corresponding translations, we define the two following operations:

$$\tilde{\alpha} = f_0, \quad \tilde{\beta} = (\omega - \omega^2) f_0.$$

Then we have

$$\Gamma'' = \langle \Gamma, \tilde{\alpha}, \tilde{\beta}, \tilde{\gamma} \rangle \quad (= \langle \Gamma, \tilde{\alpha}, \tilde{\gamma} \rangle).$$

We next proceed to assign  $\Gamma$ -invariant colors  $1, 2, \dots, 9$  to the points in  $L[f]$  and  $10, 11, 12$  to the points in  $L[e]$  not belonging to  $L[f]$ . The quotient  $L[f]/L[h]$  (which identifies with  $L[f]$  modulo  $\Gamma$ ) consists of the following 9 classes  $L_1, \dots, L_9$ :

$$\begin{array}{lll} L_4 = 2\omega f_0 + L[h] & L_7 = (1 + 2\omega) f_0 + L[h] & L_1 = (2 + 2\omega) f_0 + L[h] \\ L_2 = \omega f_0 + L[h] & L_5 = (1 + \omega) f_0 + L[h] & L_8 = (2 + \omega) f_0 + L[h] \\ L_9 = L[h] & L_3 = f_0 + L[h] & L_6 = 2f_0 + L[h] \end{array}$$

In addition, let

$$L_{10} = \Gamma e_1 = G_6 e_1 + L[h]$$

$$L_{11} = \tilde{\alpha} L_{10}, \quad L_{12} = \tilde{\alpha} L_{11}.$$

Since  $L_{10} \cup L_{11} \cup L_{12} = L[e] - L[f]$ , the coloring is now completed.

Let us define

$$\begin{aligned} \tilde{\delta}: (z_1, z_2) &\longmapsto (-\overline{z_2}, -\overline{z_1}) && \text{(conjugation with respect to } F), \\ \tilde{\epsilon}: (z_1, z_2) &\longmapsto (\overline{z_2}, \overline{z_1}) && \text{(conjugation with respect to } iF). \end{aligned}$$

Then one can readily check that  $\tilde{\alpha}, \tilde{\beta}, \tilde{\gamma}, \tilde{\delta}$  and  $\tilde{\epsilon}$  act on the colors  $1, \dots, 12$  exactly as  $\alpha, \beta, \gamma, \delta$  and  $\epsilon$  acted on vertices in § 1 :

$$\tilde{\eta} L_i = L_{\eta(i)} \quad i = 1, \dots, 12$$

where  $\eta = \alpha, \beta, \gamma, \delta$  and  $\epsilon$ .

In particular, by sending  $\tilde{\alpha} \mapsto \alpha, \tilde{\beta} \mapsto \beta, \tilde{\gamma} \mapsto \gamma$ , we get

$$\Gamma''/\Gamma \cong G.$$

In the sequel the colors introduced here will enable one to speak of the type and the color of simplices with vertices in  $L[f]$ .

Recall that as decided in § 1 and § 3, these twelve colors are organized into the following families

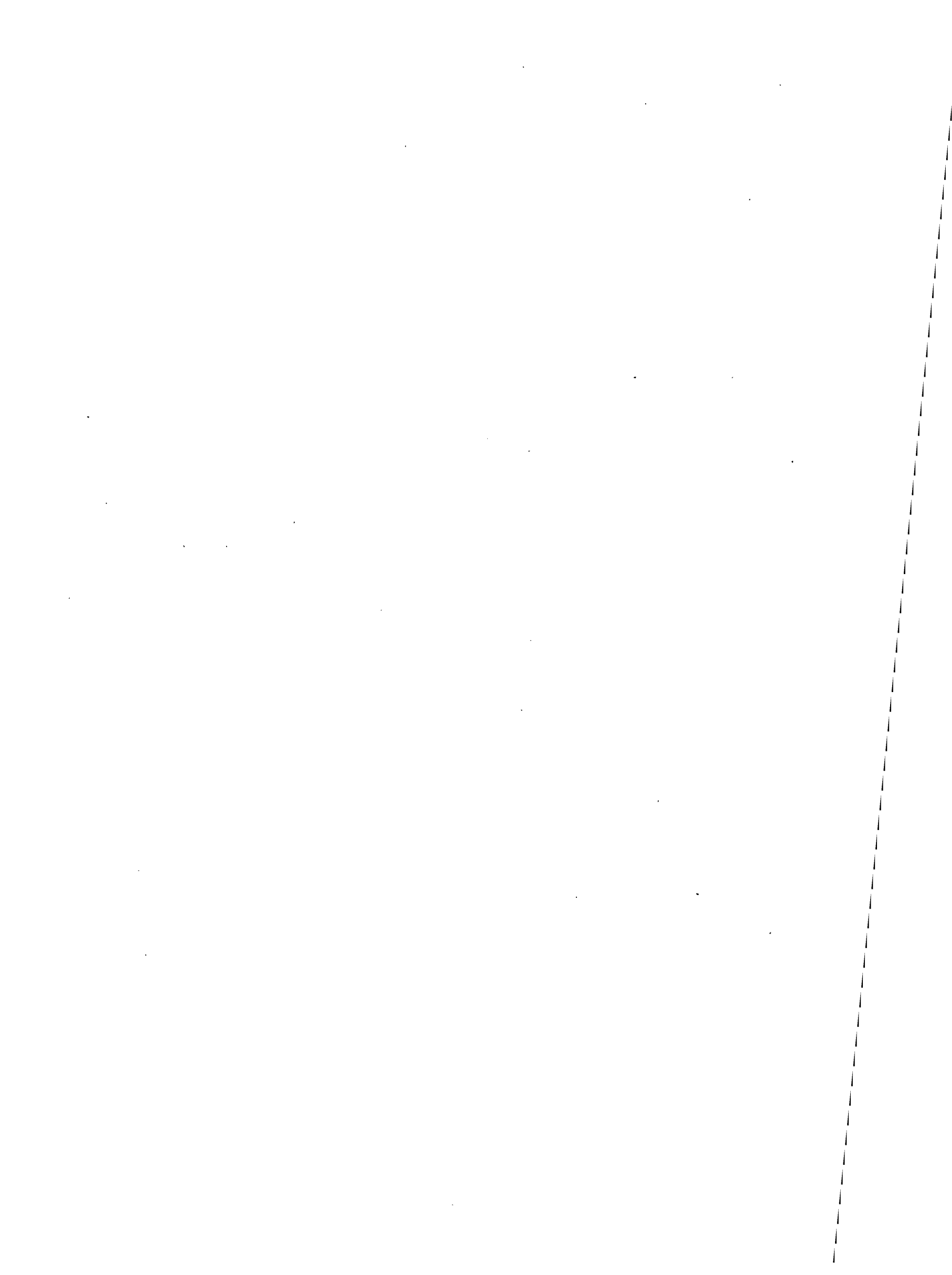
{1,2,3,10} , {4,5,6,11} and {7,8,9,12}

respectively considered as blue, white and red. Of one insists on bearing in mind actual colors, rather than numbers, we suggest substituting for the array

1	4	7
2	5	8
3	6	9
10	11	12

the following palette:

sky blue	white	pink
royal blue	gray	sparkling red
navy blue	black	scarlet
green	yellow	orange



§ 8 The rectilinear triangulation  $\tilde{\mathcal{K}}$  of  $\mathbb{C}^2$

In  $\mathbb{C}^2$  consider the real hyperplane

$$\begin{aligned} \Pi &= F + \mathbb{C}f_0 & (F &= \sum_{j=0}^2 \mathbb{R}f_j) \\ &= \{(z_1, z_2) \in \mathbb{C}^2 \mid \operatorname{Re}(z_1 + z_2) = 0\}, \end{aligned}$$

and the collection of hyperplanes

$$\Sigma = \Gamma'' \Pi.$$

Since

$$|\Sigma| = \bigcup_{\gamma \in \Gamma''} \gamma \Pi$$

is  $\Gamma''$ -invariant, the intersection pattern of hyperplanes in  $\Sigma$  is the same at each point of  $L[f]$ . Here is the intersection pattern at the origin.

A. The 9 hyperplanes of  $\Sigma$  passing through the origin are

$$\Pi_{jk} : \operatorname{Re}(\omega^j z_1 + \omega^k z_2) = 0 \quad j, k \in \mathbb{Z}/3\mathbb{Z}.$$

B. In  $\mathbb{Z}/3\mathbb{Z} \times \mathbb{Z}/3\mathbb{Z}$  let  $(j, k) \neq (j', k')$ .

- (i) If  $k - j = k' - j'$  then  $\Pi_{jk} \cap \Pi_{j'k'}$  is the complex line  $\mathbb{C}f_{k-j}$ .
- (ii) If  $k + j = k' + j'$  then  $\Pi_{jk} \cap \Pi_{j'k'}$  is the real plane  $\omega^{k+j}F$ .
- (iii) If  $j = j'$  (or  $k = k'$ ) then  $\Pi_{jk} \cap \Pi_{j'k'}$  is the real plane  $H(j; k, k')$  spanned by  $p_{jk}$  and  $p_{j'k'}$ .

(or the real plane  $V(j, j', -k)$  spanned by  $P_{jk}$  and  $P_{j', k}$ ) where

$$\begin{pmatrix} P_{00} & P_{01} & P_{02} \\ P_{10} & P_{11} & P_{12} \\ P_{20} & P_{21} & P_{22} \end{pmatrix} = \begin{pmatrix} \ell_1 & k_2 & m_3 \\ \ell_2 & k_3 & m_1 \\ \ell_3 & k_1 & m_2 \end{pmatrix} .$$

The nine vectors appearing in the second array have been defined in the list concluding § 6 (see also Figure 6-3).

C. Along each of the three complex lines  $\mathbb{C}f_j$  and each of the three real planes  $\omega^j F_j$  ( $j = 0, 1, 2$ ), three  $\pi_{jk}$ 's intersect.

D. Along each of the nine  $H$ 's and each of the nine  $V$ 's defined in (iii) above, only two  $\pi_{jk}$ 's intersect.

E. Along each of the six real lines spanned by  $k_7, \ell_7, m_7$ ,  $k_{-7}, \ell_{-7}$  and  $m_{-7}$  respectively (recall that these are defined at the end of § 6), three  $\pi_{jk}$ 's intersect.

F. Along each of the nine real spanned by the  $p_{jk}$ 's defined in (iii), five  $\pi_{jk}$ 's intersect.

Claim 1 The connected components of the open set  $\mathbb{C}^2 - |\Sigma|$  are of two types: either 4-simplices or 4-cells with 6 vertices and 9 simplicial hyperfaces. The latter type will be referred



to as cells of type 3-3 (the colors of vertices of such cells will indeed appear later to fill two columns of the array  $\begin{pmatrix} 1 & 4 & 7 \\ 2 & 5 & 8 \\ 3 & 6 & 9 \end{pmatrix}$  of § 1).

Proof We first prove the claim near the origin, by studying the convex hull  $\bar{N}$  of the 30 vertices of  $\bar{M}$  listed in § 6 (See subclaim below). Remember that the closed points to the origin in  $L[f]$  are the 18 points at distance  $\sqrt{2}$  from the origin listed in § 6. If we take the convex hull  $W$  of these 18 points, we get a polytope with 12 octahedral and 18 tetrahedral hyperfaces. Observe that the barycenters of these octahedra are the midpoints of the segments joining  $k_9$  to the 12 elements of  $L[f]$  at distance  $\sqrt{3}$  from the origin, and that the hyperplanes carried by the octahedra are the perpendicular bisectors of these segments. In order to understand how the boundary of this polytope is organized, we proceed as follows. First notice that 6 of the 12 octahedra are glued together in a hexagonal pattern, in such a way that one octahedron touches its two neighbors along two of its opposite faces so that their union is a solid torus shown in Figure 8-1. Although it does not live in the boundary of the same polytop, it is helpful to have in mind that the present picture is Figure 6-1 with the notches deleted.

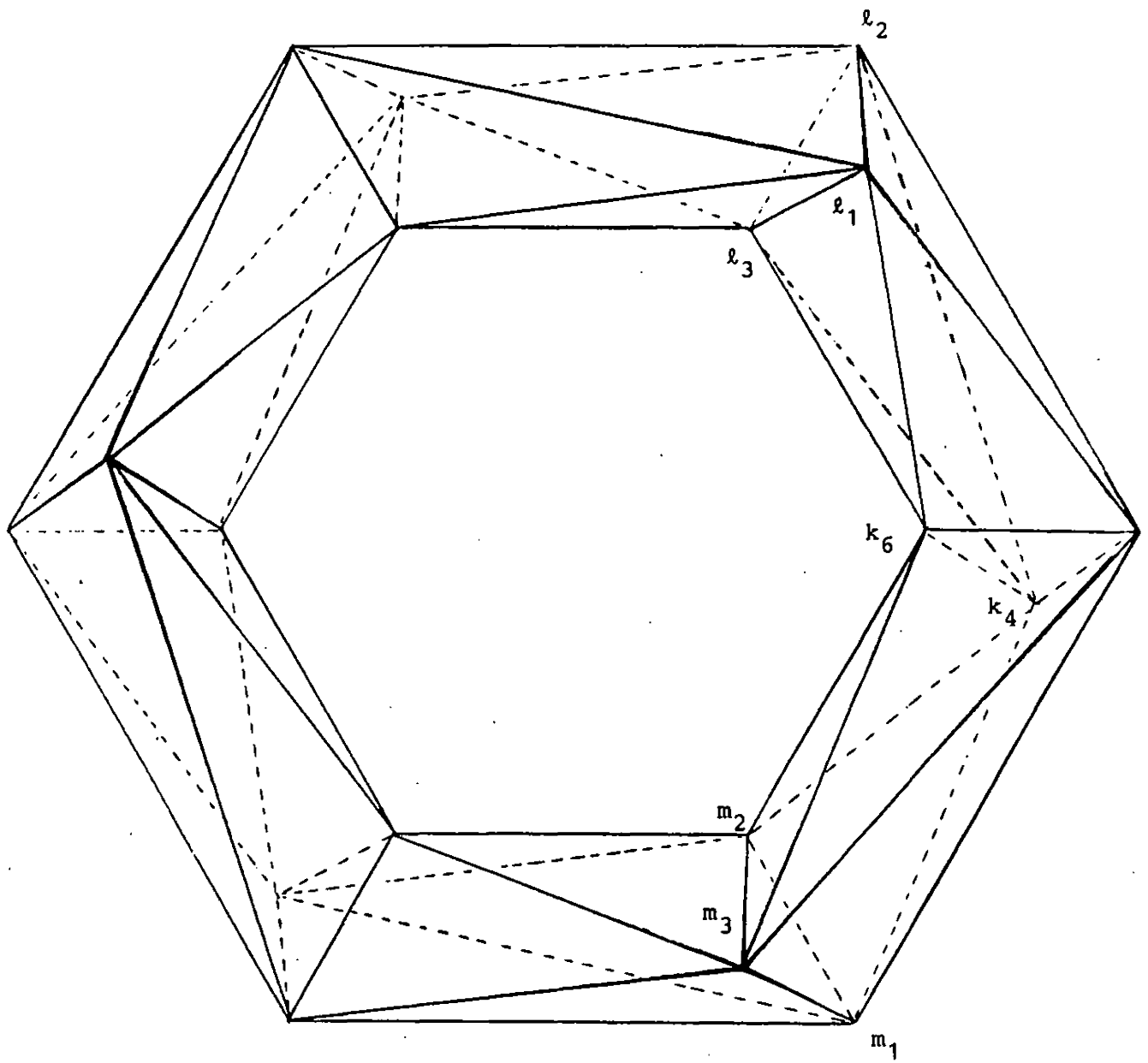
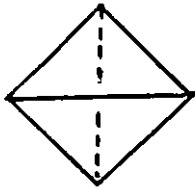


Figure 8-1

Secondly notice that one can think of the union of the six remaining octahedra as a second solid torus linking the first one in  $S^3$ . Now the complement in  $S^3$  of the union of these two solid tori is the union of 18 tetrahedra touching each other along an edge. Each tetrahedron is connected to 4 other tetrahedra along all of its edges except two opposite ones. In order to understand this patchwork of tetrahedra, one must think of a tetrahedron as a very flat object almost equal to its projection to the square.



The 18 squares thus obtained are matched together in order to produce a quilted torus as shown in Figure 8-2. We remark that the group  $G_{18}$  acts transitively on the 18 squares.

## The Quilted Torus

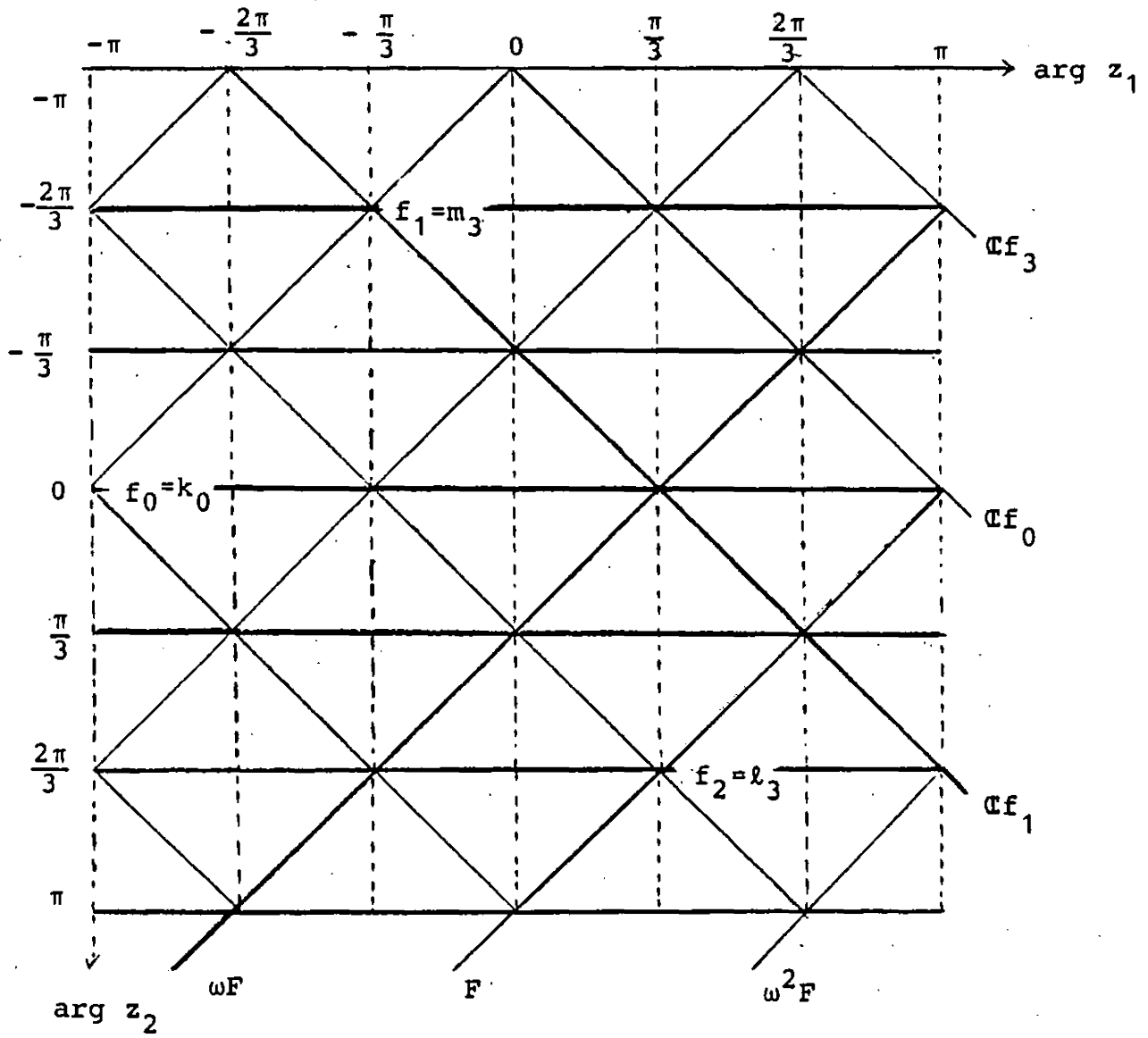


Figure 8-2

The 18 hyperplanes carrying the tetrahedra are in  $\Sigma$ , while the 12 hyperplanes carrying the octahedra are not. For instance, the tetrahedron  $k_5 m_1 k_4 l_2$  is carried by the hyperplane

$$\operatorname{Re}(z_1 + z_2) = 3/2$$

which is parallel to  $\Pi = \Pi_{00}$  and belongs to  $\Sigma$ . But the octahedron  $m_1 m_2 m_3 k_4 k_5 k_6$  is carried by the hyperplane

$$\operatorname{Im}(\omega z_2) = \sqrt{3}/2$$

which is not in  $\Sigma$ . Besides the tetrahedron  $k_5 m_1 k_4 l_2$  the hyperplane  $\operatorname{Re}(z_1 + z_2) = 3/2$  happens also to contain

$$k_7, k_8, m_{-7} \text{ and } m_{-8}.$$

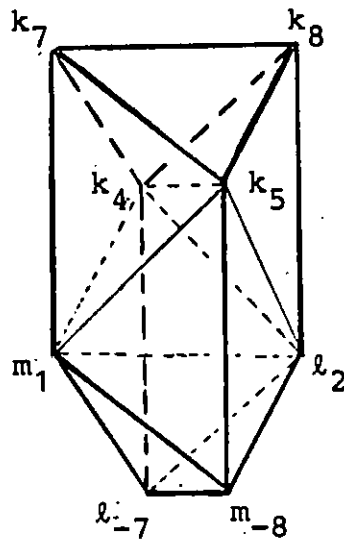
This remark proves that  $\bar{N}$  is a polytope with 18 hyperfaces carried by those hyperplanes of  $\Sigma$  belonging to the  $G_{18}$ -orbit of  $\operatorname{Re}(z_1 + z_2) = 3/2$ . All these faces have the same shape and will be referred to as pegs. Check that these 18 hyperplanes are the closet hyperplanes of  $\Sigma$  to the origin not passing through the origin and that, up to similarity, the polytope  $W$  (the convex hull of the 18 points in Figure 6-5) previously considered is dual to  $\bar{N}$ . We now describe the peg carried by  $\operatorname{Re}(z_1 + z_2) = 3/2$ , which is one of the two hypersurfaces parallel to  $\Pi$ . It is the convex hull

---

 $k_5 \quad m_1 \quad k_4 \quad l_2 \quad k_7 \quad k_8 \quad m_{-7} \quad m_{-8}$ 

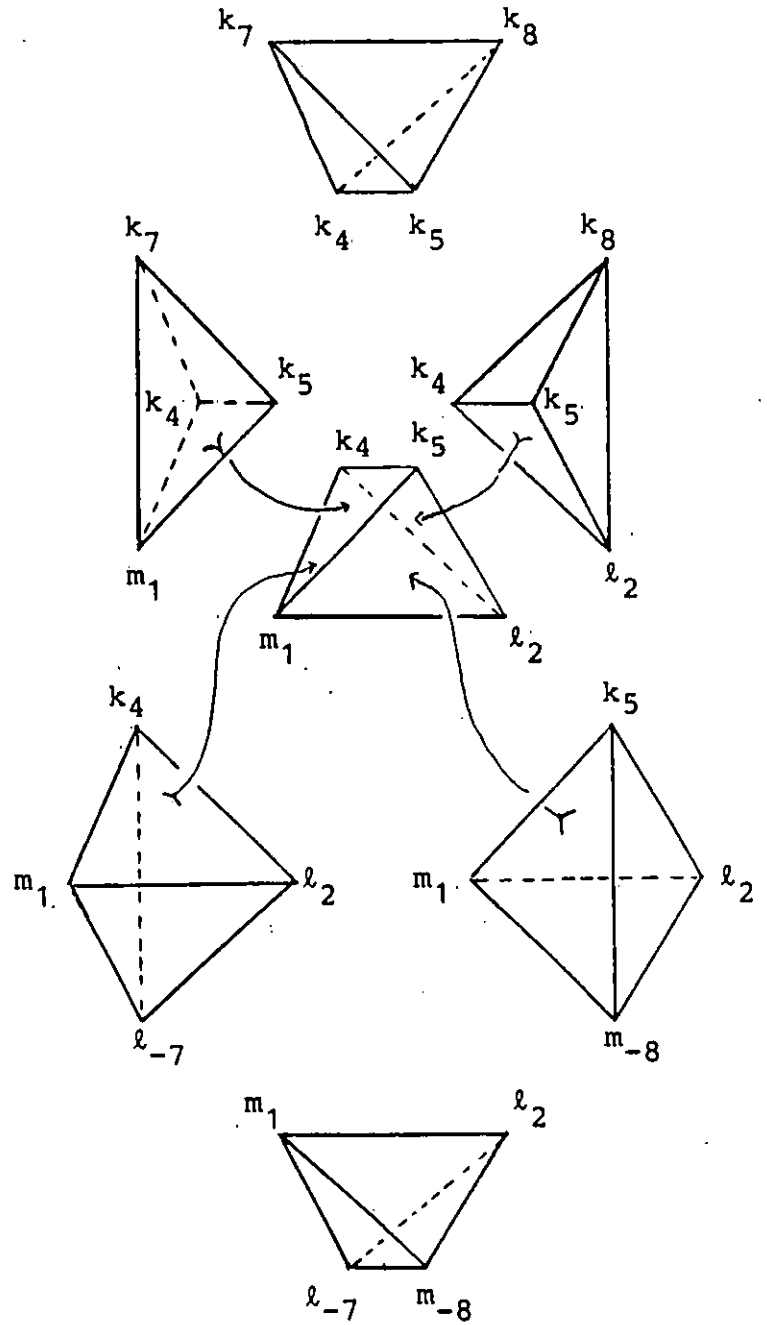
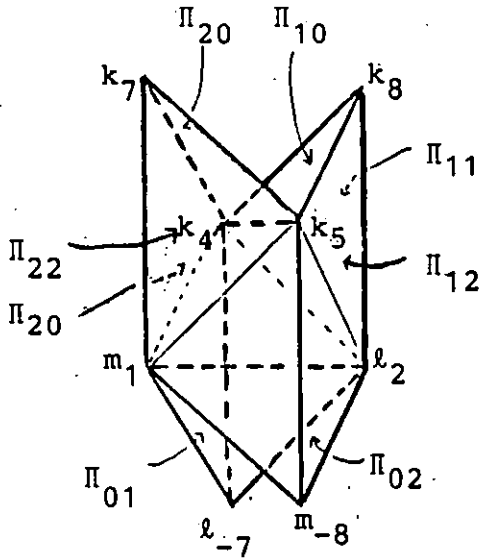
which is a polyhedron with 8 vertices, 10 edges and 8 faces. Four of the faces (called lateral faces) are rhombi and the others (called wedge faces) are isocoles triangles (see below).

Peg



It can be considered as the intersection of a prism based on the square of side  $\sqrt{6}/2$  with the tetrahedron whose faces are obtained by producing the four wedge faces of the peg.

The 8 hyperplanes  $\Pi_{ij}$   $(i,j) \neq (0,0)$  meet the peg and split it into the seven following tetrahedra.

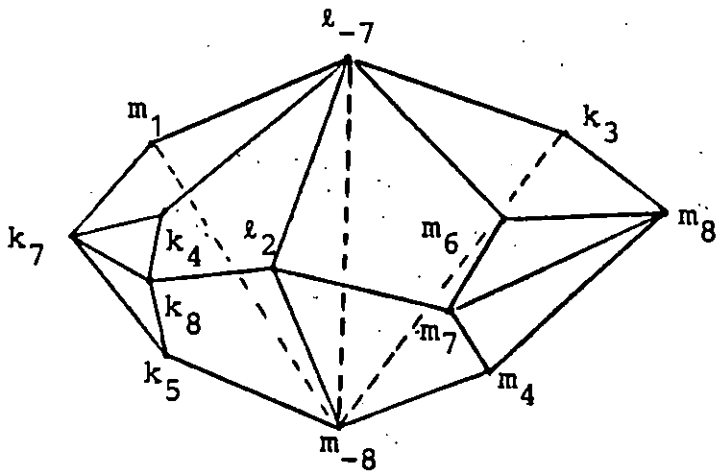


Observe that contrary to the lateral faces, the wedge faces are not intersections of the peg with the  $\Pi_{ij}$ 's but only with hyperplanes carrying the neighbouring pegs. So that five of the seven 3-simplices - the saturated ones - have all their faces contained in some  $\Pi_{ij}$ 's, while two of them (situated on the top and the bottom of the previous picture) -

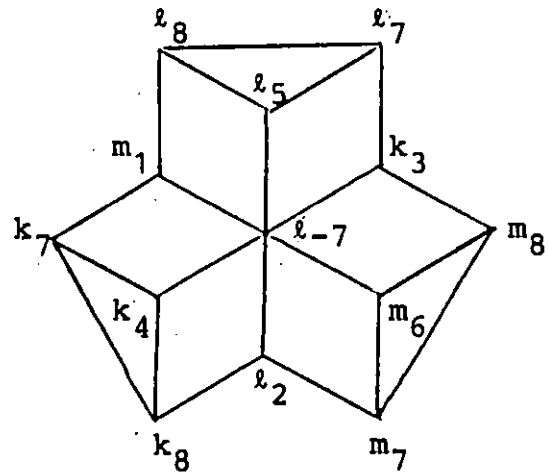
the wedge simplices - have only two faces satisfying this property.

Each of the segments  $\overline{\ell_{-7}m_{-8}}$  and  $\overline{k_7k_8}$  is the intersection of three of the 18 pegs limiting  $N$ . The following picture indicates how the three pegs meeting along  $\overline{\ell_{-7}m_{-8}}$  match together.

Two Pegs



Three Pegs from above

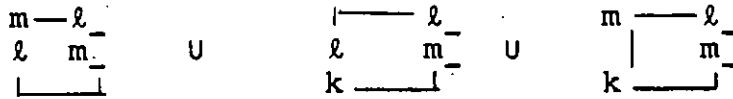


Let us define a cap to be either one of the two unions of three 3-simplices

$$\begin{bmatrix} & k & k \\ k & k & \\ k & k & \end{bmatrix} \cup \begin{bmatrix} & k & \\ k & k & \\ k & \perp & \end{bmatrix} \cup \begin{bmatrix} k & k & \\ & k & \\ k & \perp & \end{bmatrix}$$

and





or one of their images under the action of  $G_6$ . Notice that the convex hull  $\overline{\{k_9\} \cup C}$  (where  $C$  is any cap) is a 3-3 cell on the boundary of which the cap is sitting.

The following assertion should now be clear.

Subclaim The collection  $\Sigma$  splits  $\bar{N}$  into 90 4-simplices of type 2-2-1 (namely all the cones on saturated simplices of  $\partial\bar{N}$  with vertex at the origin) and 12 cells of type 3-3 (namely the convex hull of  $k_9$  and each of the 12 caps just considered).

In order to finish the proof of Claim 1, apply  $L[f]$  to the  $|\Sigma|$ -decomposition of the convex hull  $\bar{N}$ .

Finishing the construction of  $\tilde{K}$  The 2-2-1 simplices of  $\tilde{K}$  are the simplices of  $\mathbb{C}^2 - |\Sigma|$ . The 3-2 simplices of  $\tilde{K}$  are obtained by linearly subdividing each 3-3 cell into three 3-2 simplices. Since this must be done in a  $\Gamma$ -invariant fashion, we need only to split a given 3-3 cell. The splitting can be achieved in two different ways, so that a choice must be made. In fact the choice has already been dictated to us in [K-B] where it has been decreed that  $K$  should contain  $\begin{bmatrix} \cdot & \cdot \\ \cdot & \cdot \end{bmatrix}$ . Had they wished, the authors could

have chosen  $\begin{bmatrix} \cdot & \cdot \\ \cdot & \cdot \end{bmatrix}$  is place of  $\begin{bmatrix} \cdot & \cdot \\ \cdot & \cdot \end{bmatrix}$ . In order to obey them, and to complete the definition of  $\tilde{K}$ , it suffices to set

$$k_4 k_5 k_6 k_7 k_8 k_9 = \begin{bmatrix} k & k \\ k & k \\ k & \end{bmatrix} \cup \begin{bmatrix} k \\ k & k \\ k & k \end{bmatrix} \cup \begin{bmatrix} k & k \\ k \\ k & k \end{bmatrix}$$

Observe that the open set  $\mathbb{C}^2 - |\Sigma|$  is  $\delta$  and  $\tilde{\epsilon}$ -invariant but that the necessity we had to triangulate 3-3 cells forced us to exhibit a  $\delta$ -invariant but not  $\tilde{\epsilon}$ -invariant triangulation. The choice we had to make was infact between the triangulations  $\tilde{K}$  and  $\tilde{\epsilon}\tilde{K}$ . Note also that all 1-simplices of type 1-1 in  $\tilde{K}$  are of length  $\sqrt{2}$  while those of type 2-0-0 are of length  $\sqrt{3}$ , and that all 4-simplices of types 2-2-1 and of 3-2 have volume  $3/32$ .

Claim 2 As an abstract complex,  $\tilde{K}/\Gamma$  is isomorphic to  $K$ .

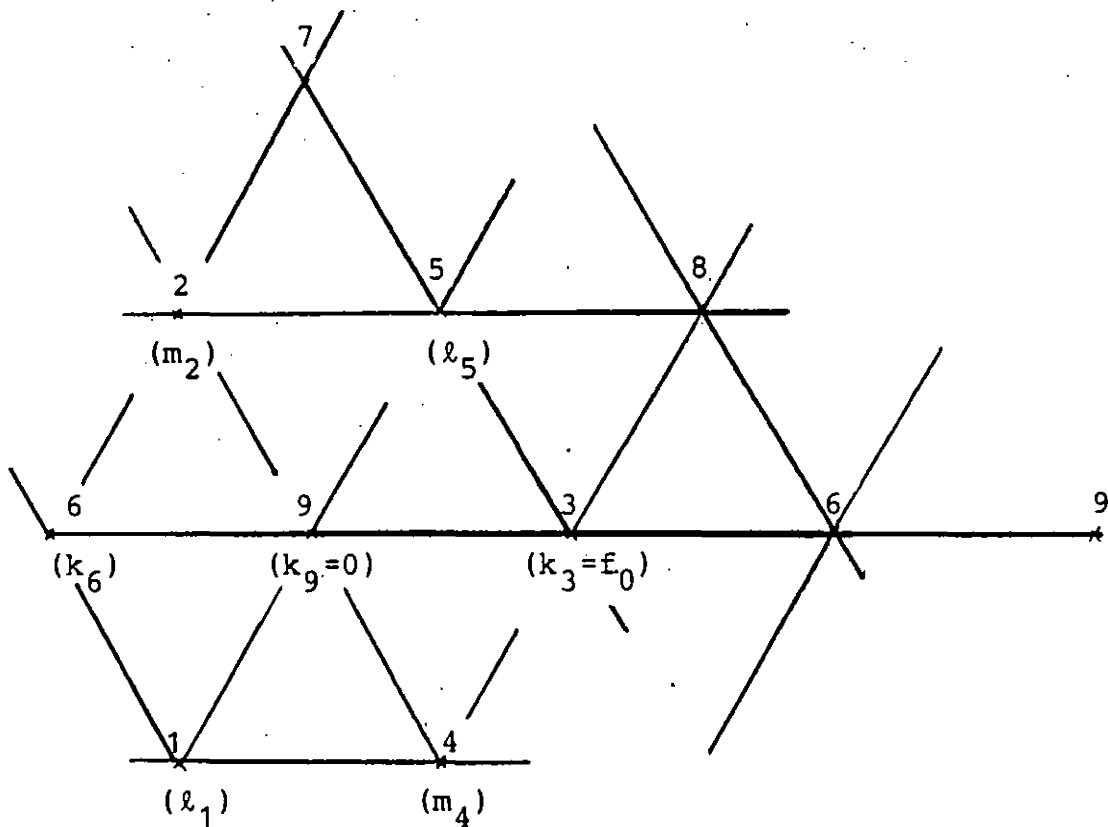
Proof Let  $c_1, \dots, c_5$  be the colors of a given simplex in  $\tilde{K}$ . There exists an element  $g$  in  $\Gamma$  which maps the vertex of color  $c_1$  to the origin  $k_9$ . Let  $\bar{g}$  be the image of  $g$  in  $G = \Gamma/\Gamma$ . Now  $(\bar{g}(c_1), \dots, \bar{g}(c_5))$  is a simplex in  $K$  and therefore also  $(c_1, \dots, c_5)$ .

Remarks

1 The inverse image of  $K''$  in  $\tilde{K}$  is the union of all the 3-3 cells in  $\mathbb{C}^2 - |\Sigma|$ . We observe that the set of barycenters of these cells is  $L[e] - L[f]$  and that the colors correspond to their images 10,11,12 in  $|K|$ .

The inverse image of the subdivision  $\bar{K}$  of  $K$  is obtained by considering the subdivision generated by  $\tilde{K}$  and  $\tilde{\tilde{K}}$ .

The inverse image of  $|T|$  is the union  $A$  of all the axes of reflections in  $\Gamma$ . Figure 8-4 shows how the vertices contained in the typical axis of reflection are colored.



$\mathbb{C}f_0$  - plane

Figure 8-4

2 The quotient  $|\tilde{K}|/L[h]$  is homeomorphic to the torus  $(S^1)^4$  decomposed into  $6 \times 36$  4-simplices with 9 vertices. This decomposition is an improper triangulation. This 4-torus is a 6 fold cover of  $|K|$  branched over  $|T|$ . In order to get a properly triangulated 4-torus, one has to consider some 9 fold cover of  $\tilde{K}/L[h]$ , for instance  $\tilde{K}/3L[f']$  where

$$L[f'] = L(\omega) f'_0 + L[\omega] f'_1 + L[\omega] f'_2$$

with

$$f'_0 = (1, 1), \quad f'_1 = (\omega, \omega^2), \quad f'_2 = (\omega^2, \omega)$$

(see § 13). The triangulation has 81 vertices and  $9 \times 6 \times 36 = 1944$  4-simplices. The 4-torus  $\tilde{K}/3L[f]$  would have worked equally well but it will turn out in § 13 that the Dirichlet domain of  $3L[f']$  at the origin is the convex hull of all points in  $L[f]$  at distance not exceeding 3. This remark provides a very good grasp on  $\tilde{K}/3L[f']$ . In order to understand this quotient, the Kühnel-Banchoff coloring, used throughout this paper since § 1, is no longer satisfactory. This explains why § 13 sets up a much more logical system of 81 colors that will prove very efficient. Nevertheless we decided not to use this powerful tool, devised by Marin, in the presentation of our material in order to supply the reader with a smooth transition between [K-B] and § 13.

§ 9 An explicit triangulation of  $\mathbb{C}P^2$  by  $K$

Let  $L$  be a lattice in  $\mathbb{C}$  and let  $\varphi$  be an embedding of the torus  $\mathbb{C}/L$  into a complex projective plane  $M^V$  as a non-singular cubic curve  $C$  such that  $\varphi(0)$  is a point of inflexion of  $C$ . Let  $M$  be the complex projective plane dual to  $M^V$ , that is, the set of lines in  $M^V$ . Let  $N$  be the hyperplane of  $\mathbb{C}^3$  (with co-ordinates  $u_0, u_1$  and  $u_2$ ) defined by

$$u_0 + u_1 + u_2 = 0.$$

We shall introduce a map

$$Y : N \longrightarrow M.$$

In order that the three points  $\varphi(u_0), \varphi(u_1)$  and  $\varphi(u_2)$  be colinear it is necessary and sufficient that  $(u_0, u_1, u_2)$  belongs to  $N$  (Abel's theorem). Thus if at least two of the three points are distinct, one can define  $Y$  geometrically by mapping  $(u_0, u_1, u_2)$  to the line through  $\varphi(u_j)$  ( $j = 0, 1, 2$ ). Since  $Y$  is defined up to a set of co-dimension two,  $Y$  extends uniquely to a holomorphic map on the whole plane  $N$ .

By this definition, the following claims are clear.

Claim 1 The map  $Y$  is invariant under translation by the lattice  $L \oplus L \oplus L \cap N$  and under the symmetric group permuting  $u_0, u_1$  and  $u_2$ .

Claim 2 The map  $Y$  is just the quotient by the crystallographic group acting on  $N$  generated by the lattice above and the above symmetric group.

Claim 3 The set of critical points of  $Y$  is the union of lines defined by

$$(9.1) \quad u_j = u_k \pmod{L} \quad (j, k = 0, 1, 2, j \neq k).$$

Claim 4 The set of critical values of  $Y$  is the dual curve  $C^V \subset M$  of  $C \subset M^V$ , where  $C^V$  is defined as the set of lines tangent to  $C$ .

Recall that, corresponding to the 9 inflection points of  $C$  (which are the images of the 3-torsion points of  $\mathbb{C}/L$ ), the curve  $C^V$  has 9 cusps.

In order to fit into the context of the previous sections, we let  $L = L(\omega)$  and make everything explicit as follows. Let  $p(u)$  be the Weierstrass function belonging to the lattice  $L(\omega)$ :

$$p(u) = \frac{1}{u^2} + \sum_{\substack{\zeta \in L(\omega) \\ \zeta \neq 0}} \left( \frac{1}{(u-\zeta)^2} - \frac{1}{\zeta^2} \right)$$

and let  $E$  be the positive real number  $p(1/2)$ . The function  $p$  and its derivative  $p'$  are related by the following well-known formula:

$$(p')^2 - 4p^3 + 4E^3 = 0.$$

If we let

$$\begin{aligned}\xi_0 &= \xi_0(u) = -p'(u) + a, \\ \xi_1 &= \xi_1(u) = p'(u) + a, \\ \xi_2 &= \xi_2(u) = b p(u),\end{aligned}$$

where

$$a = p'(1/3) = -2\sqrt{3} E\sqrt{E}, \quad b = \sqrt{16/3}\sqrt{E},$$

then one can easily check that the above formula becomes

$$(9.2) \quad (\xi_0)^3 + (\xi_1)^3 + (\xi_2)^3 = 0.$$

Let  $[\xi_0, \xi_1, \xi_2]$  be homogeneous coordinates on  $M^V$  and let  $C \subset M^V$  be the non-singular curve defined by (9.2). Define the map  $\varphi: \mathbb{C} \rightarrow M^V$  by

$$\varphi(u) = [\xi_0(u), \xi_1(u), \xi_2(u)].$$

The map  $\varphi$  defines the embedding

$$\mathbb{C}/L(\omega) \xrightarrow{\sim} C \subset M.$$

Let  $[y_0, y_1, y_2]$  be homogeneous coordinates of  $M$ . Then the map  $Y: N \rightarrow M$  is given explicitly as follows:

$$y_0 = \det \begin{pmatrix} \xi_1(u_1) & \xi_2(u_1) \\ \xi_1(u_2) & \xi_2(u_2) \end{pmatrix}, \quad y_1 = \det \begin{pmatrix} \xi_2(u_1) & \xi_0(u_1) \\ \xi_2(u_2) & \xi_0(u_2) \end{pmatrix},$$

$$y_2 = \det \begin{pmatrix} \xi_0(u_1) & \xi_1(u_1) \\ \xi_0(u_2) & \xi_1(u_2) \end{pmatrix},$$

and the dual curve  $C^V$  is given by

$$(y_0)^6 + (y_1)^6 + (y_2)^6 - 2((y_0 y_1)^3 + (y_1 y_2)^3 + (y_2 y_0)^3)$$

Notice that the cusps of  $C^V$  are the points  $v_1, \dots, v_9$  defined at the end of § 4.

With the notations of § 7, identify  $N$  with  $\mathbb{C}^2$  by setting

$$e_1 = \frac{1}{3}(\omega, 1, 2),$$

$$e_2 = \frac{1}{3}(\omega^2, 1, 1).$$

We then have

$$h_0 = (1, 0, -1), \quad h_1 = (-1, 1, 0), \quad h_2 = (0, -1, 1)$$

$$3f_0 = (1, -2, 1), \quad 3f_1 = (1, 1, -2), \quad 3f_2 = (-2, 1, 1).$$

Now one has

$$L(\omega) \oplus L(\omega) \oplus L(\omega) \cap N = \sum_{j=0}^2 L(\omega) h_j \quad (= L[h])$$

while the critical set of  $Y$  (cf. 9.1)) becomes the union  $A$  of all the lines of the form

$$\mathbb{C}f_j + \zeta \quad (j = 0, 1, 2, \quad \zeta \in L[f]).$$



Using the identification, one concludes from Claim 2 that the map  $Y$  is invariant under the action on  $\mathbb{C}^2$  of the crystallographic group  $L[h] \rtimes G_6$  (the group  $\Gamma$  defined in § 7) and that  $Y/\Gamma$  identifies  $\mathbb{C}^2/\Gamma$  with  $\mathbb{C}P^2$ .

Furthermore, one has

$$Y(L_i) = v_i \quad i = 1, \dots, 12.$$

Put

$$\hat{\alpha} = \begin{pmatrix} 0 & 0 & 1 \\ 1 & 0 & 0 \\ 0 & 1 & 0 \end{pmatrix} \quad \hat{\beta} = \begin{pmatrix} 1 & 0 & 0 \\ 0 & \omega & 0 \\ 0 & 0 & \omega^2 \end{pmatrix} \quad \hat{\gamma} = \begin{pmatrix} 1 & 0 & 0 \\ 0 & 1 & 0 \\ 0 & 0 & \omega \end{pmatrix}$$

and denote by  $\hat{\delta}$  the complex conjugation map

$$[y_0, y_1, y_2] \mapsto [\overline{y_0}, \overline{y_1}, \overline{y_2}]$$

of  $M(= \mathbb{C}P^2)$  and by  $\hat{\varepsilon}$  the composition of  $\hat{\delta}$  and the mapping represented by the matrix below.

$$\begin{pmatrix} 0 & 1 & 0 \\ 1 & 0 & 0 \\ 0 & 0 & 1 \end{pmatrix}$$

We then have

$$\hat{\eta} \circ Y = Y \circ \tilde{\eta}$$

so that

$$\tilde{\eta} v_j = v_{\eta(j)} \quad j = 1, \dots, 12$$

where  $\eta = \alpha, \beta, \gamma, \delta, \varepsilon$ .

## Chapter III Additional material

§ 10 Two interesting fundamental domains for  $\Gamma$  in  $\tilde{K}$ 

The Dirichlet domain  $P$  of  $\Gamma$  with respect to  $e_1 = k_{10}$   
 Notice that the isotropy group  $\Gamma_{10}$  of  $k_{10}$  in  $\Gamma$  is the abelian group generated by the following two elements of order 3

$$\sigma_{10} = e_1 \sigma(-e_1) \quad \text{and} \quad \tilde{\gamma}_{10} = e_1 \tilde{\gamma}(-e_1)$$

while the isotropy group of  $k_{10}$  in  $\Gamma$  is trivial.

Let  $\bar{\Gamma}_{10}$  be the group generated by  $\Gamma_{10}$  and by the two involutions

$$\tilde{\delta}_{10} = \tilde{\delta} \tau \quad \text{and} \quad \tilde{\varepsilon}_{10} = e_1 \tilde{\varepsilon}(-e_1).$$

We now construct a  $\bar{\Gamma}_{10}$ -invariant polytope  $P$  and show that  $P$  is the Dirichlet domain of  $\Gamma$  with respect to  $k_{10}$ . In the orbit  $L_{10} = \Gamma k_{10}$  of  $k_{10}$  under the action of  $\Gamma$  the closest points to  $k_{10}$  are at distance  $\sqrt{2}$ . There are nine of them listed below:

$$\begin{aligned} (1 - \omega, -1) &= \tau_{67}(k_{10}) & (1 - \omega^2, -1) &= \tau_{68}(k_{10}) \\ (1 - \omega, -\omega) &= \tau_{57}(k_{10}) & (1 - \omega^2, -\omega) &= \tau_{58}(k_{10}) \\ (1 - \omega, -\omega^2) &= \tau_{47}(k_{10}) & (1 - \omega^2, -\omega^2) &= \tau_{48}(k_{10}) \end{aligned}$$

$$(0, -1) = \tau_{69}(k_{10})$$

$$(0, -\omega) = \tau_{59}(k_{10})$$

$$(0, -\omega^2) = \tau_{49}(k_{10})$$

The  $\tau_{ij}$ 's are 2 fold reflections in  $\Gamma$  with the following axes of reflections:

$$\begin{aligned} \tau_{67} &: D(2, -f_0) & \tau_{68} &: D(1, -f_0) \\ \tau_{57} &: D(0, -\omega^2 f_1) & \tau_{58} &: D(2, -\omega^2 f_1) \\ \tau_{47} &: D(1, -\omega f_2) & \tau_{48} &: D(0, -\omega f_2) \\ & & \tau_{69} &: D(0, -f_0) \\ & & \tau_{59} &: D(1, -\omega^2 f_1) \\ & & \tau_{49} &: D(2, -\omega f_2) \end{aligned}$$

where

$$D(i, \zeta) = \mathbb{C}f_i + \zeta \quad (\zeta \in L[f]) .$$

Next we find the following twelve points at distance  $\sqrt{3}$  of  $k_{10}$ :

$$\begin{aligned} (1, \omega^2 - 1) &= \sigma_6(k_{10}) & (2 - \omega, 0) &= \sigma_7(k_{10}) \\ (1, \omega - 1) &= \sigma_6^2(k_{10}) & (-2\omega, 0) &= \sigma_7^2(k_{10}) \\ (1, 1 - \omega) &= \sigma_5(k_{10}) & (-2\omega^2, 0) &= \sigma_8(k_{10}) \\ (1, \omega^2 - \omega) &= \sigma_5^2(k_{10}) & (2 - \omega^2, 0) &= \sigma_8^2(k_{10}) \\ (1, \omega - \omega^2) &= \sigma_4(k_{10}) & (\omega^2, 0) &= \sigma_9(k_{10}) \\ (1, 1 - \omega^2) &= \sigma_4^2(k_{10}) & (\omega, 0) &= \sigma_9^2(k_{10}) \end{aligned}$$

where the  $\sigma_i$ 's are the rotations of order 3 in  $\Gamma$  given as follows:

$$\begin{aligned} \sigma_6 &= \sigma(-f_0) & \sigma_7 &= \sigma^{-1}(\omega^2 f_2 - f_0) \\ \sigma_5 &= \sigma(-\omega^2 f_1) & \sigma_8 &= \sigma^{-1}(-\omega f_2 - \omega^2 f_0) \\ \sigma_4 &= \sigma(-\omega f_2) & \sigma_9 &= \sigma^{-1} \end{aligned}$$

By definition, the Dirichlet domain of  $\Gamma$  relative to  $k_{10}$  is contained in the intersection  $P$  of half spaces containing  $k_{10}$ . Furthermore, the hyperplanes bounding this domain are the perpendicular bisectors of the line segments joining  $k_{10}$  to the 21 points at distance not greater than  $\sqrt{3}$ . Let

$$\Pi = \mathbb{C}f_0 + F \text{ (as in § 8) and } \Pi' = \mathbb{C}e_1 + \mathbb{R}e_2$$

be the real hyperplanes satisfying

$$\operatorname{Re}(z_1 + z_2) = 0 \quad \text{and} \quad \operatorname{Im}(z_2) = 0$$

respectively. As indicated in the following table, the 21 hyperplanes considered are the transforms of  $\Pi$  (for the nine first) and of  $\pi'_9 = \tilde{\gamma}^2 \tau \Pi'$  (for the twelve last) by elements of  $\Gamma_{10}$ .

$\tau_{67} : \tilde{\gamma}_{10} \sigma_{10}^2$	( $\Pi$ )	$\tau_{68} : \tilde{\gamma}_{10}^2 \sigma_{10}$	( $\Pi$ )
$\tau_{57} : \tilde{\gamma}_{10}^2$	( $\Pi$ )	$\tau_{58} : \sigma_{10}^2$	( $\Pi$ )
$\tau_{47} : \sigma_{10}$	( $\Pi$ )	$\tau_{48} : \tilde{\gamma}_{10}$	( $\Pi$ )
		$\tau_{69} :$	$\Pi$
		$\tau_{59} : \tilde{\gamma}_{10} \sigma_{10}$	( $\Pi$ )
		$\tau_{49} : \tilde{\gamma}_{10}^2 \sigma_{10}^2$	( $\Pi$ )

$$\begin{array}{ll}
\sigma_6 : \tilde{\epsilon}_{10} \tilde{\delta}_{10} & (\Pi'_9) & \sigma_7 : \tilde{\gamma}_{10}^2 & (\Pi'_9) \\
\sigma_6^2 : \tilde{\epsilon}_{10} & (\Pi'_9) & \sigma_7^2 : \tilde{\gamma}_{10}^2 \tilde{\delta}_{10} & (\Pi'_9) \\
\sigma_5 : \tilde{\gamma}_{10}^2 \tilde{\epsilon}_{10} \tilde{\delta}_{10} & (\Pi'_9) & \sigma_8 : \tilde{\gamma}_{10} & (\Pi'_9) \\
\sigma_5^2 : \tilde{\gamma}_{10}^2 \tilde{\epsilon}_{10} & (\Pi'_9) & \sigma_8^2 : \tilde{\gamma}_{10} \tilde{\delta}_{10} & (\Pi'_9) \\
\sigma_4 : \tilde{\gamma}_{10} \tilde{\epsilon}_{10} \tilde{\delta}_{10} & (\Pi'_9) & \sigma_9 : & \Pi'_9 \\
\sigma_4^2 : \tilde{\gamma}_{10} \tilde{\epsilon}_{10} & (\Pi'_9) & \sigma_9^2 : \tilde{\delta}_{10} & (\Pi'_9)
\end{array}$$

In fact as we now intend to show,  $P$  is indeed the Dirichlet domain we are looking for. In order to see this, consider  $P$  as the convex hull of its vertices, thus enabling one to compute its volume. The vertices of  $P$  are the 15 points of  $L[f]$  at distance not greater than  $\sqrt{2}$  of  $k_{10}$ , namely six at distance 1 and nine at distance  $\sqrt{2}$  as tabulated below.

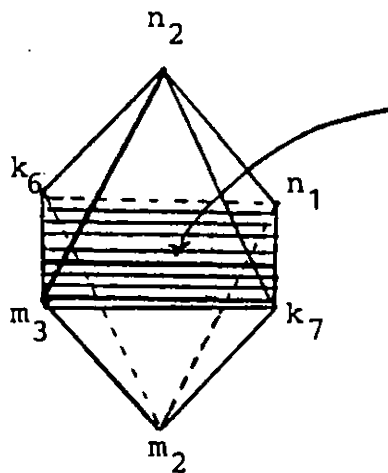
$$\begin{array}{l}
k_j \quad (4 \leq j \leq 9), \quad \ell_j \quad (1 \leq j \leq 3), \quad m_j \quad (1 \leq j \leq 3), \\
n_1 = (2, \omega), \quad n_2 = (2, \omega^2), \quad n_3 = (2, 1)
\end{array}$$

(Notice that the indexing is compatible with the coloring defined in § 1 and § 7). One can check that the set of 15 vertices of  $P$  is invariant under the group  $\bar{\Gamma}_{10}$ . The boundary of  $P$  is the union of the nine octahedra and the twelve tetrahedra shown below. The table also indicates how the  $\tau_{ij}$ 's and  $\sigma_k$ 's act on the faces.

Nine Octahedra

$$\begin{array}{ll} \tau_{67} \curvearrowright (m_3, n_2, n_1, m_2, k_6, k_7) & \tau_{68} \curvearrowright (n_2, l_1, l_3, n_1, k_6, k_8) \\ \tau_{57} \curvearrowright (m_1, n_3, n_2, m_3, k_5, k_7) & \tau_{58} \curvearrowright (n_3, l_2, l_1, n_2, k_5, k_8) \\ \tau_{47} \curvearrowright (m_2, n_1, n_3, m_1, k_4, k_7) & \tau_{48} \curvearrowright (n_1, l_3, l_2, n_3, k_4, k_8) \end{array}$$

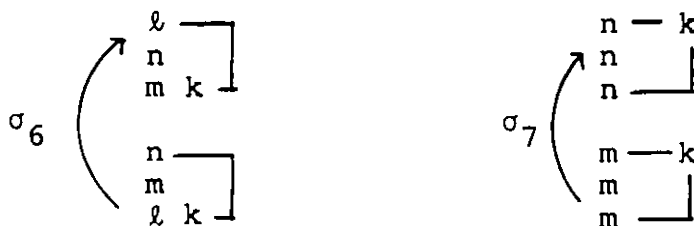
$$\begin{array}{l} \tau_{69} \curvearrowright (l_1, m_3, m_2, l_3, k_6, k_9) \\ \tau_{59} \curvearrowright (l_2, m_1, m_3, l_1, k_5, k_9) \\ \tau_{49} \curvearrowright (l_3, m_2, m_1, l_2, k_4, k_9) \end{array}$$

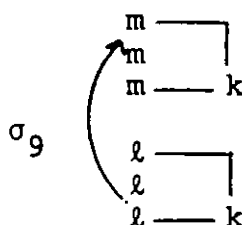
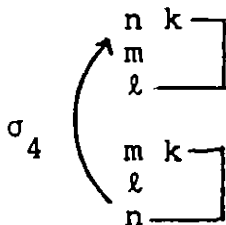
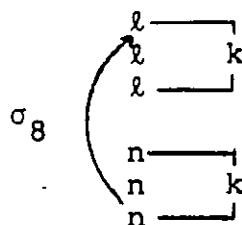
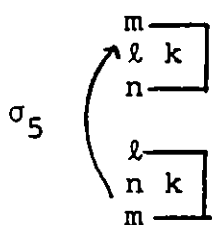


The mirror of the reflection  $\tau_{67}$

(Note that the axis of the reflection  $\tau_{ij}$  is the complex line joining  $k_i$  and  $k_j$  for  $4 \leq i \leq 6$ ,  $7 \leq j \leq 9$ .)

Twelve Tetrahedra





(Note that  $\sigma_i$  fixes  $k_i$   $4 \leq i \leq 9$ )

The convex hulls of  $k_{10}$  and each of the hyperfaces of the polytope decompose  $P$  into nine hyperpyramids of height  $\sqrt{2}/2$  with octahedral bases each of volume  $\sqrt{2}$  and twelve hyperpyramids of height  $\sqrt{3}/2$  with tetrahedral bases each of volume  $\sqrt{3}/4$ . The volume of  $P$  is therefore

$$\begin{aligned} V(P) &= \frac{1}{4} \left\{ 9 \times \frac{\sqrt{2}}{2} \times \sqrt{2} + 12 \times \frac{\sqrt{3}}{2} \times \frac{\sqrt{3}}{4} \right\} \\ &= 27/8 \\ &= V(\mathbb{E}^2/\Gamma) \quad (\text{cf. } \S 8) \end{aligned}$$

which shows that  $P$  is the Dirichlet domain of  $\Gamma$  with respect to  $k_{10}$ . Using the Poincaré theorem, one readily checks from this fact that  $\Gamma$  is generated by the nine  $\tau_{ij}$  ( $4 \leq i \leq 6, 7 \leq j \leq 9$ ) bound by the relations



$$\tau_{48} \tau_{47} \tau_{57} \tau_{59} \tau_{69} \tau_{68} = 1$$

$$\tau_{i9} \tau_{i8} = \tau_{i8} \tau_{i7}$$

$$\tau_{4j} \tau_{5j} = \tau_{5j} \tau_{6j}$$

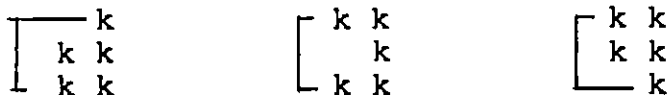
and

$$\tau_{ij}^2 = 1 \quad (\text{for } 4 \leq i \leq 6, 7 \leq j \leq 9).$$

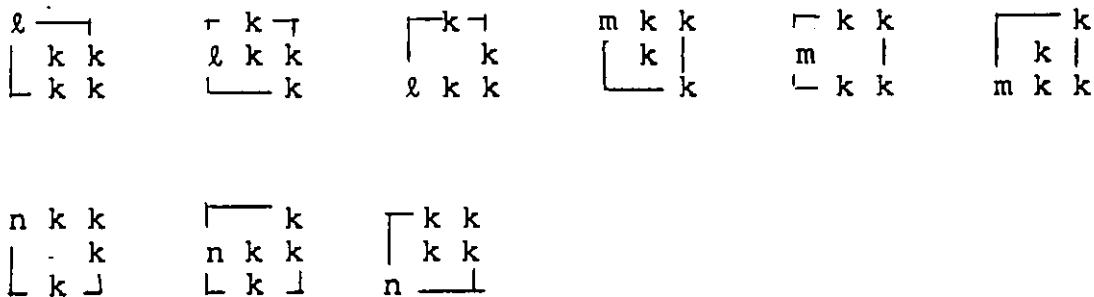
Compare this presentation with the one given in [Y2].

The polytope  $P$  is rectilinearly triangulated by the 36 4-simplices each of volume  $3/32$  listed below.

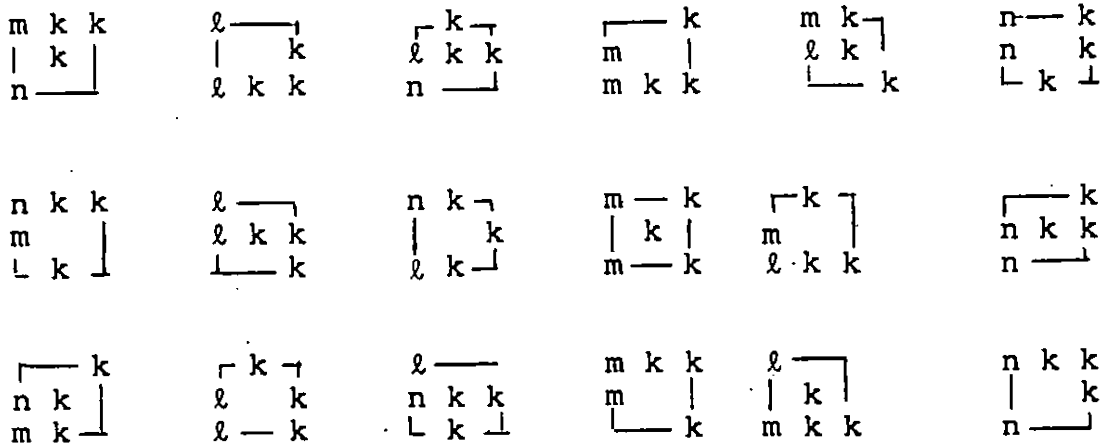
Decomposition of the central core:



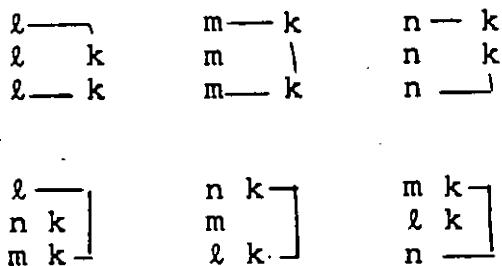
Teeth:



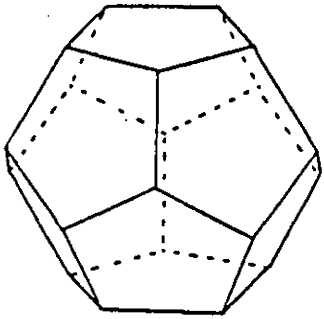
Bridges:



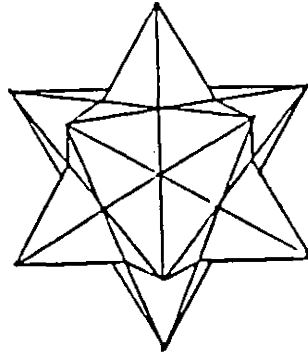
Notches:



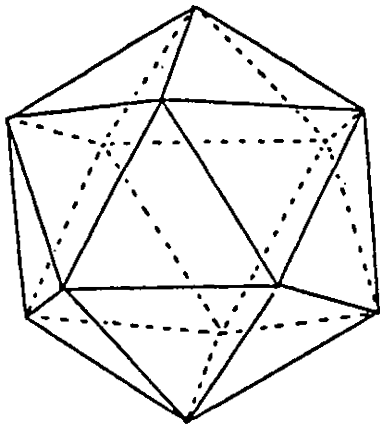
The construction of P by adding layers of simplices to the central core is exactly analogous to the following sequence of operations. Take a regular dodecahedron and stellate it in order to obtain the small starred dodecahedron (due to Kepler). Next, bridge the teeth of the starred solid to get the great Poinset dodecahedron and finally fill in the craters so as to end up with the convex hull of the starred Kepler polytope, which is a regular icosahedron.



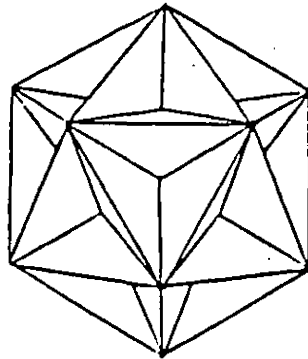
Dodecahedron



Small Dodecahedron



Icosahedron



Great Dodecahedron

In the previous list, the first 33 simplices are in  $\tilde{K}$  but the last three are in  $\tilde{\varepsilon} \tilde{K}$ . In order to get a fundamental domain  $P'$  (which is unfortunately not convex) for  $\tilde{K}$ , it suffices to replace the last three (undesired) simplices by the three following ones:

$$\begin{array}{ccc} \left[ \begin{array}{c} k' \\ n \ k \\ m \ k \end{array} \right] & \left[ \begin{array}{c} n \ k \\ l \ k' \\ l \ k \end{array} \right] & \left[ \begin{array}{c} m \ k \\ l \ k \\ l \ k' \end{array} \right] \end{array}$$

where

$$k'_4 = -k_4 + k_5 + k_6$$

$$k'_5 = k_4 - k_5 + k_6$$

$$k'_6 = k_4 + k_5 - k_6$$

The prismatic Marin fundamental domain MaD

After carefully reading § 12 below (due to A. Marin), we feel able to plug the fundamental domain described there into our display of  $\tilde{K}$  and to prove with our techniques that it is indeed a fundamental domain for the action of  $\Gamma$  both in  $\mathbb{C}^2$  and in  $\tilde{K}$ .

Claim The set MaD of vectors in  $\mathbb{C}^2$  of the form  $z + w$  where

$$z \in (\overline{k_9 \ m_1 \ k_5}) \quad \text{and} \quad w \in (\overline{k_4 \ \ell_2 \ m_4 \ k_2 \ \ell_4 \ m_2})$$

is a fundamental domain for  $\Gamma$  both in  $\mathbb{C}^2$  and in  $\tilde{K}$ .

Dictionary Observe that  $(\overline{k_9 \ m_1 \ k_5})$ ,  $(\overline{k_9 \ k_4 \ \ell_2})$ ,  $(\overline{k_4 \ \ell_2 \ m_4 \ k_2 \ \ell_4 \ m_2})$  and MaD respectively stand for Marin's  $\Delta, \Delta', H$  and  $\Delta \times H$ . Indeed one has

$$\begin{array}{lll} m_j \longrightarrow h_j & (j = 0, 1, 2), & \\ s_0 \longrightarrow k_9, & s_1 \longrightarrow m_1, & s_2 \longrightarrow k_5, \\ & s'_1 \longrightarrow k_4, & s'_2 \longrightarrow \ell_2 \end{array}$$

where the symbols on the left are Marin's notation (see § 12).

Description of MaD. The polytope MaD has the 21 following vertices:

$k_9$	$m_1$	$k_5$
$k_9 + k_4 = k_4$	$m_1 + k_4 = p_8$	$k_5 + k_4 = n_3$
$k_9 + l_2 = l_2$	$m_1 + l_2 = k'_6$	$k_5 + l_2 = p_7$
$k_9 + m_4 = m_4$	$m_1 + m_4 = m_{-8}$	$k_5 + m_4 = p_3$
$k_9 + k_2 = k_2$	$m_1 + k_2 = l_6$	$k_5 + k_2 = m_{-7}$
$k_9 + l_4 = l_4$	$m_1 + l_4 = l_8$	$k_5 + l_4 = m_3$
$k_9 + m_2 = m_2$	$m_1 + m_2 = p_6$	$k_5 + m_2 = k_7$

where  $p_3, p_6, p_7$  and  $p_8$  appear here for the first time.

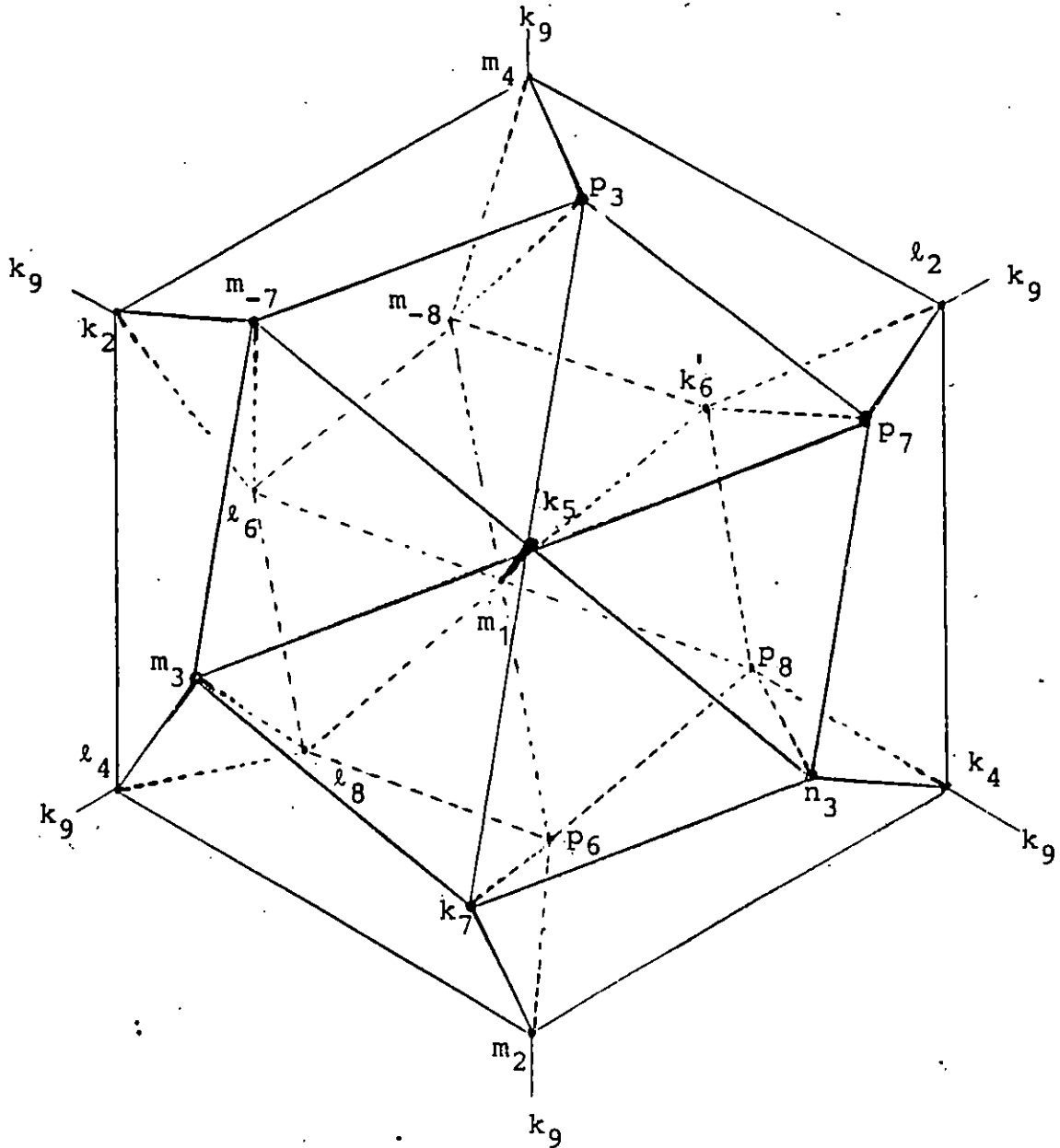
The polytope MaD is invariant under the action of  $m_1\sigma$ .

The action of  $m_1\sigma$  on these 21 vertices is given as follows:

$k_9 \mapsto m_1$	$m_1 \mapsto k_5$	$k_5 \mapsto k_9$
$k_4 \mapsto m_{-8}$	$p_8 \mapsto p_3$	$n_3 \mapsto m_4$
$l_2 \mapsto l_6$	$k'_6 \mapsto m_{-7}$	$p_7 \mapsto k_2$
$m_4 \mapsto l_8$	$m_{-8} \mapsto m_3$	$p_3 \mapsto l_4$
$k_2 \mapsto p_6$	$l_6 \mapsto k_7$	$m_{-7} \mapsto m_2$
$l_4 \mapsto p_8$	$l_8 \mapsto n_3$	$m_3 \mapsto k_4$
$m_2 \mapsto k'_6$	$p_6 \mapsto p_7$	$k_7 \mapsto l_2$

The boundary  $\partial\text{MaD}$  of this polytope decomposes into six triangular prisms whose union is a solid torus with a complementary torus which decomposes into three hexagonal prisms. These two solid tori are glued to each

other along their common boundary, which is a hollow torus  $T_0$ , decomposed into  $6 \times 3$  quadrilaterals.

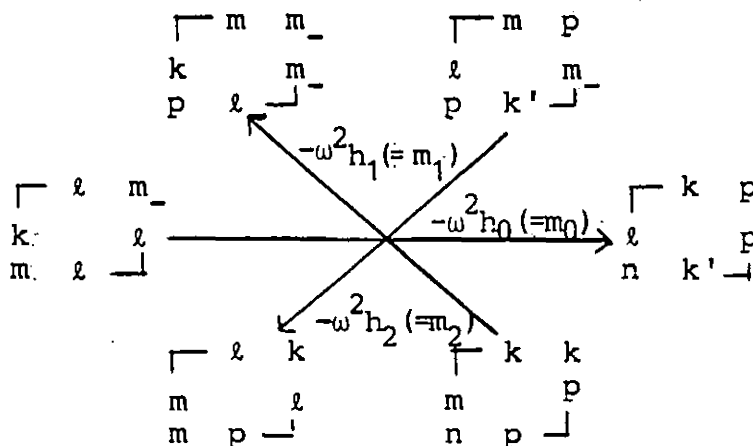


$\partial \text{MaD}$

In this picture (displaying a skewed stereographic projection of  $S^3$ ), the vertex  $k_9$  is at infinity and all the edges of  $\partial\text{MaD}$  are shown except  $\ell_6 k_9$  and  $k_9 k_3$ . Once  $\partial\text{MaD} - \{k_9\}$  has been identified with  $S^3 - \{\infty\} = \mathbb{R}^3$ , the boundary of the 2-simplex  $(k_9 m_1 k_5)$  becomes the vertical axis of  $\mathbb{R}^3$ , while (although zigzagging) the core of the hexagonal solid torus (union of the six triangular prisms) works like a horizontal circle in  $\mathbb{R}^3$  whose axis is  $\partial(k_9 m_1 k_5)$ . On the picture the action of  $m_1 \sigma$  is a rotation through  $2\pi/3$  around the  $\partial(k_9 m_1 k_5)$ -axis combined with a rotation fixing the core of the torus and moving  $\partial(k_9 m_1 k_5)$  through an angle of  $2\pi/3$ .

Proof of the claim

Translations of  $\Gamma$  permute the triangular prisms in  $\partial\text{MaD}$  as indicated now.



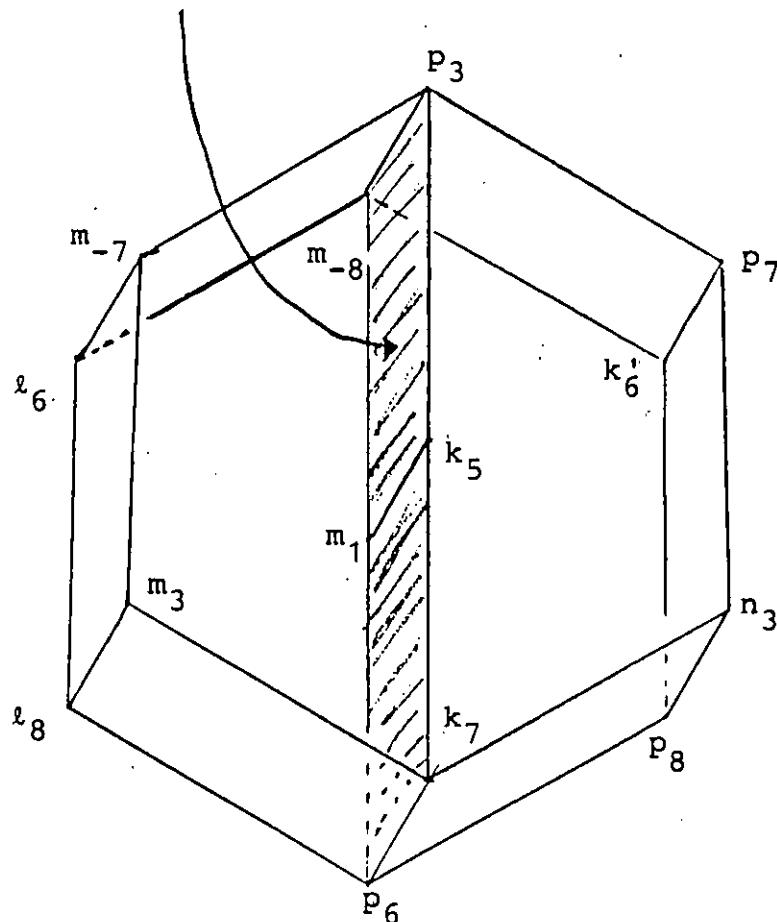


Here we are abusing the Braille notation to indicate the triangular prisms. On each of the 3 hexagonal prisms in  $\partial\text{MaD}$ , a reflection in  $\Gamma$  acts as follows,

$$\begin{aligned} \sigma^{-1}\tau\sigma (= \tau_2) & : (k_4, \ell_2, m_4, k_2, \ell_4, m_2) \mapsto (k_4, m_2, \ell_4, k_2, m_4, \ell_2) \\ & (p_8, k'_6, m_{-8}, \ell_6, \ell_8, p_6) \mapsto (p_8, p_6, \ell_8, \ell_6, m_{-8}, k'_6) \\ \sigma\tau\sigma^{-1} (= \tau_1) & : (n_3, p_7, p_3, m_{-7}, m_3, k_7) \mapsto (p_3, p_7, n_3, k_7, m_3, m_{-7}) \\ & (k_4, \ell_2, m_4, k_2, \ell_4, m_2) \mapsto (m_4, \ell_2, k_4, m_2, \ell_4, k_2) \\ \tau - \omega^2 h_0 & : (n_3, p_7, p_3, m_{-7}, m_3, k_7) \mapsto (m_3, m_{-7}, p_3, p_7, n_3, k_7) \\ (= \tau_0 + m_0 = \tau'_0) & (p_8, k'_6, m_{-8}, \ell_6, \ell_8, p_6) \mapsto (\ell_8, \ell_6, m_{-8}, k'_6, p_8, p_6) \end{aligned}$$

Here Marin's notation is given in parentheses.

The mirror of the reflection  $\tau - \omega^2 h_0$



Since the three translations and the three reflections just introduced generate the group  $\Gamma$  (see § 12), one sees that MaD is a fundamental domain of  $\Gamma$  in  $\mathbb{E}^2$ .

The fundamental domain MaD naturally splits into the six following polytopes - called Marin hyperprisms -

$$\Delta \times \Delta' = (k_9, m_1, k_5 ; k_4, p_8, n_3 ; l_2, k'_6, p_7)$$

$$\Delta \times \Delta' \tau_1 = (k_9, m_1, k_5 ; m_4, m_{-8}, p_3 ; l_2, k'_6, p_7)$$

$$\Delta \times \Delta' \delta = (k_9, m_1, k_5 ; m_4, m_{-8}, p_3 ; k_2, l_6, m_{-7})$$

$$\Delta \times \Delta' \tau_1 \delta = (k_9, m_1, k_5 ; l_4, l_8, m_3 ; k_2, l_6, m_{-7})$$

$$\Delta \times \Delta' \delta^2 = (k_9, m_1, k_5 ; l_4, l_8, m_3 ; m_2, p_6, k_7)$$

$$\Delta \times \Delta' \tau_2 = (k_9, m_1, k_5 ; k_4, p_8, n_3 ; m_2, p_6, k_7)$$

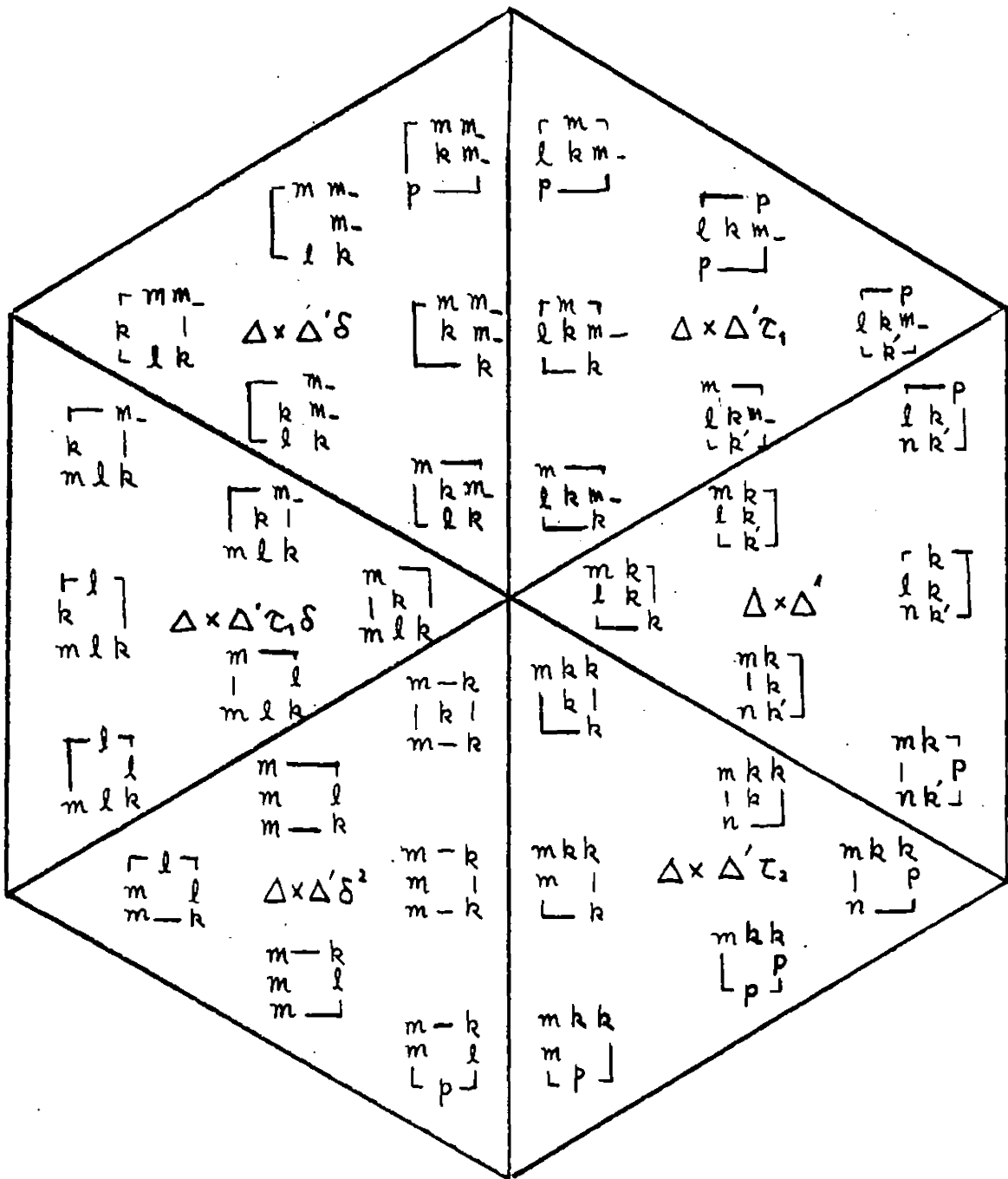
where the notations  $\tau_1, \delta$  etc. are explained in § 12.

If we use our colors to paint the Braille cell used by Marin in § 12 we get the following array,

9	1	5
4	8	3
2	6	7

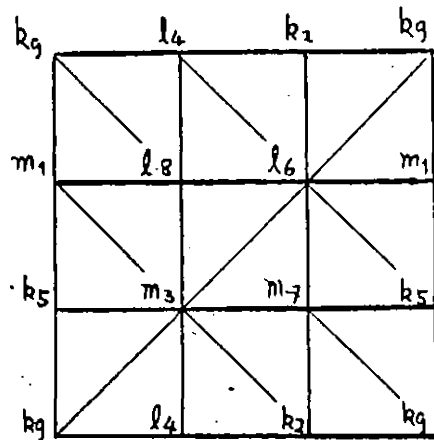
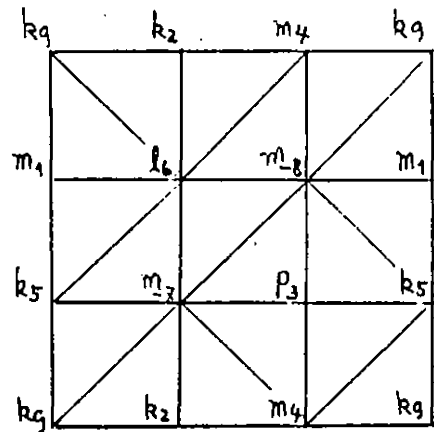
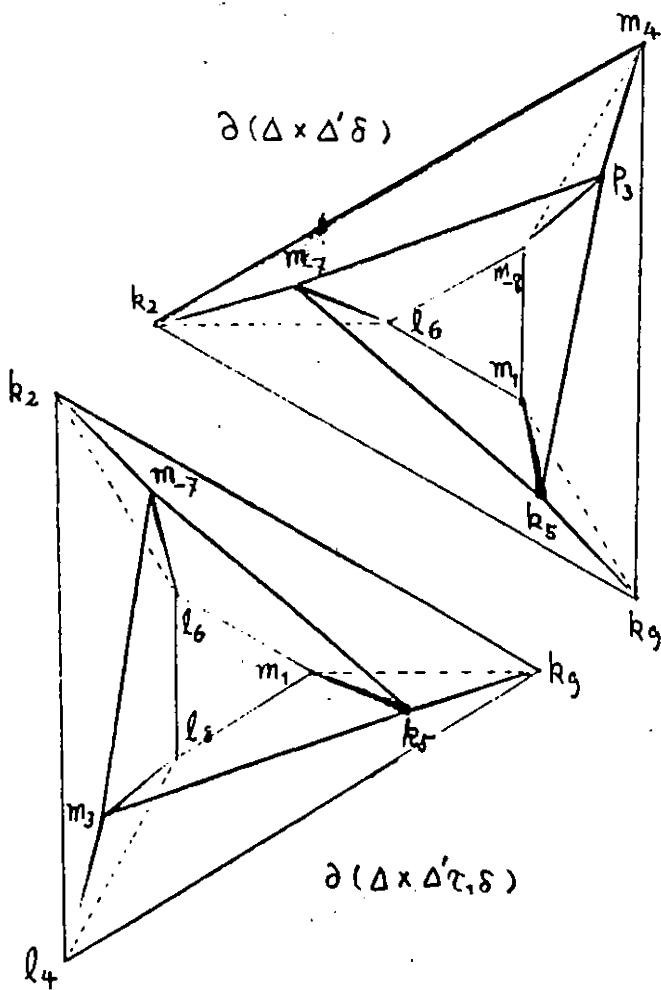
According to our conventions, the table in § 12 becomes

The triangulation of MaD

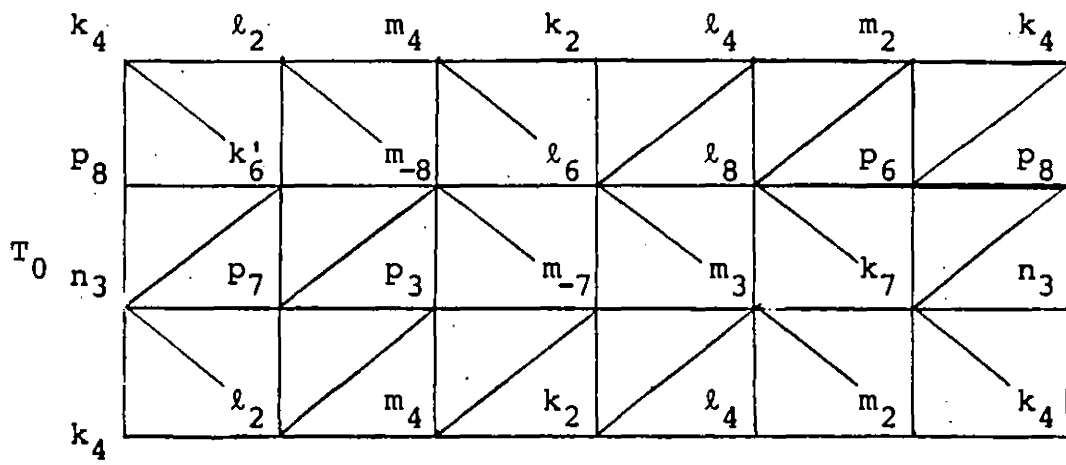


One can now easily check that the 36 4-simplices tabulated above are in  $\tilde{K}$ . If we replace letters by dots in the cells of the previous table we get the Kühnel list of § 1. This completes the proof of the claim.

The triangulation induced by  $\tilde{K}$  on the boundaries of the 6 Marin hyperprisms. Note that, because of the symmetry properties a Marin hyperprism has, the triangulation of such a prism, using only vertices of the prism, is determined by its restriction to the boundary (i.e. the union of the six triangular prisms). Each boundary splits into two complementary solid tori, whose common boundary  $T_1$  is the union of 9 quadrilaterals. Each solid torus splits in turn into 3 triangular prisms. In order to determine the triangulation of the whole boundary of a Marin hyperprism, it suffices to know what the triangulation does on  $T_1$ . Here are the splitting of the boundaries of two of the Marin hyperprisms together with the triangulations induced by  $\tilde{K}$  on the corresponding  $T_1$ 's. To obtain the boundaries of the four others, apply first once and then twice the operation  $m_1\sigma$ .



Observe that four hyperfaces of a Marin hyperprism are visible (i.e. are contained in  $\partial \text{MaD}$ ), while each of the two others is shared by another Marin hyperprism. Therefore inside  $\partial \text{MaD}$ , one has 6 invisible prisms which can be thought of as walls separating two adjacent Marin hyperprisms. The following figure shows the triangulation induced by  $\tilde{K}$  on the torus  $T_0$  considered above (see the picture of  $\partial \text{MaD}$ ).



§ 11 How does  $\mathbb{R}P^2$  fit into the picture

Let  $M_{\mathbb{R}} \cong \mathbb{R}P^2$  be the subset of  $M = \mathbb{C}P^2$  fixed by the complex conjugation  $\hat{\delta}$  defined in § 9. In this section, we exhibit the inverse image  $Y^{-1}(M_{\mathbb{R}})$  of  $M_{\mathbb{R}}$  in the complex plane  $N$  (see § 9). On  $N = \mathbb{C}^2$  define the following two complex conjugations which fix the real planes

$$E = \sum_{j=1}^2 \mathbb{R} e_j$$

and

$$F = \sum_{j=0}^2 \mathbb{R} f_j$$

respectively, by setting

$$\tilde{\delta}_E : \begin{cases} (u_0, u_1, u_2) \mapsto (\overline{u_2}, \overline{u_1}, \overline{u_0}) \\ (z_1, z_2) \mapsto (\overline{z_1}, \overline{z_2}) \end{cases}$$

$$\tilde{\delta}_F = \tilde{\delta} : \begin{cases} (u_0, u_1, u_2) \mapsto (\overline{u_0}, \overline{u_1}, \overline{u_2}) \\ (z_1, z_2) \mapsto (-\overline{z_2}, -\overline{z_1}) \end{cases} .$$

Observe that the  $Y$  is covariant with respect not only to  $\tilde{\delta}_E$  and  $\hat{\delta}$  but also to  $\tilde{\delta}_F$  and  $\hat{\delta}$ . This means that the following relations hold.

$$Y \circ \tilde{\delta}_E = \hat{\delta} \circ Y$$

$$Y \circ \tilde{\delta}_F = \hat{\delta} \circ Y .$$

In  $\Gamma$ , let  $\Gamma_E$  and  $\Gamma_F$  be the isotropy subgroups of  $E$

and  $F$  respectively. These are real crystallographic subgroups of the complex crystallographic group  $\Gamma$ . Since one has

$$\Gamma_E = \{g \in \Gamma \mid g\tilde{\delta}_E = \hat{\delta}_E g\}$$

and

$$\Gamma_F = \{g \in \Gamma \mid g\tilde{\delta}_F = \tilde{\delta}_F g\}$$

it follows that  $\Gamma_E$  is the semi-direct extension of a two dimensional lattice  $\mathbb{Z} \oplus \mathbb{Z}$  by a group of order 2 generated by a real reflection and that  $\Gamma_F$  is the affine Weyl group of type  $A_1$  (i.e. the semi-direct extension of a two dimensional lattice by the symmetric group  $S_3$ ). Here are fundamental domains  $D_E$  and  $D_F$  of  $\Gamma_E$  and  $\Gamma_F$  in  $E$  and  $F$  respectively, on which colors of points in  $L[e] \cap D_E$  and  $L[e] \cap D_F$  are shown.

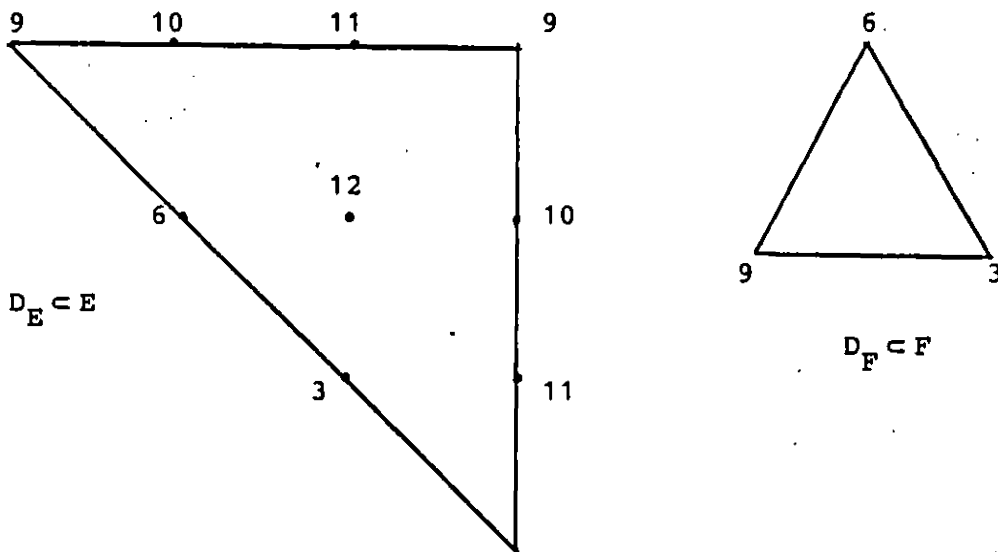


Figure 11-1



Since  $E/\Gamma_E$  is the Möbius strip obtained by identifying the vertical and horizontal sides of  $D_E$  (following the indicated color code) and since  $F/\Gamma_F$  is an equilateral triangle, one can conclude that

$$E/\Gamma_E \cup_{\partial(936)} F/\Gamma_F \cong \mathbb{R}P^2.$$

Moreover  $M_{\mathbb{R}}$  splits into  $Y(E) \cup Y(F)$  so that

$$Y^{-1}(\mathbb{R}P^2) = \left( \cup_{g \in \Gamma} gE \right) \cup \left( \cup_{g \in \Gamma} gF \right).$$

The following picture shows the intersection of  $\tilde{K}$  with  $E$ .

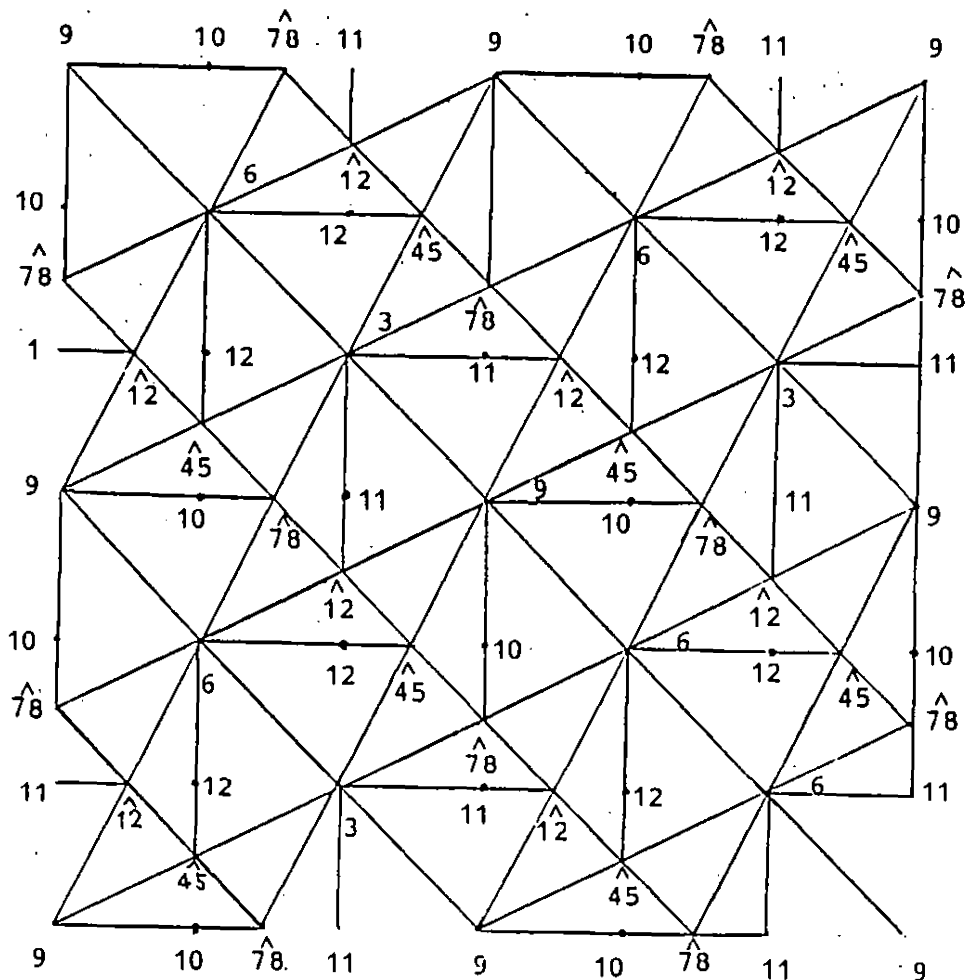


Figure 11-2

Here  $\overset{\wedge}{12}$  is the color attached to the midpoint of a segment of length  $\sqrt{3}$  whose endpoints are colored by 1 and 2. Similarly for  $\overset{\wedge}{45}$  and  $\overset{\wedge}{78}$ . Figures 11-1 and 11-2 tell us that the triangulation  $\tilde{K}$  induces on  $M_{\mathbb{R}}$  the Möbius decahedral triangulation of  $\mathbb{R}P^2$  obtained by quotienting the boundary of the regular icosahedron by the antipodal map (cf. [Mö]). The six vertices of the Möbius decahedron map to

$$3, 6, \overset{\wedge}{9}, \overset{\wedge}{12}, \overset{\wedge}{45} \quad \text{and} \quad \overset{\wedge}{78} .$$

Notice that the use of the map  $Y$  forces us to define a rectilinear embedding of the decahedron in  $|K|$  which is precisely the embedding constructed in [K-B] for quite different reasons.

§ 12 The ontological proof forcing  $\mathbb{C}P^2$  to admit  
the triangulation  $K$  (A. Marin)

The  $n$ -dimensional complex projective space is a complex crystal.

Does it have a tight triangulation with  $(n+1)^2$  vertices?

### 0. Introduction

To each elliptic curve and each integer  $n$  there is associated an  $n$ -dimensional complex crystal <sup>1)</sup> invariant under the action of a group  $I_{n+1}$  isomorphic to  $\mathbb{Z}/(n+1)\mathbb{Z} \oplus \mathbb{Z}/(n+1)\mathbb{Z}$ . This crystal is naturally isomorphic, as a complex space, to the  $n$ -dimensional complex projective space  $\mathbb{C}P^n$ . It is also the union of  $(n+1)!$  flat prisms  $\Delta^{n \times n}$ , and the symmetry group  $I_{n+1}$  respects this decomposition into primes. All these prisms have the same vertices (they are  $(n+1)^2$  in number) <sup>2)</sup>.

One is then faced with the following:

Main Problem Find a triangulation of the crystal, having  $(n+1)^2$  vertices, invariant under the group  $I_{n+1}$  and giving a linear subdivision of each prism.

In the case  $n = 2$  a systematic search gives essentially one solution: the Kühnel triangulation of  $\mathbb{C}P^2$ . We were unfortunately unable to make the same search for other values of  $n$  (except of course for  $n = 1$ ). We ask the reader

to work out the case  $n = 3$ , and, why not, to solve the more general problem of finding a triangulation of the  $\mathbb{C}P^n$  crystal with  $(n + 1)^2$  vertices.

Behind the Main Problem is the following:

Question A If the above problem has a solution, does it define a substantial tight embedding of the complex projective space  $\mathbb{C}P^n$  into the boundary of the  $n^2 + 2n$  dimensional simplex ?

For tightness theory, consult the following survey article by N. Kuiper [K]. Let us just recall that if  $hF_n$  is the real affine space of hermitian forms of trace one in  $(n + 1)$  variables, then the set  $V_n$  consisting of those forms which are the product of a linear form and its conjugate is a substantial tight submanifold of  $hF_n$ . The manifold  $V_n$  is diffeomorphic to  $\mathbb{C}P^n$  and the affine space  $hF_n$  is of (real) dimension  $n^2 + 2n$ .<sup>3)</sup> Observe also that  $V_n$  lies on the boundary of the open convex set of all positive definite trace one hermitian forms.

Observe also that a triangulation of  $\mathbb{C}P^n$  must have at least  $(n + 1)^2$  vertices. In fact: If there is a map  $f$  from a  $2n$ -dimensional complex  $K_n$  to  $\mathbb{C}P^n$  which is non zero on  $H_{2n}(K_n, \mathbb{Z}/2\mathbb{Z})$  then  $K_{2n}$  has at least  $(n + 1)^2$  vertices.

[Make the map transversal to a  $\mathbb{C}P^{n-1}$  disjoint from the image of a  $2n$ -simplex  $\Delta$  of  $K_n$ . Deduce that, in the full subcomplex of  $K_n$  generated by the vertices not lying in  $\Delta$ , there is a subcomplex  $K_{n-1}$  of dimension  $2n-2$  which is a mod 2  $2n-2$  cycle  $[K_{n-1}]$ , such that  $f_*([K_{n-1}])$  is non zero. Conclude by induction on  $n$  <sup>4)</sup>.] We conjecture that if  $K_n$  has exactly  $(n+1)^2$  vertices such a map  $f$  is a homotopy equivalence. If this conjecture is true, it is easy to prove (by the same sort of induction as above) that such a complex is a tight subcomplex of  $\Delta^{n^2+2n}$ . This would provide an affirmative answer to Question A. (It would in fact be enough if  $f$  gave an isomorphism in homology mod 2).

Recall that Kuiper proved that any smooth substantial tight embedding of  $\mathbb{C}P^2$  into  $\mathbb{R}^8$  has an image congruent under a projective transformation of  $\mathbb{R}^8$  to the "hermitian form model"  $V_2$  (The Kühnel triangulation is a counter example to the conjecture of Kuiper that you can release the smoothness hypothesis in this last statement).

We can foolhardily extend a question Kuiper asked in the above cited survey:

Question B Let  $f: \mathbb{C}P^n \rightarrow \mathbb{R}^{n^2+2n}$  be a substantial topological tight embedding. Is its image congruent under a projective transformation of  $\mathbb{R}^{n^2+2n}$  either to the "hermitian form model"  $V_n$  or to the subcomplex of the  $n^2 + 2n$  dimensional simplex given by some solution of the Main Problem ?

Recall that Kuiper and Pohl answered affirmatively the analogous question for substantial tight embeddings of  $\mathbb{R}P^2$  into  $\mathbb{R}^5$ . (The image is congruent either to the Veronese surface or to the subcomplex of the boundary of the 5 simplex realising the triangulation of  $\mathbb{R}P^2$  which is the quotient by the antipodal map of the isocahedron).

Let us now leave aside the speculations, clarify the above statements and give some hints as to how to prove them.

Notes

1) A crystal is an orbifold which is the quotient of a flat torus by a finite group of isometries, equivalently (by Bieberbach's theorem) a crystal is the quotient of a euclidean space by a discrete uniform group of isometries (a crystallographic group) which is called the group of the crystal .

2) Unlike the natural isomorphism between the crystal and  $\mathbb{C}\mathbb{P}^n$  this decomposition of the crystal into prisms depends not only on the elliptic curve, but also on a splitting of it, as a real Lie group, into a product  $\mathbb{R}/\mathbb{Z} \times \mathbb{R}/\mathbb{Z}$  (i.e. a choice of basis for the lattice  $L = \pi_1(E)$ ).

3) A formula for this Veronese type embedding is

$$\phi([z_0 : \dots : z_n]) = \left( \sum_{i=0}^n |z_i|^2 \right)^{-1} (z_i \bar{z}_j) .$$

4) This sketch of proof gives also: If there is a map from a complex  $K_n$  to  $\mathbb{C}\mathbb{P}^n$  which is non zero on  $H_{dn}(K_n; \mathbb{Z}/2\mathbb{Z})$  then  $K_n$  has at least  $1 + (d+1) + \dots + (nd+1) = \frac{(n+1)(dn+2)}{2}$  vertices. Here  $\mathbb{K}$  is one of the fields  $\mathbb{R}, \mathbb{C}$  or  $\mathbb{H}$  (the quaternions) and  $d$  its dimension over  $\mathbb{R}$ . Observe that this bound is one more than the dimension over  $\mathbb{R}$  of the space of trace one hermitian forms over  $\mathbb{K}$  in  $n+1$

#### 12.4.II

variables, in which  $k\mathbb{P}^n$  embeds as the subset of trace one forms which split into the product of a linear form and its conjugate. When  $d = 4$  and  $n = 2$ , the minimum number of vertices is fifteen; this bound is actually attained, since W. Kühnel recently produced an explicit triangulation of  $HP^2$  with 15 vertices ([B-K]).



1 The unique degree  $n+1$  embedding of an elliptic curve in the  $n$ -dimensional complex projective space  $\mathbb{C}P^n$ .

Let  $E$  be an elliptic curve. \*) By the Riemann-Roch theorem there exists a degree  $n+1$  embedding  $\varphi$  of  $E$  into  $\mathbb{C}P^n$ . Abel's theorem asserts that the sum in  $E$  of the  $n+1$  points of a hyperplane section of  $\varphi(E)$  is independent of the section. Composing  $\varphi$  with a translation in  $E$  we may assume that this sum is zero (the embedding  $\varphi$  is then unique up to projective transformations of  $\mathbb{C}P^n$ ). Let  $E_{n+1}$  be the subgroup of points of order  $n+1$  in  $E$ , it is isomorphic to  $\mathbb{Z}/(n+1)\mathbb{Z} \oplus \mathbb{Z}/(n+1)\mathbb{Z}$  and is mapped by  $\varphi$  to the points of hyperinflection of the curve  $\varphi(E)$ .

---

(\*) An elliptic curve  $E$  is the quotient of the Gauss plane  $\mathbb{C}$  by a lattice  $L$ .

## 2 The complex crystal structure on $\mathbb{C}P^n$ .

Consider the abelian variety

$A^n = \{(z_0, \dots, z_n) \in E^{n+1} \mid z_0 + \dots + z_n = 0\}$  and the holomorphic mapping  $\Pi$  from  $A$  to the complex projective space  $\hat{\mathbb{C}P}^n$  of hyperplanes in  $\mathbb{C}P^n$  which associates to the point  $(z_0, \dots, z_n)$  of  $A$  the hyperplane of  $\mathbb{C}P^n$  passing through the points  $\varphi(z_0), \dots, \varphi(z_n)$ . (If  $k$  of the points  $\varphi(z_i)$  are equal, interpret passing through these  $k$  points as having there a contact of order  $k$  with the curve  $\varphi(E)$ .) The Riemann-Roch theorem implies that there is a unique such hyperplane.

We call the abelian variety  $A$  symmetric because the symmetric group  $\mathcal{S}_{n+1}$  acts on  $A$  on the right by permutation of the coordinates. (\*) The complex projective space  $\hat{\mathbb{C}P}^n$  is isomorphic via  $\Pi$  to be the quotient  $A/\mathcal{S}_{n+1}$ .

The points of  $A$  fixed by  $\mathcal{S}_{n+1}$  are the diagonal points  $(z, \dots, z)$  where  $z$  is in  $E_{n+1}$  (because  $(z, \dots, z)$  is in  $A$  if and only if  $0 = z + \dots + z = (n+1)z$ ). These points form a subgroup  $I_{n+1}$  of  $A$ . Since the translations by elements of  $I_{n+1}$  commute with the action of  $\mathcal{S}_{n+1}$  they induce an action on the left of the group  $I_{n+1}$  on the crystal  $\hat{\mathbb{C}P}^n = A/\mathcal{S}_{n+1}$ .

---

(\*) Recall that  $E^{n+1}$  is the space of mappings from the set  $\{0, 1, \dots, n\}$  to  $E$  and that a permutation  $\sigma$  of  $\{0, 1, \dots, n\}$  acts on each  $x$  of  $E^{n+1}$  by composition in the source. This action is given by the formula

$$(z_0, \dots, z_n) \cdot \sigma = (z_{\sigma(0)}, \dots, z_{\sigma(n)}).$$

3 The symmetric Abelian variety  $A$  splits into the product  $T \times T'$  of two symmetric real tori (the action of  $\mathcal{S}_{n+1}$  being diagonal).

Let  $L$  be a lattice in  $\mathbb{C}$  such that the elliptic curve  $E$  is isomorphic to  $\mathbb{C}/L$  and let  $(e, e')$  be a basis of  $L$ . Then  $E$  splits, as a real Lie group, into a product  $\mathbb{R}e/\mathbb{Z}e \times \mathbb{R}e'/\mathbb{Z}e' (\cong \mathbb{C}/L \cong E)$ . Accordingly  $A^n$  splits into a product  $T^n \times T'^n$  where  $T^n$  and  $T'^n$  are two copies of the symmetric  $n$ -dimensional real torus:

$$T^n = \{(x_0, \dots, x_n) \in (\mathbb{R}/\mathbb{Z})^{n+1} \mid x_0 + \dots + x_n = 0\}.$$

The symmetric group  $\mathcal{S}_{n+1}$  acts on the right on  $T$  by permutation of the coordinates. The fixed points of that action form a cyclic subgroup  $J_{n+1}$  of order  $n+1$  of  $T$  which acts on the left on the crystal  $T/\mathcal{S}_{n+1}$ . The original action of  $\mathcal{S}_{n+1}$  on  $A$  corresponds to the diagonal action of  $\mathcal{S}_{n+1}$  on  $T \times T'$ .

4 The real crystal  $T/\mathcal{S}_{n+1}$  .

In the euclidean space  $\mathbb{R}^{n+1}$ , equipped with its canonical basis  $(e_0, \dots, e_n)$ , consider the hyperplane  $P$  with equation  $x_0 + \dots + x_n = 0$ ; let  $M$  denote the lattice  $P \cap \mathbb{Z}^{n+1}$ . The lattice  $M$  is generated by the vectors  $m_1, \dots, m_n$  where  $m_i = e_i - e_{i-1}$ ; in addition, let  $m_0 = e_0 - e_n$  (in the sequel all indices are to be thought of as modulo  $n+1$ ).

The symmetric group  $\mathcal{S}_{n+1}$  acts linearly and isometrically on the right on  $P$  by permuting the coordinates. For example the transposition  $\tau_i$  exchanging the  $i$ -th and  $(i-1)$ th coordinates gives the linear reflection which fixes the linear hyperplane  $H_i$  of  $P$  orthogonal to  $m_i$ . The figure below<sup>(\*)</sup> depicts the case  $n=2$ . Observe that when  $n=2$ , choosing the orientation of  $P$  given by the basis  $(m_1, \dots, m_n)$ , the circular permutation  $\delta = \tau_n \dots \tau_1$  acts as a direct (or anticlockwise) rotation through  $2\pi/3$ .

---

(\*) For the time being, mentally erase the as yet undefined elements  $\hat{H}_0$ ,  $\Delta_i$  and  $s_i$  of that figure. Their meaning will be explained in due course.

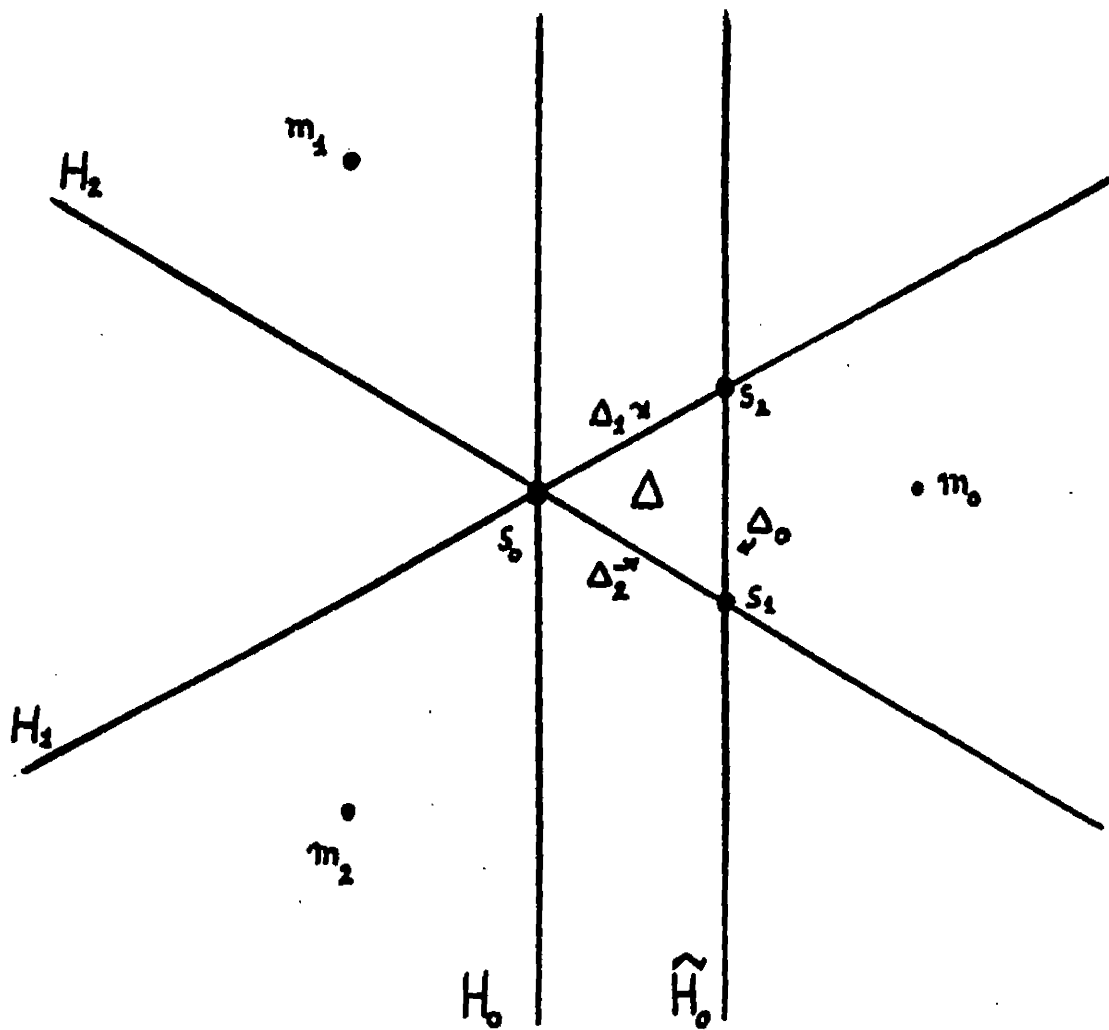


Figure 12-1

Let  $G$  be the crystallographic group generated by  $s_{n+1}$  and the translations of the lattice  $M$ . We shall use the notations  $\rho: P \rightarrow P/M = T$ ,  $\pi: P \rightarrow P/G$  and  $\bar{\pi}: T \rightarrow T/s_{n+1}$  to indicate the quotient maps.

Consider the  $n$ -simplex

$$\Delta = \{x \in P \mid (x|m_i) \leq 0 \text{ for } i = 1, \dots, n \text{ and } (x|m_0) \leq 1\}$$

which is bounded by the hyperplanes of symmetry of the reflections  $\hat{\tau}_0 = \tau_0 m_0, \tau_1, \dots, \tau_n$ . Let  $\Delta_0, \Delta_1, \dots, \Delta_n$  denote the corresponding faces of  $\Delta$ ,

Claim 1 The angle between two "consecutive" faces  $\Delta_i$  and  $\Delta_{i-1}$  is  $\pi/3$ , and, in the remaining cases, the angle between  $\Delta_i$  and  $\Delta_j$  is  $\pi/2$ .

This is true because  $m_i$  is orthogonal to  $\Delta_i$ , and the scalar products of the  $m_i$  are  $(m_i | m_i) = 2$ ,  $(m_i | m_{i-1}) = -1$  and  $(m_i | m_j) = 0$  in the other cases. ■

Claim 2 The simplex  $\Delta$  is a fundamental domain for the action of  $G$  on  $P$ . □

Since the angles between faces of  $\Delta$  are submultiples of  $\pi$ , you can prove, just as in the case of the Schwarz triangle groups, (\*) that  $\Delta$  is a fundamental domain for the action on  $P$  of the group  $G_0$  generated by the reflections  $\hat{\tau}_0, \tau_1, \dots, \tau_n$ . But since  $\tau_1, \dots, \tau_n$  generate the symmetric group  $S_{n+1}$ ,  $m_0 = \tau_0 \hat{\tau}_0$  and  $m_i = \delta^{-1} m_{i-1} \delta$  where  $\delta = \tau_n \dots \tau_1$  is induced by the cyclic permutation of the coordinates  $i \mapsto i - 1$ , the group  $G_0$  is equal to the group  $G$  and the simplex  $\Delta$  is a fundamental domain for the action of  $G$  on  $P$ . ■

---

(\*) See for example the account in paragraph 2 (p. 178-181) of [M1].

We can express the last claim in the following commutative diagram, where the natural maps on the bottom line are isomorphisms.

$$(1) \quad \begin{array}{ccccc} \Delta & \hookrightarrow & P & \xrightarrow{\rho} & T = P/M \\ \downarrow \cong & & \downarrow \pi & & \downarrow \bar{\pi} \\ \Delta & \xrightarrow{\cong} & P/G & \xrightarrow{\cong} & T/\mathfrak{S}_{n+1} \end{array}$$

Claim 2' The polyhedron  $H = \bigcup_{\sigma \in \mathfrak{S}_{n+1}} \Delta \cdot \sigma$  is the Dirichlet domain at the origin of the lattice  $M$ .

□

The face of the simplex  $\Delta \cdot \sigma$  which does not contain the origin is  $\Delta_0 \cdot \sigma$ . As the angles between this face and the other faces of  $\Delta \cdot \sigma$ , being  $\pi/3$  or  $\pi/2$ , are less than or equal to  $\pi/2$ , the polyhedron  $H$  is convex and is equal to  $\bigcap_{\sigma \in \mathfrak{S}_{n+1}} \hat{H}_{0-} \cdot \sigma$ . Here  $\hat{H}_{0-} \cdot \sigma = \{x \in P \mid (x | m_0 \cdot \sigma) \leq 1\}$  is the half space consisting of points nearer to 0 than to  $m_0 \cdot \sigma$  (its boundary is the hyperplane  $\hat{H}_0 \cdot \sigma$  carrying the face  $\Delta_0 \cdot \sigma$  of  $\Delta \cdot \sigma$ ). The polyhedron  $H$  contains the Dirichlet domain at 0 of the lattice  $M$ . It is in fact equal to that Dirichlet domain because, by diagram (1) they have the same volume.

■

The polyhedron  $H$  in case  $n = 2$

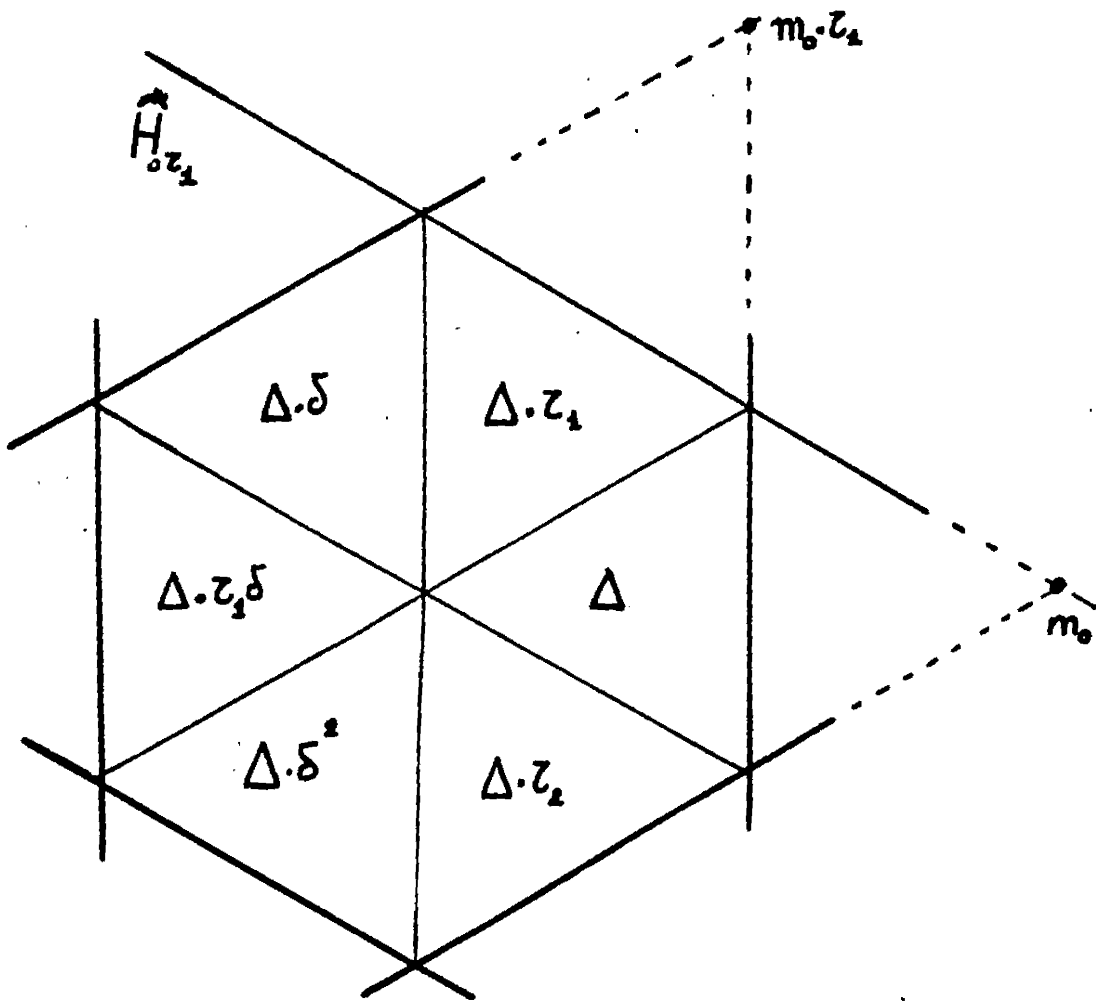


Figure 12-2



Claim 3 The images in the torus  $T$  of the vertices of  $\Delta$  are the points of  $J_{n+1}$ .

□

The image of  $\Delta$  in  $T$  is a fundamental domain for the action of  $\mathcal{S}_{n+1}$  and so the images of the  $n+1$  vertices of  $\Delta$  are fixed by  $\mathcal{S}_{n+1}$ . The claim then follows because the fixed point set  $J_{n+1}$  of the action of  $\mathcal{S}_{n+1}$  on  $T$  also has  $n+1$  elements.

■

Let  $\mathcal{S}_n$  be the isotropy subgroup of the last letter  $n$ .

Claim 4 The polyhedron  $K = \bigcup_{\sigma \in \mathcal{S}_n} \Delta \cdot \sigma$  is a parallelepiped which is a fundamental domain for the lattice  $\bar{M} = \rho^{-1}(J_{n+1})$ , and whose vertices form a set of generators for the group  $\bar{M}$ .

□

Let  $n_0, \dots, n_{n-1}$  be the orbit of  $m_0$  under the group  $\mathcal{S}_n$  ( $n_i$  has  $-1$  as last ( $n^{\text{th}}$ ) coordinate,  $1$  as  $i$ th coordinates and zeros elsewhere). Since  $n_{n-1} = -m_n$ , the set  $n_0, \dots, n_{n-1}$  is also the orbit of  $-m_n$  under  $\mathcal{S}_n$ . Clearly  $K$  is included in

$$\begin{aligned} & \{x \in P \mid (x \mid m_n \cdot \sigma) \leq 0 \quad \text{and} \quad (x \mid m_0 \cdot \sigma) \leq 1 \quad \text{for all } \sigma \text{ in } \mathcal{S}_n\} \\ &= \{x \in P \mid 0 \leq (x \mid n_i) \leq 1 \quad \text{for } i = 0, \dots, n-1\} \end{aligned}$$

This is a parallelepiped  $\tilde{K}$ . As  $\mathcal{S}_n$  is of index  $n+1$

in  $\mathcal{S}_{n+1}$  (the classes being represented by  $\delta^k$  for  $k = 0, \dots, n$ ) and the polyhedron  $H$  is the non overlapping union of the  $n+1$  parallelepipeds  $\tilde{K} \cdot \delta^k$ , it follows that the polyhedron  $K$  is equal to the parallelepiped  $\tilde{K}$ . Since the vertices of this parallelepiped are in the  $\mathcal{S}_n$  orbit of the vertices of  $\Delta$ , Claim 3 asserts that the lattice generated by these points is included in  $\bar{M} = \rho^{-1}(J_{n+1})$ . A final index (or volume) consideration tells us that this is in fact an equality and  $K$  is thus a fundamental domain for the lattice  $\bar{M}$ . The set of those vertices of  $K$  which are joined to the origin by an edge of  $K$  must then be a basis for  $\bar{M}$ .

Let us denote by  $s_i$  the vertex of  $\Delta$  opposite to the face  $\Delta_i$ .

The polyhedron  $K$  in the case  $n = 2$

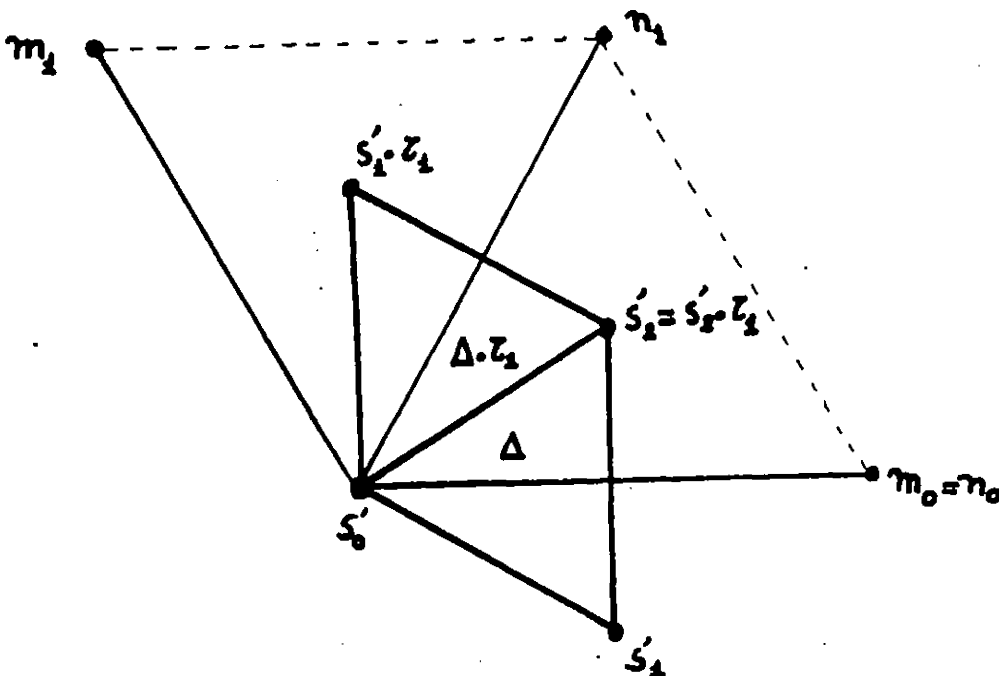


Figure 12-3

Claim 5 The image in  $T$  of the vertex  $s_1$  generates the group  $J_{n+1}$  and we have  $s_i - s_1 = s_{i-1} \cdot \delta$  for  $i = 0, 1, \dots, n$ .

□

First note that  $s_1 + s_n = m_0$  (note that  $s_1 + s_n$  is an eigenvector of the isometry which maps  $m_i$  to  $m_{-i}$ . As  $s_1$  and  $s_n$  are orthogonal to  $m_2, \dots, m_{-1}$  and the plane  $H'_0$  perpendicularly bisecting  $Om_0$  the eigenvector  $s_1 + s_n$  must be  $m_0$ ).

Now since  $\delta$  cyclically permutes the  $m_i$  ( $m_{i-1} \cdot \delta = m_i$ ) and the  $m_i$  are orthogonal to the faces  $\Delta_i$  of  $\Delta$ , the simplex  $\Delta \cdot \delta$  is a translate of  $\Delta$ . In  $\Delta \cdot \delta$  the origin is opposite to the face  $\Delta_0 \delta$  which is parallel to  $\Delta_1$ , the face opposite to  $s_1$  in  $\Delta$ , so that we must have  $\Delta \cdot \delta = \Delta - s_1$ . The angle condition of claim 1 gives a cyclic order on the faces and hence on the vertices of  $\Delta$  leaving two possibilities for  $s_i - s_1$ :

Either  $s_i - s_1 = s_{1-i} \cdot \delta$  for  $i = 1, \dots, n, n+1$  which is ruled out by the relation  $s_1 + s_n = m_0$  (this relation with  $-s_1 = s_0 - s_1 = s_1 \cdot \delta$  implies  $s_n = s_1 \cdot \delta + m_0$  contradicting the fact that distinct points in  $\Delta$  are not congruent under the group  $G$  (Claim 2)).

Or the formula of Claim 5

$$s_i - s_1 = s_{i-1} \cdot \delta \quad \text{for } i = 0, 1, \dots, n.$$

As the  $\delta^k$  exhaust the classes of  $s_n$  in  $s_{n+1}$  this formula implies that the image of  $-s_1$  is of order  $n+1$  in the cyclic group  $J_{n+1}$  proving that  $-s_1$  hence  $s_1$  is a generator of that group. ■

Claim 5' The cyclic group  $J_{n+1}$  acts on  $T/s_{n+1}$  viewed as the simplex  $\Delta$  by permutation of its vertices. The generator  $s_1$  acts by  $s_i \mapsto s_{i+1}$ . ■

If you prefer to verify the claims of this paragraph by calculus, the coordinates in  $\mathbb{R}^{n+1}$  of the  $i^{\text{th}}$  vertex  $s_i$  of  $\Delta$  are:

$$s_i = \left( \underbrace{1 - \frac{i}{n+1}, \dots, 1 - \frac{i}{n+1}}_{i \text{ times}}, \frac{-i}{n+1}, \dots, \frac{i}{n+1} \right)$$

5 The prismatic decomposition of  $T \times T' / \mathcal{S}_{n+1}$  . Looking for a triangulation of the crystal  $\mathbb{CP}^n$  with  $(n+1)^2$  vertices

The first projection  $T \times T' \rightarrow T$  induces a map  $p: T \times T' / \mathcal{S}_{n+1} \rightarrow T / \mathcal{S}_{n+1} \approx \Delta$ , which is an orbifold fibration with generic fiber  $T'$ . Over a point  $x$  of the boundary  $\Delta$ , the fiber  $T'$  is folded by the subgroup of  $\mathcal{S}_{n+1}$  generated by the reflections  $\tau_i$  along the faces  $\Delta_i$  of  $\Delta$  which contain  $x$ .

The polyhedron  $\Delta \times H'$  (\*) is then a fundamental domain in  $P \times P'$  for the action of the group  $G$  on the crystal  $T \times T' / \mathcal{S}_{n+1}$ . This fundamental domain is the union of the  $(n+1)!$  flat prisms (\*\*)  $\Delta \times \Delta' \cdot \sigma$  for  $\sigma$  in  $\mathcal{S}_{n+1}$ .

The Main Theorem is: Find the triangulations of the crystal  $T \times T' / \mathcal{S}_{n+1}$ , invariant under the symmetry group  $I_{n+1}$  ( $= J_{n+1} \times J'_{n+1}$ ), and which are good for that decomposition into flat prisms, in the sense that they induce on each prism  $\Delta \times \Delta' \cdot \sigma$  a linear subdivision which does not add any new vertex.

Since by claim 5 of § 4 a generator of the group  $J'_{n+1}$

---

(\*) Recall that  $T'$  is a second copy of  $T$  so that  $P', \Delta', H', K'$ , and  $J'_{n+1}$  will be the corresponding copies of  $P, \Delta, H, K$  and  $J_{n+1}$ .

(\*\*) A flat prism in a crystal  $X = P/G$  is a subset  $Y$  of  $X$  such that there exist in the euclidean space  $P$  an affine prism  $\Delta_1 \times \Delta_2$  such that the quotient  $\pi: P \rightarrow P/G$  induces a homeomorphism between  $\Delta_1 \times \Delta_2$  and  $Y$ .

sends the prism  $\Delta \times \Delta' \cdot \sigma$  to the prism  $\Delta \times \Delta' \cdot \delta\sigma$  (\*)  
 no prism of the crystal  $T \times T' / \mathcal{S}_{n+1}$  is conversed by a  
 non trivial element of  $J'_{n+1}$ . Therefore we have to find  
 the simplicial decompositions of the crystal  $J'_{n+1} \backslash T \times T' / \mathcal{S}_{n+1}$ ,  
 invariant under the group  $J_{n+1}$  and good for the  
 decomposition into prisms  $\Delta \times \Delta' \cdot \sigma$ ,  $\sigma \in \mathcal{S}_n$

A flat fundamental domain for this last crystal is the  
 polyhedron  $\Delta \times K'$  (Claim 4 of §§ 4) the main problem reduce  
 then to find a linearsubdivision S of the decomposition  
into prisms of that polyhedron which does not add any new  
vertex and satisfies the following:

Compatibility and invariance conditions.

1) First Compatibility Condition

The restriction of the subdivision to the facet  $\Delta_1 \times K'$   
is invariant under  $\text{id} \times \tau_1$ .

2) Second Compatibility Condition

The restriciton of the subdivision to the facets  $\Delta \times F'_{i0}$   
and  $\Delta \times F'_{i1}$  are isomorphic via the translation which  
maps one of these facets to the other (Here  $F'_{ij}$  are :

---

(\*) Recall that  $J_{n+1}$  is the fixed point set of the action  
 of  $\mathcal{S}_{n+1}$  on  $T'$  so that:  $\Delta' \cdot \sigma - s'_1 = \Delta' \cdot \sigma - s'_1 \cdot \sigma = (\Delta' - s'_1) \cdot \sigma$   
 $= (\Delta' \cdot \sigma) \cdot \sigma = \Delta' \cdot \delta\sigma.$

the facets of the parallelepiped  $K'$ : for  $j = 0, 1$   
 and  $i = 0, \dots, n-1$  the facet  $F'_{ij}$  is  
 $\{x \in K' \mid (x \mid n_i) = j\}$ .

### 3) Invariance Condition

For all  $\sigma$  in  $\mathfrak{S}_n$  the affine mapping sending

$$(s_i, s'_j \cdot \sigma) \text{ to } (s_{i-1}, s'_{j-(1+\sigma(0))} \cdot \delta \delta^{\sigma(0)} \sigma \delta^{-1})$$

induces an isomorphism between the restrictions of

the subdivision to the prisms  $\Delta \times \Delta' \cdot \sigma$  and  $\Delta \times \Delta' \cdot \delta \delta^{\sigma(0)} \sigma \delta^{-1}$ .

Note that  $\delta^{\sigma(0)} \sigma(0) = 0$  hence  $\delta \delta^{\sigma(0)} \sigma \delta^{-1}$  is in  $\mathfrak{S}_n$   
 (fixes  $n$ ): the mapping in the third condition is the  
 generator  $-s_1$  of  $J_{n+1}$  acting on  $\Delta \times \Delta' \cdot \sigma$ . (By claim 5 of  
 §§ 4 this generator maps  $\Delta \times \Delta' \cdot \sigma$  to  $\Delta \cdot \delta \times \Delta' \cdot \sigma$ . Use the  
 diagonal action to send this prism to  $\Delta \times \Delta' \cdot \sigma \delta^{-1}$  which is  
 in  $\Delta \times H'$ ; then by claim 5 a suitable element of  $J'_{n+1}$   
 maps it into  $\Delta \times K'$ .)

The first condition is the folding condition over  $\Delta_1$ :  
 the folding conditions over the other faces  $\Delta_i$  are implied  
 by the invariance condition.

The second condition asserts that the subdivision of  
 $\Delta \times P$  invariant under the action of  $\bar{M}$ .

Note that the resulting decomposition into (open) simplices  
 may not be a triangulation of the crystal  $X = J'_{n+1} \backslash T \times T' / \mathfrak{S}_{n+1}$   
 (because in  $X$  there are only  $n+1$  vertices and  $\dim(X) = 2n > n$ ).

To get a triangulation of the crystal  $\hat{\mathbb{C}P}^n = T \times T' / \mathcal{S}_{n+1}$  you have to add.

(4) The Triangulation Condition:

The  $\bar{M}'$  and  $G$  invariant linear subdivision of  $P \times P'$  extending  $S$  induces a triangulation of  $P \times P'/G$  (the  $G$ -orbit of a simplex is uniquely determined by the  $G$ -orbits of its vertices.).

6 If  $n = 2$  there is just one solution to the Main Problem: the KÜHNEL triangulation of  $\mathbb{C}P^2$ .

To solve the Main Problem, a naïve approach is, as follows.

a) List all simplicial subdivisions of the polyhedron  $\Delta \times K'$  which do not add any new vertex.

b) Rule out the ones which fail to satisfy the compatibility and invariance conditions of the above paragraph.

This brute force attack works in the case  $n = 1$ .

The two subdivisions of the square are solutions and induce a triangulation of  $\mathbb{C}P^1$  combinatorially equivalent to the boundary of a 3-simplex. In the case  $n = 2$  this method gives four solutions, whose universal covers (in the orbifold sense) are cyclically permuted by the quarter turn rotation with matrix  $\begin{pmatrix} 0 & -1 \\ 1 & 0 \end{pmatrix}$  acting on  $P \times P'$ . Furthermore, these solutions satisfy the triangulation condition.

Let us list the 4-simplices of one of these triangulations.



Denote a  $k$ -simplex of a prism  $\Delta \times \Delta' \cdot \sigma$  by its braille:  $k+1$  points in a 3 by 3 matrix where a point on the  $i^{\text{th}}$  column and  $j^{\text{th}}$  row means that  $(s_i, s_j \cdot \sigma)$  is a vertex of the 4-simplex.

Figure 12-4 shows the parallelogram  $K'$  which is the union of the 2! triangles  $\Delta'$  and  $\Delta' \cdot \tau_1$ . In each of these triangles we write the brailles of the six 4-simplices subdividing the corresponding prism.

One of the four solutions of the Main Problem in the case  $n=2$

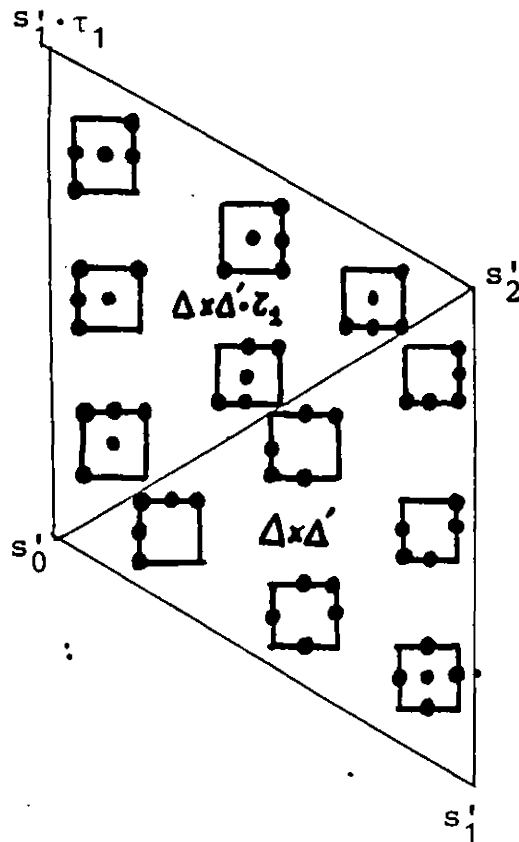


Figure 12-4

We leave it as an exercise for the reader to check that the simplices depicted in figure 12-4 give a triangulation of the polyhedron  $\Delta \times K'$  which satisfies the compatibility and invariance conditions. (For example the triangulations of each prism restrict to the same triangulation  $(\begin{array}{c} \cdot \quad \cdot \quad \cdot \\ \cdot \quad \cdot \quad \cdot \\ \cdot \quad \cdot \quad \cdot \end{array} \quad \begin{array}{c} \cdot \quad \cdot \quad \cdot \\ \cdot \quad \cdot \quad \cdot \\ \cdot \quad \cdot \quad \cdot \end{array} \quad \begin{array}{c} \cdot \quad \cdot \quad \cdot \\ \cdot \quad \cdot \quad \cdot \\ \cdot \quad \cdot \quad \cdot \end{array})$  of their common face  $\Delta \times \Delta'_1$  and the generator  $-s_1$  of  $J_{n+1}$  acts on the simplices of  $\Delta \times \Delta'$  and  $\Delta \times \Delta' \cdot \tau_1$  by a clockwise (respectively anticlockwise) rotation through  $\frac{2\pi}{3}$  in each of the triangles  $\Delta'$  and  $\Delta' \cdot \tau_1$  of figure 12-4).

The philosophy of chapter XII is: "To make the crystal  $\mathbb{C}P^n$  and its triangulation easier to understand, factor by the biggest symmetry group giving a quotient crystal possessing a nice prism decomposition". However, let us now lean toward the philosophy of the rest of the paper: "The more symmetry a fresco has, the more enticing it is". Unfold the triangulation of the polyhedron  $\Delta \times K'$  which we described above into a triangulation of the fundamental domain  $\Delta \times H'$  of the group  $G$  of the crystal  $T \times T' / \mathfrak{S}_3 \simeq \hat{\mathbb{C}P}^2$ .

An unfolded solution of the Main Problem for  $n = 2$

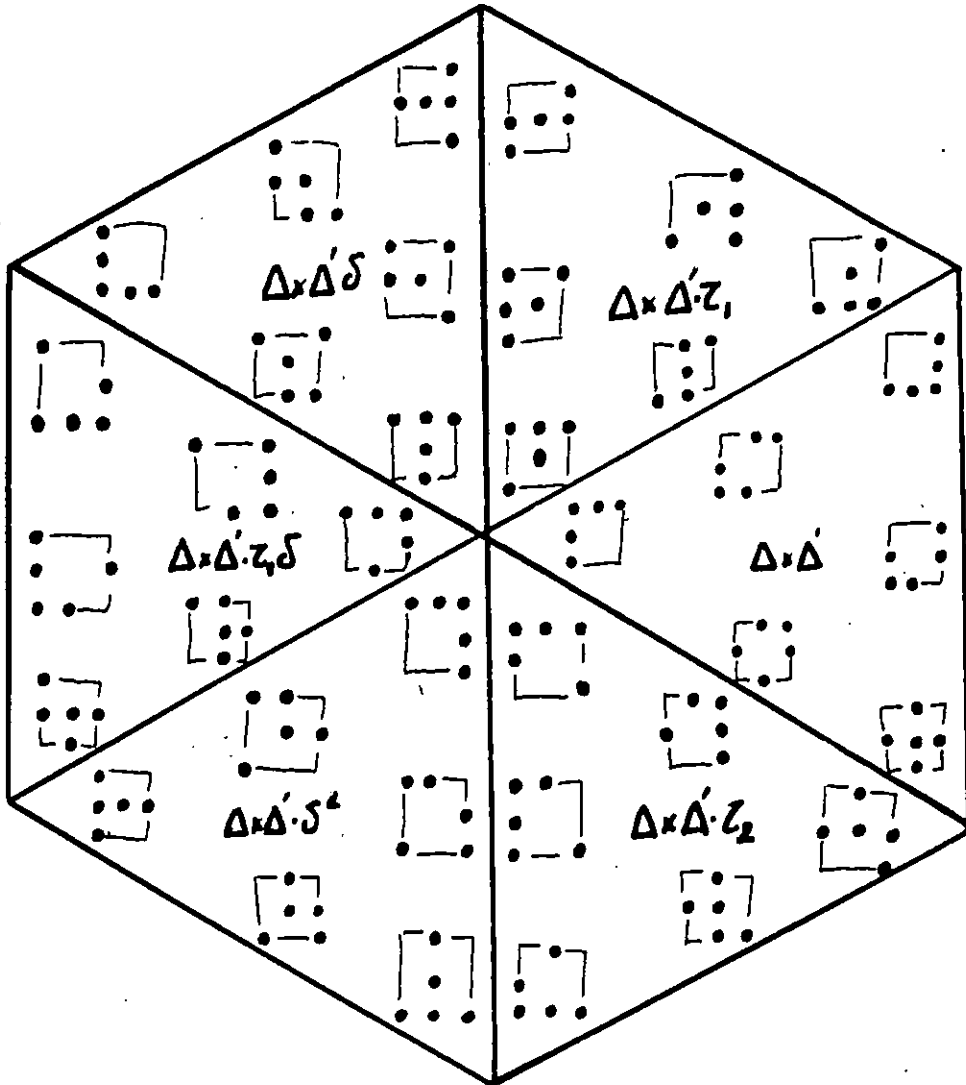


Figure 12-5

To recognize the thirty six 4-simplices of the KÜHNEL COMPLEX, our braille must be coloured according to the following scheme

9	1	5
4	8	3
2	6	7

Thus our braille has a different meaning from that of chapter I. (Recall that the braille of chapter I was coloured

$$\begin{pmatrix} 1 & 4 & 7 \\ 2 & 5 & 8 \\ 3 & 6 & 9 \end{pmatrix} .$$

Note that on the present braille the generators of  $J'_3$  and  $J_3$  act by permuting the rows and columns; they are  $1 \times \delta$  and  $\delta \times \delta$  and correspond to the permutations  $\alpha\beta^{-1}$  and  $\beta$  of chapter I.

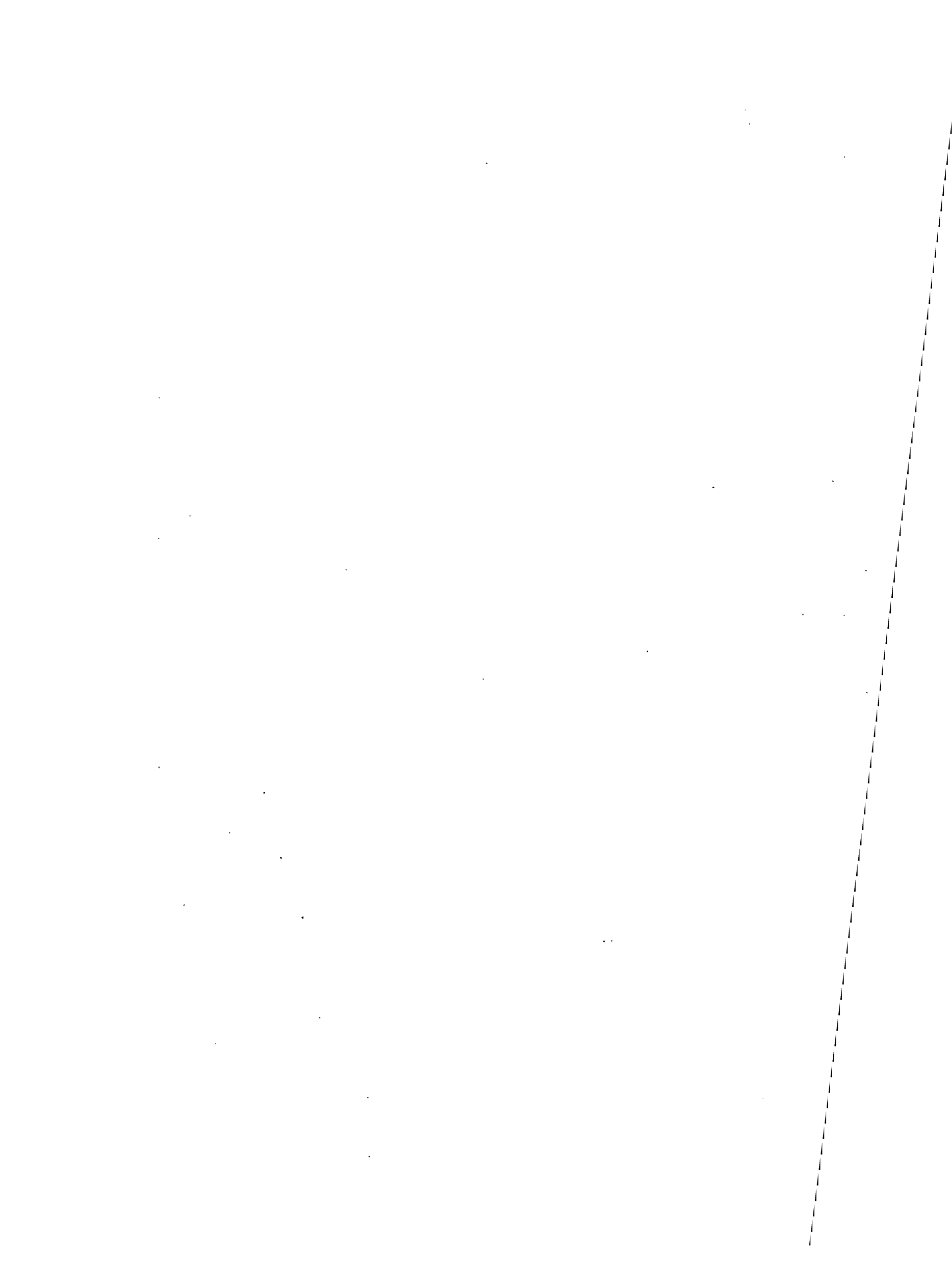
In the case of an elliptic curve associated to a hexagonal lattice, the crystal  $T \times T' / \mathfrak{S}_{n+1}$  has one more symmetry of order three, which in the case  $n=2$  corresponds to the permutation  $\gamma$  of chapter I. But as this  $\frac{2\pi}{3}$  rotation of the curve  $E$  does not preserve any splitting of  $E$  it cannot preserve the prismatic decomposition. Nevertheless, choosing the basis  $(\exp(\pi i/3), \exp(2\pi i/3))$  for the hexagonal lattice, this new symmetry acts isometrically on  $T \times T'$  via the matrix  $\begin{pmatrix} -1 & -1 \\ 1 & 0 \end{pmatrix}$  and, in the case  $n=2$ , respects the triangulation we described. We obtain precisely Marin-Yoshida's rectilinear triangulation of the two dimensional complex vector space  $\mathbb{C}^2$ .

Note that in  $T \times T'$  the matrix  $\begin{pmatrix} 0 & -1 \\ -1 & 0 \end{pmatrix}$  which gives complex conjugation also respects the triangulation (it is the translation of the  $\delta$  of chapter I). Observe also that choosing the basis  $(1, \exp(\pi i/3))$  would not give the Kühnel complex, but its image under the  $\varepsilon$  of chapter I

(the Kühnel complex of course being given by two of the three other solutions of the Main Problem).

Remark We do not give the proof of the uniqueness of the solution of the main problem, because that proof is a tedious verification (which took us a whole afternoon the first time we tried it). Furthermore, we do not yet understand what really makes it work: a nice proof would answer the Main Problem in all dimensions. Let us just mention that in the case  $n = 2$  the invariance condition splits into two invariance conditions (one on each prism): you essentially have to consider the prisms one after the other and these invariance conditions very soon limit the number of cases to consider. But for  $n \geq 3$  the generator of  $J_{n+1}$  permutes some of the prisms, so you have to consider all the prisms at the same time: the incompatibilities come much later. We hope nevertheless that some reader, more careful than us, will "catch the tight triangulations" and solve the Main Problem. Even finding a triangulation of  $\mathbb{C}P^3$  with sixteen vertices would be a step forward!

§ 13 and § 14 are in preparation



## REFERENCES

- [B] M. Brückner
- [B-K] U. Brehm and W. Kühnel, A 5-neighborly triangulation of the quaternionic projective plane with 15 vertices Univ. Duisburg- preprint.
- [E-K] J. Eells and N.H. Kuiper, Manifolds which are like projective planes, Publ. IHES 14 (1962)
- [G1] B. Grünbaum, Convex polytopes, Wiley-Interscience (1967)
- [G2] \_\_\_\_\_, Polytopes, graphes and complexes, Bull. AMS (1970) 1131-1201.
- [G-S] B. Grünbaum and V.P. Sreedharan, An enumeration of simplicial 4-polytopes with 8 vertices, J. Comb. Th. 2 (1967) 437-465.
- [Jä] B. Morin, The Kühnel triangulation of  $\mathbb{C}P^2$ . Note taken by K. Jänich (1981), unpublished.
- [K] N. Kuiper, Geometry in Total Absolute Curvature theory, in Anniversary of Oberwolfach 1984, Perspectives in Mathematics Birkhäuser Verlag Basel, p. 377-392.
- [K-B] W. Kühnel and T.F. Banchoff, The 9-vertex complex projective plane, Math. Intelligencer 5-3 (1983) 11-22.
- [K-L] W. Kühnel and G. Lassmann, The unique 3-neighborly 4-manifold with few vertices. J. Comb. Th. (A) 35 (1983).
- [Mi] J. Milnor, On the 3-dimensional Brieskorn Manifold  $M(p,q,r)$  in Knots, Groups and 3-manifolds ed. L.P. Neuwirth, Ann. of Math. Studies 84.
- [Mö] A. Möbius, Gesammelte Werke (~1865)
- [Moi] E.E. Moise, Affine structures on 3-manifolds V, Ann. of Math. 56 (1952) 96-114.
- [R-S] C.P. Rourke and B.I. Sanderson, Introduction to piecewise linear topology, Springer Erg. Math. Bd 69.

- [S] R.J. Stern, Instantons and the topology of 4-manifolds, Math. Intelligencer 5-3 (1983) 39-44.
- [Sie] L.C. Sieberman, Exercise sur les noeuds rationels, Preprint. Orsay (1975).
- [Wh1] J.H.C. Whitehead, Simplicial spaces nuclei and  $m$ -groups. Proc. London Math. Soc. 45 (1939) 243-327.
- [Wh2] \_\_\_\_\_, On  $C^1$ -complexes, Ann. of Math. 41, 809-824 (1940).
- [Y1] S. Tokunaga and M. Yoshida, Complex crystallographic groups I, J. Math. Soc. Japan 34 (1982) 581-593.
- [Y2] J. Kaneko, S. Tokunaga and M. Yoshida, Complex crystallographic groups II, J. Math. Soc. Japan 34 (1982).